Temperature Dependence of the Leachability of Cemented Paste Backfill

By

Andrew Bull

Thesis submitted to the
Faculty of Graduate and Postdoctoral Studies
in Partial Fulfillment of the Requirements
for the M.A.Sc Degree in Environmental Engineering

Ottawa-Carleton Institute for Environmental Engineering
Civil Engineering Department
Faculty of Engineering
University of Ottawa

Temperature Dependence of the Leachability of Cemented Paste Backfill

Submitted by

Andrew Jaret Bull

In partial fulfillment of the requirements for the degree of

Master of Applied Science

In

Environmental Engineering

_____

Dr. M. Fall (Thesis Supervisor)

Contents

List of Figures

List of Tables

List of Abbreviations

AO: aesthetic objective

BFS: blast furnace slag (Slag)

CH: portlandite

CML: cumulative mass leached

CPB: cemented paste backfill

CRF: cemented rock fraction

C-S-H: calcium-silicate-hydrate

d_c: critical pore diameter

d_{th}: threshold pore diameter

D_e: diffusion coefficient

IFL: incremental fraction leached

MAC: maximum acceptable concentration

MCL: maximum contaminant level

MCLG: maximum contaminant level goal

NA: no value or not yet developed

OG: operational guidance value

OPC: ordinary Portland cement

Rd: rate of mass removal (interchangeable with rate of diffusion)

TT: treatment technique

URF: Uncemented rock fraction

wt%: percent by weight

K: hydraulic conductivity

K_i: intrinsic permeability

γ: specific weight

μ: dynamic viscosity

Acknowledgement

I would like to sincerely thank Dr. Mamadou Fall and the University of Ottawa for accepting me as a M.A.Sc. Student. Dr. Fall has helped to guide me in my research while challenging me to think critically and solve problems independently. He has directly overseen my research and provided me with valuable tools to be successful as an environmental engineer, beyond the mine tailings management field. Thank you, Dr. Fall, for providing me with such a great opportunity, and the tools for a successful future.

Over the two years spent working on my research I have had the opportunity to work with many great people in Dr. Fall's research unit, and in other faculties and disciplines within the University. I would like to thank all my colleagues who have helped me along the way. I owe specific thanks to: Jean-Claude Celestin for providing advice, humour, and ensuring orders were made, and materials received; Patrick D'Aoust for discussing ideas with me and providing me with access to his lab; Dr. Nimal De Silva and Smitarani Mohanty for helping me with leachate analysis and providing me with ideas on how to best display my results. I wish to thank both Dr. Paul Simms and Dr. Majid Sartaj for providing positive contributions to my research, and academic career outside of research. I also owe thanks to many other great professors who made the course-based component of this degree both interesting and informative.

Without the help of my family none of my success would have been possible. I want to thank my parents Dave and Cathy, and my sister Jaimee. They have taught me that hard work and true grit are the keys to success. The have also provided me with every opportunity possible to follow my passion.

The two years I spent in Ottawa were made memorable by the many friends I made along the way. I am very fortunate to have spent two years here with many great people and have developed connections that will last a lifetime.

Abstract

Underground mining is a mineral acquisition technique that is critical to global economies, and human technological advancements. As shallow resource reserves are depleted, mine depths are increasing to accommodate global mineral demand. Increases in mine throughputs and excavation depths pose increased environmental concerns. Tailings surface disposal, and underground mine support are two considerable environmental and geotechnical factors of concern in current day mining. Underground waste disposal has been adopted by the mining industry in many forms. Cemented paste backfill (CPB) is a common best management practice developed to tackle these two specific resource industry related issues worldwide. CPB is a cement-stabilized material composed of tailings, water, and hydraulic binder. Tailings disposal areas on the earth's surface are reduced by disposing of tailings in subsurface stopes that have been previously excavated. This increases underground safety by providing structural support to the mine. There are also economic benefits to this practice, as the additional support allows for adjacent pillars to be excavated. Although CPB greatly reduces tailings exposure to atmospheric elements, there are still underground environmental factors that must be considered with respect to environmental performance. CPBs are porous media, meaning they are susceptible to leaching of naturally occurring metals that are no longer in a stable condition as they were when incorporated in the parent rock. Arsenic and lead are metals of concern due to their association with many ore bodies. Leaching of these unstable metals may be influenced by the backfill curing temperature and the chosen hydraulic binder. Curing temperatures may be influenced by geographic location, local stope geology and depth, hydration and transport, among others. Hydraulic binders are chosen based on availability, cost, and desired mechanical properties of the paste. In this research, the effect of curing temperature and binder composition on the leachability of CPB are studied. ASTM C 1308 leaching protocol is used to determine the leachability of six CPBs. In addition, microstructural techniques (Powder X-Ray Diffraction, Mercury Intrusion Porosimetry, and Scanning Electron Microscopy) are used to relate the microstructural properties of the CPB to the leaching characteristics. Results reveal that CPBs cured with ordinary Portland cement (OPC) leach significantly less than CPBs cured with an OPC/Blast furnace slag (Slag) binder (50% blending ratio) as a result of CH consumption in slag hydration. Both CH and C-S-H are responsible for immobilizing arsenic in cement stabilized materials. OPC-CPBs contain greater relative quantities of CH, which aids in arsenic immobilization. Between the range of 2°C and 35°C OPC-CPB performed better at lower curing temperatures. Lower curing temperatures are favoured in OPC-CPB because the pore surface greater than the threshold pore diameter is reduced. Alternatively, OPC/Slag-CPB exhibited a decrease in cumulative mass leached at higher curing temperatures. The difference in cumulative mass leached by the OPC/Slag-CPBs is also related to the pore surface, and threshold pore diameter.

Chapter 1 - Introduction

1.1 Background and problem statement

Hard rock (underground) mining operations are vital for the acquisition of metals used globally, in a wide range of industries. Current mining operations produce substantial amounts of waste annually. Waste from hard rock mines in the form of tailings pose many challenging environmental and geotechnical issues. Tailings are commonly stored on the earth surface as vast deposits of potentially toxic material with poor geotechnical engineering properties.

Underground mining is used to excavate metal bearing ore. It is practiced in countries across the world that have a broad range of surface and subsurface climatic conditions. Each climate faces unique challenges with respect to mine waste management. Cemented paste back-fill (CPB) is an emerging technology that has become extensively used in Canada and other countries to both reduce surface disposal of tailings, and act as a geotechnical support measure for underground mines. CPB is hydraulically pumped and/or transported by gravity from surface facilities that mix tailings, water, and a hydraulic binder to subsurface stopes where it is contained by support barricades and left to cure until design strength is achieved. This increasingly common technology can be implemented during active mining operations or upon mine closure. The high strength and low binder proportions of modern CPB make the technology desirable from both environmental and geotechnical standpoints.

Since CPB is a relatively modern technology, there are many unknowns regarding its long term environmental and geotechnical performance. CPB, like other cement structures is porous, meaning that when cured as a monolith between rock mass of significantly lower permeability, the CPB structure acts as the path of least resistance for water migration. The water table in underground mines is often artificially lowered by pumping during mining operations. As mines are closed and pumping is discontinued, the water table will return to its natural state by the upward migration of water through the CPB structure. The leachability of the CPB is a potential concern due to the possible presence of hazardous materials, such as heavy metals. CPB structures are susceptible to various temperatures during their curing period due to both external

and internal temperature sources. Thus, it is important to understand the effect of curing temperature on the leachability of CPB structures.

1.2 Research Objectives and Scope

The primary objective of this research is to determine if the thermal conditions that CBP structures are subject to during the curing period influence the leachability of heavy metals, particularly arsenic and lead from the mature CPB monolith. Natural gold mine tailings will be used to determine how curing temperature affects the leaching of samples prepared using two binder compositions. Microstructural analysis of the samples cured at three different temperatures using two different binder compositions will be conducted to determine if the temperature dependence on leaching is related to variations in the microstructure of the cement matrix. This experiment aims to:

- Determine if curing temperature influences leachability of mature CPB
- Assess if the hydraulic binder used changes the leachability of CPB cured at three curing temperatures
- Evaluate the influence of binder composition and curing temperature on the microstructure of the CPB
- Relate the microstructural properties to the temperature dependent leaching characteristics of the CPB

1.3 Research Approach and Methods

Previous research regarding the leachability of metals from CPB is limited. Past studies (e.g., Mácsik and Jacobsson 2006; Yin et al. 2007; Kogbara and Al-Tabbaa 2013, Poon et al. 2001; Vollpracht and Brameshuber 2016; Dell'Orso et al. 2012) have been conducted with interest of the leachability of other cementitious material and cement stabilized wastes. Leach tests used for these experiments have been divided into two categories; single extraction batch tests, and multiple extraction dynamic tests. Within each category there are many tests designed to simulate a variety of leaching conditions for a range of materials. CBP is monolithic in the field, thus a leaching protocol designed to simulate long term leaching of a monolith is ideally suited for this application. ASTM C1308-08 is a standard test method developed for determining the

diffusive release of contaminates from solidified waste forms. This protocol was reapproved in 2017 suggesting it is the most current standard procedure developed for determining the accelerated long-term leaching characteristics of monolithic waste forms.

The ASTM C1308-08 procedure was carried out on samples cured at 2°C, 20°C, and 35°C using a constant binder proportion of 4.5 wt%. Two binder compositions were used; Ordinary Portland Cement (OPC), and an OPC – Blast Furnace Slag (BFS or Slag) mix at a blending ratio of 50%. These curing temperatures and binder conditions were chosen because they are both commonly observed in the practice of cemented paste backfilling in shallow to mid-level underground mining practice. Natural tailings were used in this experiment to ensure results best simulate field conditions with respect to mix design and chemical composition of CPB. Elemental analysis of natural tailings resulted in much lower concentrations of As and Pb than expected in the field, thus tailings were doped with As and Pb to maximum observed natural concentrations to represent the worst-case leaching conditions over the 11-day leaching procedure.

Leachate collected from the ASTM C1308-08 procedure was analyzed by the Geochemistry Laboratory at the University of Ottawa using Inductively Coupled Plasma Atomic Emission Spectroscopy - Mass Spectroscopy (ICP). Leachate analysis was used to highlight the differences in the leaching characteristics between the six samples. This data was supported by microstructural analysis of the monolithic samples. Scanning Electron Microscopy (SEM), Powder X-Ray Diffraction (PXRD), and Mercury Intrusion Porosimetry (MIP) were used to characterise the microstructure and relate the microstructural characteristics to the results from ASTM C1308-08.

1.4 Thesis Outline

An outline of this thesis is presented below:

Chapter 2 – Technical and Theoretical Background. This chapter reviews literature on the technical and theoretical background of hard rock mining practice, mine waste management, mine backfilling, leaching and leaching tests, sources of temperature in mining, and sources of arsenic and lead in the mining environment.

Chapter 3 – Theory and Objectives. This chapter describes mine flooding theory and the objectives of the study which includes; the influence of curing temperature on leachability, the influence of binder composition on leachability, the combined effect of temperature and binder composition on leachability, and the influence of microstructure on leachability.

Chapter 4 – Experimental Design. This chapter outlines the design of the experiment, including materials and methods as well as analysis techniques.

Chapter 5 – Results and Discussion. This chapter highlights the findings from the ASTM C1308-08 Leaching protocol and provides evidence from microstructure analysis and past research as to why trends are observed.

Chapter 6 – Conclusion and Recommendation for Future Research. This chapter summarizes the findings from this study and provides insight to where future research is needed in the field of the environmental performance of cemented paste backfill.

Chapter 2 – Technical and Theoretical Background

2.1 Introduction

Underground mining is a vital industry for the excavation and extraction of many minerals. CPB technology has been developed as a best management practice for underground mining. There are many benefits to implementing CPB including; surface disposal area reduction, and underground mine support. As CPB has become standard practice in Canada and other nations, research has been conducted to improve the performance of the CPB structures. CPB technology allows for mine waste to be converted into an economically beneficial product. In this chapter the mining, backfilling and leaching processes are described. Several leaching tests are discussed, and water quality standards are outlined.

2.2 Mining and Mine Waste Management

In underground hard rock mining ore bodies are excavated through a series of shafts, drifts, drawpoints, and stopes. Hard rock mining has a higher operational cost than some bulk mining methods, however dilution rates (ratio of mass waste to mass excavated) are reduced by selective mining (Pareja 2000). The New Afton Mine operated by New Gold Inc. located west of Kamloops British Colombia operates at an average throughput of 15 thousand tonnes per day; 5.5 Mtpa (Rennie et al. 2015). In Canada, 500 million tonnes of hard rock mine waste is produced each year (Amaratunga and Yaschyshyn 1997). This number has presumably increased in the past two decades. This waste must be managed to ensure environmental and geotechnical stability. There are many forms of waste produced through mining operations and many methods to mitigate environmental and geotechnical concerns.

2.2.1 Ore Body Excavation

Underground mining excavation sequences differ based on the characteristics and size of the ore body. Ore bodies must be blasted for muck to be transported to the surface. This is done through a series of stopes and an engineered subsurface transport and ventilation system. Stopes (the area that is blasted and excavated) are cut and filled based on the complex geometry and structure of the ore body. Excavation sequences may require sequential backfilling during operations to aid in subsurface support (Villaescusa 2003). Figure 2.1 displays a 3D preview of the ore body at the New Afton gold and copper mine in BC (New Gold 2017). Muck (excavated rock) is transported through drawpoints at the base of the stope and brought to the surface (Ghirian 2016). Muck is stockpiled at the surface where it is classified as ore or waste rock. Ore is sent to the mill for further processing while waste rock is deposited and managed according to its acid generating potential (Waihi Gold 2015).

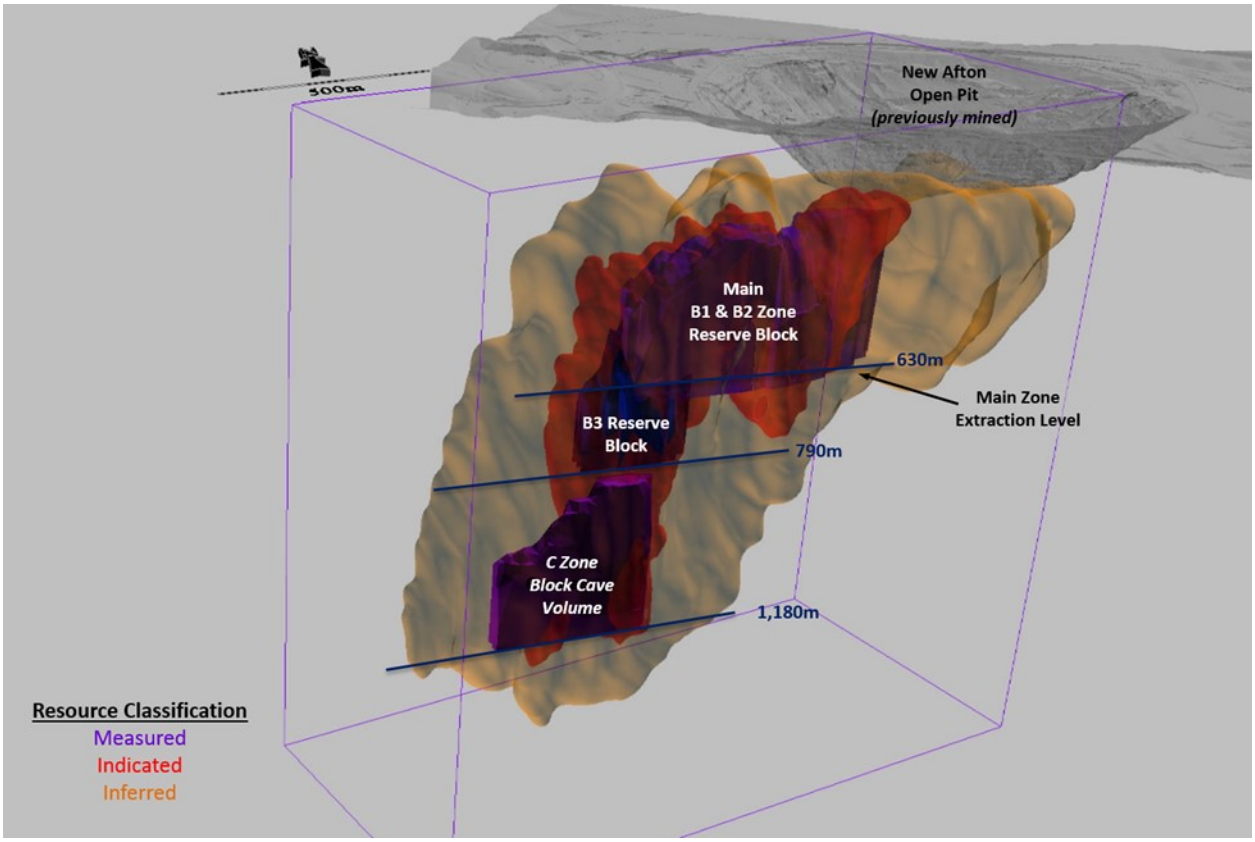

Figure 2.1. 3D preview of the block cave reserves at the New Afton Mine west of Kamloops BC (New Gold 2017).

2.2.2 Milling and Extraction

Economic rock sent to the mill must be reduced in size for transport and extraction. The milling process begins with crushing. Crushing is a dry process where particles are reduced to a maximum diameter of 16 cm by primary crushers, then progressively to pass No. 6 to No. 14 mesh by secondary crushers. Once particles are reduced by the crushers, they are ground by grinders to the micron size. This size reduction is necessary to reduce particles to a single grain for efficient liberation of individual minerals. Water is introduced at the grinders as a lubricant, and a medium to facilitate transport (Balsubramanian 2015). At the grinders, particles are reduced to a particle size range of 10 to 100 microns. Milled rock is transported through pipelines as a slurry with a relative density of 1.3 to 1.5 to the extraction plant where the target mineral is separated from gangue minerals (Blight & Bentel 1983). Figure 2.2 represents a simplified flow chart for mineral processing.

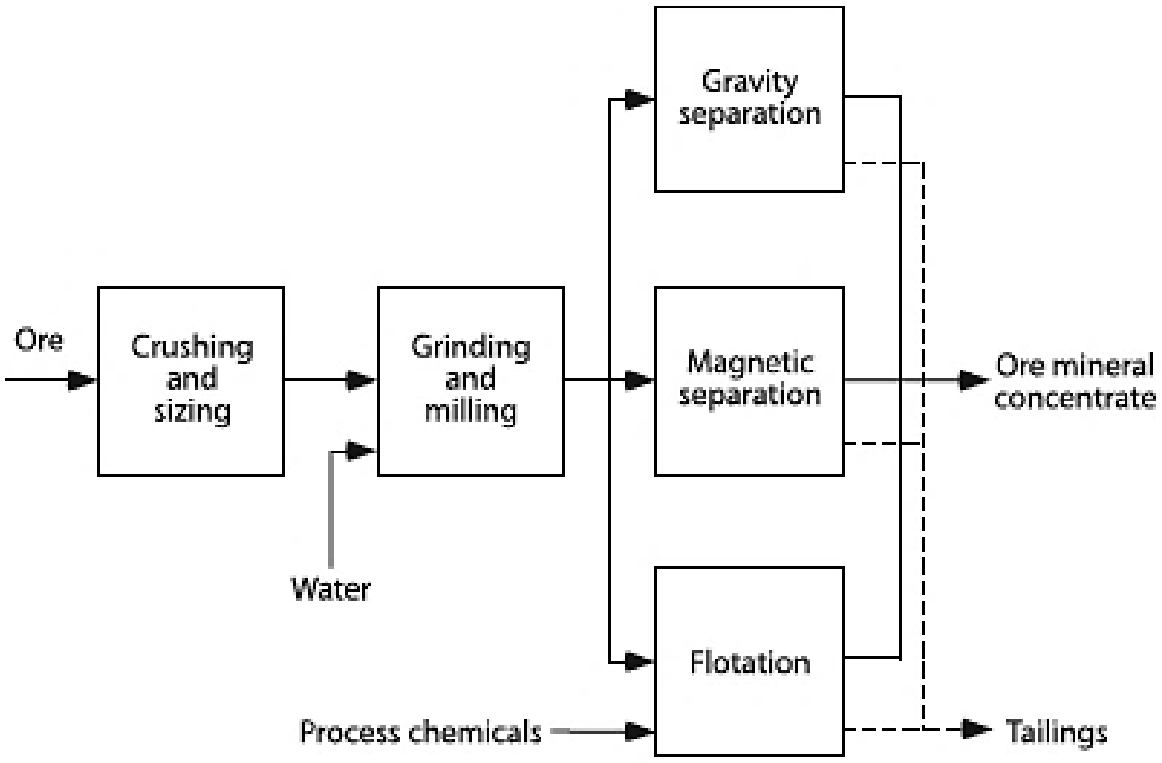

Figure 2.2. Flowchart of common hard rock mine processing operations which separate ore mineral concentrate from tailings (from Lottermoser 2007).

The particle size of 10 to 100 microns is utilized because it reduces most minerals to a single grain. The valuable portion of the slurry must be separated from the valueless sulfides in the extraction process. A common extraction method utilized in gold mining is froth flotation. Froth flotation separates minerals based on their chemical behavior. Addition of chemical reagents, or altering pH causes some minerals to become hydrophobic, while others to be hydrophilic. Air is bubbled through the slurry and hydrophobic minerals attach to the air bubbles, then collect at the surface as a froth. Froth is then skimmed from the surface, separating the valuable mineral from the waste (Wills and Finch 2015). Valuable minerals are sent for further processing, while valueless minerals must be deposited as mine tailings.

2.2.3 Mine Waste

There are two main types of mine waste that must be managed; waste rock, and tailings. Each type of waste has its own unique issues with respect to disposal and storage. Waste rock is the waste produced through the excavation that does not have a high enough yield of economic mineral to extract. Tailings are produced as the waste associated with the milling and extraction process. Cumulatively waste rock and tailings can account for fifty to ninety-eight percent of excavated ore (Nagaraj 2005).

2.2.4 Mine Waste Management

Each type of mine waste is associated with its own set of geotechnical and environmental challenges. The result of these challenges leads to different management techniques catered to each of the waste types.

2.2.4.1 Waste Rock Management

Waste rock can be notorious for acid generation, resulting in acid rock drainage. Although waste rock stacks very well, there is a three-dimensional diffusion pathway for oxygen to move through the waste rock pile resulting in the generation of protons due to sulfide oxidation. At depth, sulfides are stable. When brought to the surface and exposed to oxygen, the following sulfide oxidation reaction series with respect to pyrite poses a tremendous environmental concern:

1) $FeS_2 + 2H_2O + 3O_2 \rightarrow Fe^{2+} + 2SO_4^{2-} + 4H^+$
2) $Fe^{2+} + ¼\ O_2 + H^+ \rightarrow Fe^{3+} + ½\ H_2O$
3) $Fe^{3+} + 3H_2O \rightarrow Fe(OH)_3 + 3H^+$ (Occurs when pH > 4)
4) $FeS_2 + Fe^{3+} + 8H_2O \rightarrow 2Fe^{2+} + 2SO_4^{2-} + 16H^+$

Since the availability of oxygen is the key driver in this reaction series, the most common approach to waste rock management is to develop soil covers that limit the ingress of oxygen into the waste rock pile. At pH greater than 4, ferric iron precipitates may act as an oxidant therefore leading to an increase in acidity by accelerating the oxidation of pyrite (Singer & Stumm 1970).

2.2.4.2 Tailings Management

Acid generation is also an environmental concern with respect to tailings. Besides acid generation, large surface disposal areas also pose environmental concern. The mechanical strength of tailings is very low due to high gravimetric water contents (between 100 and 150 percent) used in tailings transport, making stacking tailings a challenge. Since in most cases tailings cannot be stacked, they consume large areas adjacent to mines due to their high volume and low strength (Vick 1983; Blight & Bentel 1983). Tailings are commonly deposited using a series of dams. The upstream dam method (Figure 2.3) is most common, however with this method dam failure is a geotechnical concern. With the upstream method, coarser particles settle first and are stacked upon each other. This creates dams made primarily of sand sized particles to retain the remaining portion of the tailings. These sands are susceptible to liquefaction in the event of seismicity, which can be natural or mine related (Vick 1983). Dam failure due to liquefaction can be catastrophic, as tailings can flow for several kilometers resulting in environmental destruction (Azam & Li 2010). To reduce the use of upstream damming, tailings can be dewatered with hopes of gaining mechanical strength. Soil covers, and water covers can then be developed to limit the ingress of oxygen to the tailings, thus reducing the risk of acid generation. Although acid generation can be mitigated using covers, the large surface disposal areas are not reduced. Backfill technology can be used to reduce the surface disposal areas by up to 60 % (Fall 2017).

Backfill technology serves environmental, geotechnical and economic purposes. Environmentally, surface disposal areas are reduced, thus reducing the risk of acid mine drainage, and decreasing the number of natural ecosystems that are destroyed. From a geotechnical standpoint reducing surface disposal areas reduces the risk of catastrophic dam failure and CBP provides structural support to the subsurface where mining activities have taken place. Economically, CPB provides enough structural support to the subsurface that pillars can be converted to stopes, allowing for a higher percentage of the ore body to be excavated (Benzaazoua et al. 2008).

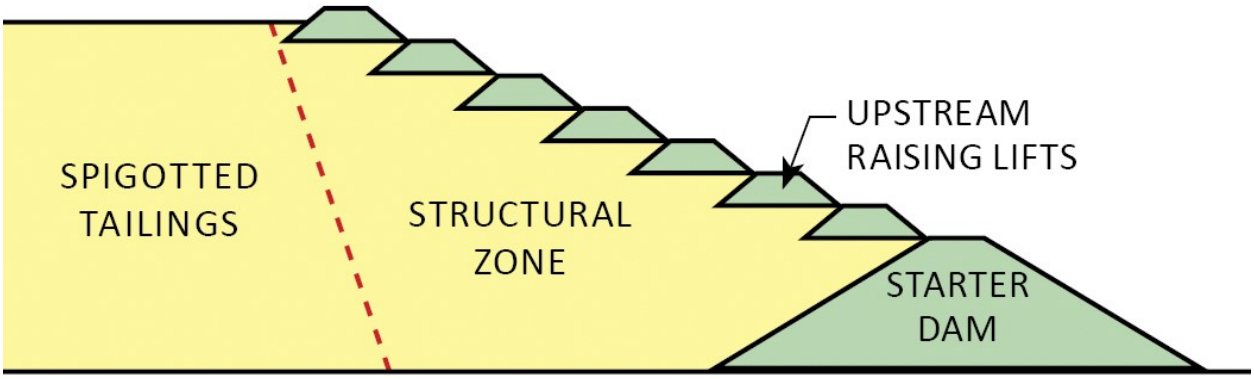

Figure 2.3. Upstream dam construction over seven sequential dam raises from the initial starter dike (McLeod and Bjelkevik 2017).

2.3 Backfill Technology

Mine backfilling is a modern technique where waste rock and/or tailings are deposited into closed stopes. Prior to backfilling, the drawpoint must be sealed with a bulkhead or barricade. Sealing the drawpoint can be done using a range of materials including rock, masonry, and concrete (Rankine and Sivakugan 2006). Backfill is composed primarily of tailings. However, the mix design of the fill depends of the type of backfill being used. Backfill can be broken down into three categories; rockfill, hydraulic fill, and paste fill (Ghirian 2016).

2.3.1 Rock Fill

Rock fill technology uses a mixture of waste rock and tailings to fill stopes. Rock fill can be classified as uncemented rock fill (URF), or cemented rock fill (CRF). With CRF, a cement paste is mixed with the remainder of the fill prior to deposition. 4% to 8%

cement can be added to the fill to increase the mechanical strength of the fill (Ghirian 2016).

2.3.2 Hydraulic Fill

Hydraulic fill is a simple method of backfilling using a slurry composed of tailings, water, and sometimes cement, additives and waste rock. Hydraulic fill is poured via pipelines or boreholes and can be mixed at the surface or underground. Drainage ports are added to the stope to facilitate dewatering of the fill (Ghirian 2016).

2.3.3 Cemented Paste Backfill

Cemented paste backfilling is an emerging mine waste management practice, that in recent years has become widely used in hard rock mining. CPB is a combination of fine tailings, water, and a hydraulic binder. Commonly, the fine tailings fraction of CPB ranges from 70-85 wt% (Fall et al. 2008). The hydraulic binder often accounts for 3-7 wt% (Benzaazoua et al. 2004). Binder percentages of up to 10 wt% are not uncommon for the first pour, where a rapid increase in mechanical strength is desired (Williams et al. 2001). The most common binder used is Ordinary Portland Cement (OPC). Additives such as blast furnace slag (BFS), and fly ash are often used as components of the hydraulic binder (Tariq and Yanful 2013). Additives can be used to cut costs, since the use of OPC can account for as high as 75% of CPB cost (Grice 1998). The remaining percentage of the paste is water, which can be fresh water or recycled mine water (Wu et al. 2015).

The result of the CPB mix components is a high-density slurry. This slurry is a non-Newtonian fluid that is sequentially pumped and/or transported by gravity into stopes. The first pour (plug) contains a higher binder percentage to ensure a high mechanical strength in early stages of curing. The second pour consists of a lower binder percentage, thus increasing the volume of tailings in the paste, and reducing costs associated with the binder. This method also reduces stress within the backfill and on the barricades by keeping a low pore water pressure (Ghirian and Fall 2015). Pore water pressure within the plug is reduced by the degree of hydration achieved prior to the second fill. The plug is cured for up to a few days before the second pour is initiated.

The higher binder content in the plug allows the CPB to hydrate rapidly and gain early age strength quickly. As CPB hydrates the material stiffens increases, and the coefficient of permeability decreases. This results in a decrease in the maximum pore water pressure within the backfill (Shahavari and Grabinsky 2016; Ghirian and Fall 2015).

CPB is a preferred practice due to its environmental, economical, and geotechnical benefits. From an environmental standpoint, CPB can reduce the surface disposal footprint of a mine, and remove acid generating tailings from earth surface conditions. Geotechnical advantages include increased structural support of the mine both during operation and upon closure (Fall and Benzaazoua 2005). Economically, CPB can allow for excavation of adjacent stopes, and reduce surface rehabilitation costs (Benzaazoua et al. 2008). Although there are many advantages to the use of CPB technology, it is important to consider the potentially harmful environmental effects of this practice. One concern regarding the use of CPB is ground water contamination due to leaching through the cement matrix. Cement is a porous medium and is therefore susceptible to the natural leaching process (Vollpracht and Brameshuber 2016). It is important to consider the leachability of the CPB when considering CPB as a waste management practice.

2.3.3.1 Mix Design of CPB

The mix design of CPB is a crucial factor in optimizing the performance, while ensuring economic viability. CPB must be both transportable and cost-effective. Factors that influence both cost and transportability are W/C ratio, tailings fineness, tailings density, and cement content (Fall et al. 2008). Economically, mix design becomes important because the cost of cement can be as high as 75% of the total backfill cost (Grice 1998).

The mix design of CPB varies depending on the mining operation. OPC is the primary binder used. BFS is commonly used as an additive to the mix. Additives including non-ferrous slag, fly ash and other pozzolanic materials are also used (Ghirian 2016). The delivery of the paste to the stope, as well as the hydration reactions resulting in the curing of the CPB require water (Benzaazoua et al. 2004). The chemistry of this

water is critical with respect to the short-term and long-term strength development of CPB. Therefore, mixing water must be analyzed prior to use (Benzaazoua et al. 2002). Figure 2.4 displays typical mix proportions found in CPB (Ghirian 2016). The water content, tailings percentage and water to cement ratio can be adjusted to meet desired rheological and hardened strength properties (Ouellet et al. 2005).

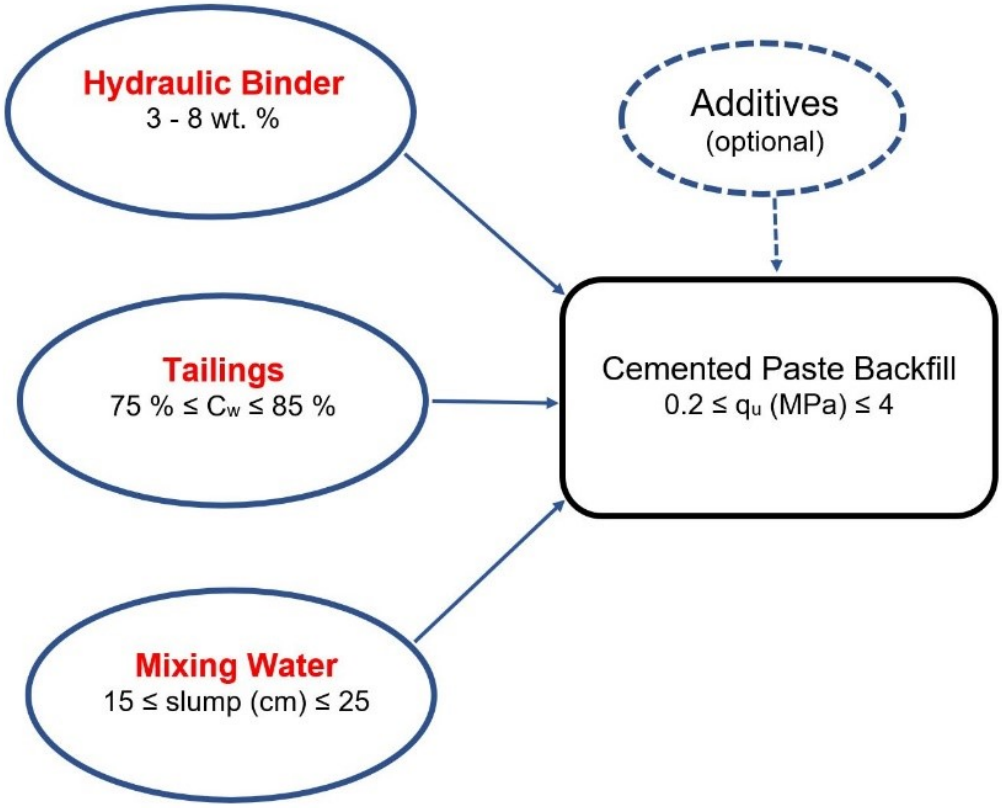

Figure 2.4. Common mix proportions of CPB (from Ghirian 2016).

2.3.3.2 CPB Preparation

With the use of conventional deposition, the solids content of tailings ranges from 35% to 60% (Ghirian 2016). Further dewatering of these tailings to a solids content of 70% - 82% is required for CPB preparation. This dewatering is typically done using disk filters, and results in the production of filter cake. Thickened tailings, in the form of filter cake, are sent to a mixer where they are combined with the choice binder of the operation, and water to achieve the desired slump (Belem and Benzaazoua 2004). Figure 2.5 displays a flow chart of a paste production plant.

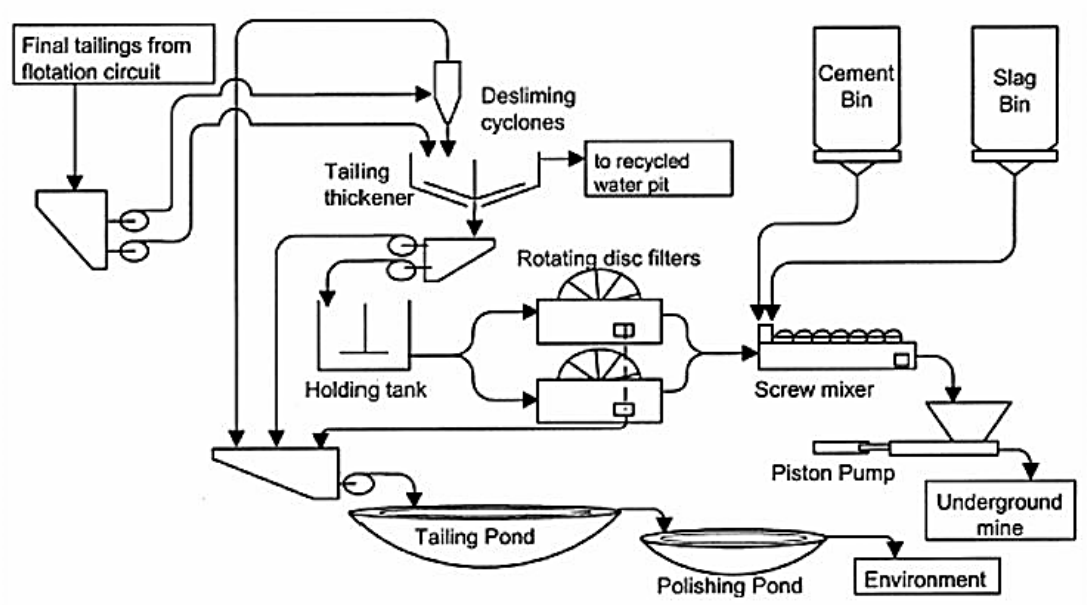

Figure 2.5. CPB production plant at Louvicourt mine Canada (from Belem and Benzaazoua 2004, after Cayouette 2003)

2.3.3.3 CPB Transportation

CPB is transported from the production plant to the subsurface using pipelines. Transport systems for CPB are designed using the rheological behavior of the paste. CPB behaves as a non-Newtonian fluid, therefore it must be transported accordingly, meaning the applied stress must exceed the yield stress. A slump test is commonly performed on the paste. Results from the slump test are correlated to the viscosity and yield stress. The applied pressure gradient can then be determined using the viscosity and yield stress provided by the slump test (Ghirian 2016). Pump/gravity systems can be implemented to decrease the energy required to transport the paste by taking advantage of flow due to gravity. An optimal ratio of vertical to horizontal distance can be determined such that the pumping energy required is minimal. In some cases systems using gravity alone can be developed (Belem and Benzaazoua 2004). Figure 2.6 outlines three basic transportation system designs that can be implemented (Belem and Benzaazoua 2004).

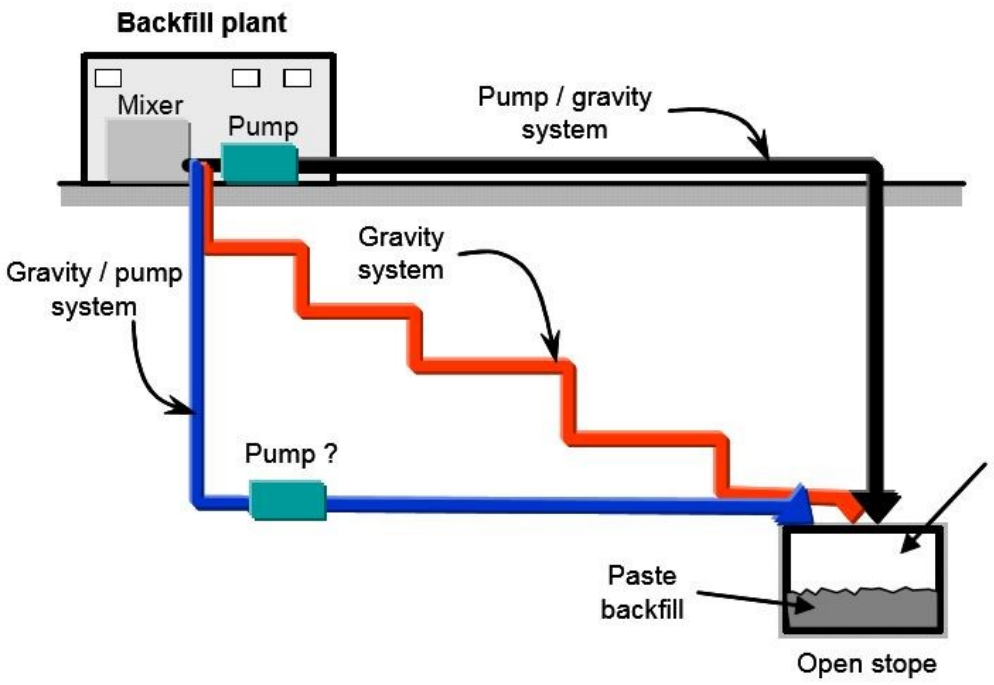

Figure 2.6. Three transportation systems for CPB that use pumps and/or gravity to move paste backfill to the stope (from Belem and Benzaazoua 2004, adapted from Thomas 1979).

2.4 Leachability

It is important to consider the leachability of CPB because it is a porous material. Tailings from hard rock mining are known to often contain heavy metals such as arsenic, zinc and lead. These metals, among others, were once stable when they were bound in rock at depth. Excavation of this rock and exposure to earth surface conditions reduces the thermodynamic stability of minerals, resulting in metal availability (Usiyama and Fukushi 2016). The presence of metals in tailings is therefore an environmental concern due to their toxic properties. Binding these metals in CPB may reduce the risk of metal contamination, however if they are able to leach from the cement matrix, then there is a risk of ground water contamination.

2.4.1 Leaching Mechanisms

According to Vollpracht and Brameshuber (2016), there are three main mechanisms that influence the leachability of cementitious material (e.g. CPB). The first mechanism is the diffusion of ions from the cement matrix to the pore water solution.

The second mechanism is solubility. The third mechanism is soluble salt wash off from the pore linings. Crossover between mechanisms must be considered. For example, changes in solubility may promote diffusion. Each mechanism is governed by a set of controls that must be considered.

2.4.1.1 Diffusion of Ions from the Cement Matrix

Leaching from a cement-based material begins with the movement of ions from the interior of the cement structure to the pore matrix and finally these ions will be leached out of the cementitious material. Compounds undergo dissolution and are then transported by the porewater through the cemented material. Most ion movement is controlled by the diffusion mechanism (Ekström 2003). Diffusion of ions from the cement structure to the pore water is dependent on concentration gradients. As ions diffuse from the cement to the pore solution, intermolecular forces also play a role in the diffusion flow of the ions. Mobility of ions depends both on diffusion from the matrix to the pore solution, and diffusion flow within the pore solution (Ekström 2003). Concentration gradients also occur between the pore water solution and the leachate. These concentration gradients result in the movement of ions from the porewater solution to the eluate (into the environment) (Vollpracht and Brameshuber 2016). Increases in the hydraulic conductivity of the cement results in an increase in the diffusion coefficient. Over time, as leaching occurs pores tend to widen, resulting in an increased w/c ratio, thus a higher diffusion coefficient (Ekström 2003).

2.4.1.2 Solubility

The mobility of a constituent within the cement matrix is commonly governed by the solubility of the constituent. Solubility relates to the saturation of the given constituent in the pore solution or leachate. Solubility of some constituents is dependent on thermodynamics, while other constituents rely on kinetics (Al 2017). Materials in cement-based material may not follow the solubility series that could be expected based on their chemical composition. This is because solubility is dependent on the chemistry of the water that encounters these materials. Therefore, the water chemistry of both the leachant and the pore water influences the order and rate at which constituents go into

solution. For example, materials of lower solubility may undergo dissolution more rapidly than materials of higher solubility based on the chemistry of the water moving through the system (Ekström 2003).

2.4.1.3 Soluble Salt Wash Off

Soluble salts accumulate on the pore linings of the cement matrix as a by-product of hydration products. Salts such as monosulfate, can precipitate in the early stages of hydration (as early as 0.5 to 1 day). Precipitates form on the pore lining and often undergo dissolution when contact with a leachant occurs. This dissolution of precipitates can be considered “soluble salt wash off” since the precipitates have accumulated exclusively on the pore lining (Vollpracht and Brameshuber 2016). Ekström 2003 refers to the “soluble salt wash-off” process as the leaching of the layer between the pore solution and the core of the specimen. The layer between the pore lining’s composition includes soluble salts and other hydration products.

2.4.2 Leaching Controls

Controls of the mechanisms discussed above are outlined by Mácsik and Jacobsson (1996). Although it is often difficult to compare laboratory tests to field measurements, the following controls are understood to influence in situ leaching of cementitious material; surface area of continuous pores that are in contact with pore water, movement of water through the pore matrix, pH of the porewater, redox conditions and pore water content, and the release of alkali and alkaline earth metals during hydration. Results from the study conducted by Mácsik and Jacobsson (1996) suggest that the binder composition is also a controlling factor with respect to the leaching mechanisms outlined by Vollpracht and Brameshuber (2016).

High pore surface area can lead to an increased concentration gradient for diffusion, and an increased area for soluble salt accumulation during hydration. As pore surface area increases, the leaching potential of the CBP increases due to an increased area for ion transfer (Vollpracht and Brameshuber 2016; Dell’Orso et al. 2012).

Pore water movement is a very important control over leachability. The hydraulic conductivity, or permeability of the CBP is the key characteristic related to pore water

movement. Factors affecting the conductivity of the CPB include mix components, curing time, temperature, mechanical damage, and stress applied (Fall et al. 2009). As hydraulic conductivity increases the movement of porewater through the cement matrix will increase. Although increased water movement decreases contact time, an increase in physical and chemical weathering of the cement will occur. This will lead to an increase in leaching of the CPB. It is important to note that based on the study conducted by Fall et al. (2009), the permeability of CPB becomes very low between the curing time of 28 and 55 days.

pH is a critical factor when considering the mobility of metals in the cement matrix. The experiment conducted by Dell'Orso et al. (2012) determines the relationship between pH and leachate concentration of zinc and lead for five leachate-to-solid ratios. The trend observed is that at low pH many metals are most mobile, as pH approaches neutral to slightly basic the mobility of metals decreases, and finally as pH becomes very basic mobility tends to slightly increase. This trend is also observed in the experiment conducted by Tabeline et al. (2014). This experiment used similar methodology to Dell'Orso et al. (2012); however, the porous medium leached was a sedimentary rock. The importance of this finding is that there is a high potential for low pH water to be present where there is mine waste. The sulfide oxidation process releases protons, causing mine waste water to often be acidic. If this low pH water enters the CPB pores, a high metal concentration in the leachate may result.

Redox conditions of the porewater become important when investigating multivalent metals. The redox state of the metal can govern its mobility. Mácsik and Jacobsson (1996) found iron to be a redox sensitive metal. Higher iron concentrations were found in leachate collected under aerobic conditions. When considering the redox conditions of the CPB, the groundwater table, and microbial activity should be considered.

Release of alkali and alkaline earth metals from the cement hydration process accumulate in the form of a soluble salt layer on the pore lining. The wash-off of these salts is seen as the first leaching step. Concentrations of sodium, calcium, magnesium, and potassium may be seen in leachate as the product of this wash off (Mácsik and Jacobsson 1996; Vollpracht and Brameshuber 2016).

Finally, a variety of binder compositions and mix ratios are used in CPB practice. The binder used influences the microstructural properties of the CPB (Wu et al. 2015). In laboratory experiments regarding cement stabilized sulphide soil, the use of ordinary Portland cement (OPC) without additives yielded the highest leachability. When OPC was combined with Slag the leachability decreased (Mácsik and Jacobsson 1996). This suggests that the use of additives such as slag and fly ash alters the microstructural properties of the CPB favourably when considering leachability. The use of additives may reduce the pore surface area, therefore reducing the contact surface between the CPB and the pore water (Mácsik and Jacobsson 1996). As discussed previously, a lower surface area will reduce the potential for ion transfer, thus reducing the leaching potential of the CPB.

2.5 Temperature Sources in Mine Backfilling

The curing temperature of CPB is highly variable and depends on several factors. The temperature of the backfill can be effected by the geographic location of the mine, geologic conditions and stope depth, the hydration and transport of the backfill, rock or backfill self-heating, and temperature variations produced by the mining operation (Fall et al. 2010).

2.5.1 Geographic Location

The geographic location of a mine is a control over the temperature that CPB is cured at. CPB's wide spread use across many different climates results in variable near surface conditions. When considering the leachability of CPB, near surface conditions are important, because near the surface is where CPB leachate could cause harmful effects to local groundwater systems. Although there is some seasonal variation, in northern Canada and other northern regions, the virgin rock temperature surrounding stopes can remain permanently below zero to depths of 1000 m (Fall et al. 2010; Udd 2006). While the average near surface temperature of a gold mine in South Africa increased from 15 to 32 °C between 0 m and 1500 m (Rawlins and Phillips 2001).

2.5.2 Local Geology and Stope Depth

The temperature of the rock adjacent to the stope is affected by the local geology and depth of the mine. Generally, temperature increases with depth because of geothermal gradients (Figure 2.7). In a deep gold mine in South Africa, the temperature of the rock corresponded to depth as follows; 35°C at 3 km, 50°C at 4 km and 70°C at 5 km (Rawlins and Phillips 2001). While studies by Martinson (1977), in South African Gold mines, found that the virgin rock temperature at a depth of 3.6 km ranged from 50°C to 70°C. Martinson also noted that the dry bulb temperature gradient in the mine was approximately 1°C per 100 m, increasing with depth. Geologic conditions govern the virgin rock temperature in deep mines. Since local geology plays an active role in mine temperature, temperature with depth can be variable for mines situated in different geologic settings (Fall et al. 2010).

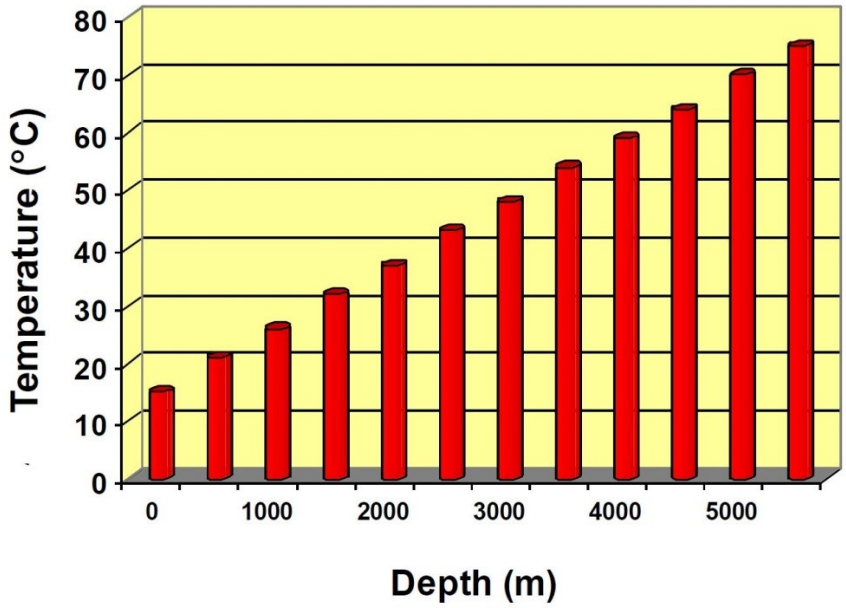

Figure 2.7. Data displaying the increase in temperature with depth due to the geothermal gradient (from Fall et al. 2014 with data from Rawlins and Phillips 2001).

2.5.3 Hydration and Transport of Backfill

The hardening of CPB is possible because of the hydration of a binder. Binder hydration produces heat as the result of an exothermic reaction. Significant heat generation through hydration does not easily dissipate thorough the cement structures due to their large size, and insulating capacity. This results in elevated temperatures

through the curing process of the CPB. Findings of temperatures of up to 47.2°C in field experiments directly measuring temperatures in hydrating CPB have been recorded. The primary source of heat in this case is the hydration reaction (Fall et al. 2010; Williams et al. 2001).

Transport of backfill from the production location to the stope can also contribute to the curing temperature of the fill. Backfill transport is conducted through pipelines that move the paste from the surface to the stope. Reasons for temperature increase during transport include; fluid compression with depth, friction loss, non-use of energy recovery systems, selection of fluid flow rate in converging pipes, and other fluid properties including thermal capacity (Fall et al. 2010; Rawlins and Phillips 2001).

2.5.4 Rock or Backfill Self-Heating

Under some circumstances, exothermic reactions between sulfide minerals, such as pyrrhotite, that may be present in the paste, or in the virgin rock adjacent to the stope with the paste can cause temperatures greater than 400°C. The self heating reactions involving sulfide minerals are rare, and therefore not well understood (Fall et al. 2010; Bernier and Li 2003).

2.5.5 Temperature Variation Produced by Mining Operations

There are many technologies and processes used in the mining operation that may cause temperature variation within the stope. One source of heat that may play a significant role in altering the curing temperature of CPB is artificial heating of CBP to increase the early strength of CPB structures. The magnitude of this induced temperature varies based on binder composition, however temperatures as high as 600°C have been experimentally tested (Orejarena and Fall 2008). Other sources of temperature variation include ventilation, blasting, fires, mine machinery, and lighting. As discussed previously the size and insulating capacity of the CPB structures result in these temperature sources having little effect on the curing temperature (Fall et al. 2010).

2.6 Possible Temperature Effects Associated with Leaching

As discussed previously, the micro-structural properties of CBP are controls over leachability. Curing temperature can have a pronounced effect on the micro-structure of the monolith, with a primary control being the continuity and surface area of pores. Within this temperature range, the hydrates that produce the pore lining vary (Fall and Samb 2009). The variability of the hydrates lining the pores may result in inconsistent leaching between samples that have a micro-structure that is near the same physically. Curing temperature influences the hydration reactions of cements and cement stabilized materials (Lothenbach et al. 2008). The formation of hydration products influences the immobilization capacity of cement stabilized materials (Stronach et al. 1977).

2.7 Standard Leaching Tests

There are several leaching tests that can be used to determine the leachability of cementitious materials. There are two general categories of leaching tests; dynamic leaching tests and static leaching tests. Dynamic leaching tests use a continuous leachant supply and are conducted as either flow-through or flow-around tests, with multiple extractions. Static leaching tests are a single extraction test (Washington State Department of Ecology 2003). Within each category there are many different tests that can be implemented. Sequential batch laboratory leaching tests (dynamic leaching tests) are developed to simulate leaching that would occur over tens or hundreds of years in a natural environment. These sequential batch tests tend to simulate the worst case leaching scenario (Mácsik and Jacobsson 1996). Some of these leaching tests will be discussed and a test that simulates the “worst case” leaching scenario of CPB will be chosen.

2.7.1 Single extraction/batch leaching tests (static leaching tests)

Single extraction tests are designed such that the leachant is not renewed throughout the duration of the protocol. The leaching fluid that becomes leachate through the test duration is removed as a single unit at the end of the leaching time. These tests are designed such that steady state equilibrium is achieved by the end of

the test to quantify the long-term leaching behavior of the material of interest (Washington State Department of Ecology 2003).

2.7.2 Sequential Batch Leaching Tests

Sequential batch leaching tests (SBLT) are designed such that a portion of leaching fluid is extracted at set increments throughout the testing period. This allows for the derivation of kinetic and constituent mobilization information (Washington State Department of Ecology 2003). This means contaminate release through time can be recorded.

2.7.3 Flow Around Tests

Flow around tests are suitable for materials that are bound as monoliths or stabilized waste. The material is suspended in allowing for leachant to flow around the sample and into pores. Leachate is renewed throughout the test duration like a sequential batch leaching test to determine kinetic information, species mobility, and cumulative fraction leached (Washington State Department of Ecology 2003).

2.7.4 Flow Through Leaching Test

Flow through leaching tests require a pressurized flow to force a leaching fluid through the pores of monolithic or compacted materials. The applied pressure required depends on the permeability of the material. The leachate that passes through the material is collected and can be analyzed at increments through the duration of the leaching period to determine both IFL and CFL.

2.7.4.1 Monolith Leaching Test using a Modified Triaxial Cell

This test is not an industry standard and has only previously been used in a few experiments to determine the leachability of cement stabilized waste. This flow through test has been developed by Butcher et al. (1993), specifically for leaching monolithic samples. This test used a triaxial cell that has been modified to create accelerated leaching conditions by use of pressurized flow to force a leachant through the pores of the monolith. This test simulates the leaching of a monolith more realistically than a flow

around test because in reality pore surfaces are the main contact area for interaction between the groundwater and the stabilized waste, so the actual leaching surface of the monolith is being exposed to accelerated leaching conditions (Butcher et al. 1993). Since there is no industry standard protocol or equipment for this test, it was ruled out for this experiment.

2.8 Leaching Protocol of Choice

Considerations must be made to determine the suitable test to be used for the leachability of a CPB sample. Past procedures will be compared and the test that appropriately suits the experiment will be chosen.

2.8.1 Protocol Considerations

Several considerations must be made when choosing a leaching test for a CPB sample. The primary consideration is that CPB is monolithic in the field. It is important to conduct leaching tests on a monolithic sample, therefore any leaching test that requires particle size reduction is not valid. If a crushed sample were to be used, the porosity and permeability of the sample for the given curing temperature would not be considered. It is also important that the test conducted is suitable for anaerobic conditions. CPB is common below the ground water table where oxygen is not available. Based on past experiments by (Aldhafeeri et al. 2016; Benzaazoua et al. 2004; Cui and Fall 2016), the properties of CPB evolve with quite rapid change between a curing time of 0 days and 120 days. Near 90-120 days, the CPB becomes relatively stable. These past experiments have recorded CPB properties at 14, 28, 56, 90, and 120 days, with some including 150 days. Based on these past experiments, CPB can be considered mature after curing for 90 days. The leaching test chosen should be conducted with a monolithic sample of mature CPB.

2.8.2 Past Tests Used for Determining Leachability of Cement Stabilized Materials

Past tests used to determine the leachability of cementitious monoliths have used multiple available leaching tests. Mácsik and Jacobsson (1996) used Sequential Leaching Tests to simulate the leaching of a LD-Slag/Portland Cement stabilized soil. In

this experiment, monolith was crushed to reduce particle size. This methodology would not yield comparable results when considering samples cured at different temperatures because the particle size distribution, and artificially created pore surface would create variability in the experiment for which there could be no account. The Sequential Batch Leachate Test does not require particle size reduction, is relatively inexpensive to perform and can be conducted in under both anaerobic and aerobic conditions (Washington State Department of Ecology 2003).

In a study performed by Yin et al. (2007), whole block leaching tests that have not been previously discussed were performed to determine the heavy metal leachability from an OPC stabilized scrap metal waste. This test protocol used 25.4 mm cubic monolithic samples suspended in 100 ml of either acetic acid (0.1 M) or de-ionized water. Leachates were collected at 1, 3, 7, 15, 31, and 63 days, then filtered and analyzed for metals. This experimental design was intended to simulate short-term leaching of a monolithic sample (Yin et al. 2007).

The NEN 7375 leaching test for monolithic samples was used by Kogbara and Al-Tabbaa (2013), when leaching a stabilized soil monolith bound with OPC. This test is like the block leaching test described above where the de-ionized water is used as a leachant and is replaced at 0.12, 1, 2.25, 4, 9, 16, 36, and 64 days. Metal analysis is performed on the extracted leachate (Kogbara and Al-Tabbaa 2013).

Flow through leaching tests using a modified triaxial cell have also been used to determine the diffusivity of heavy metals from cement stabilized waste (Poon et al. 2001). Poon et al. (2001) describes the leaching procedure used for their experiment as a flow through test. Flow through tests are suitable for monolithic cement stabilized samples that are surrounded by an impervious or less pervious material (Poon et al. 2001). In the case of CPB, a porous cement bound waste is surrounded by rock mass (an unfractured rock mass is considered in this study). Since this is a porous media surrounded by a material with lower permeability, the flow through leaching mechanism must be considered. Flow through tests have not been commonly used for monolithic samples since there is no industry standard. The methodology of the test used by Poon et al. (2001), and other researchers stems from the protocol discussed above by Butcher et al. (1993).

2.8.3 Chosen Leaching Protocol: ASTM C1308-08

ASTM C1308-08 is an ASTM standard test method that has been reapproved in 2017. The method is developed to determine leach rates from solidified matrix material (ASTM 2017). The protocol is designed such that long-term diffusive release can be estimated if the dominant leaching mechanism of a constituent of interest is mass diffusion. This information can be derived through the constituent concentrations found by analyzing leachate that is completely renewed at specified intervals through the protocol. From the complete renewal of leachate, the incremental fraction leached (IFL) and cumulative fraction leached (CFL) can be computed. The IFL refers to the mass leached at a given test interval. The CFL corresponds to the total mass leached over the duration the test.

ASTM C1308-08 was chosen because it is a standard leaching procedure designed to determine both IFL and CFL of monolithic cement stabilized materials. CPB is a cement stabilized waste therefore it is falls into the category of materials for which the ASTM C1308-08 was designed for. This protocol is developed to simulate long term leaching behavior over an 11-day leaching period, with 14 leachant renewals. The test required minimal equipment, reducing experimental cost.

The protocol allows for the calculation of IFL and CFL, however since this test was used as a comparative analysis, it was slightly modified to determine fractional and cumulative mass leached. This means that leaching interval analysis will consider mass leached as opposed to a fraction of the initial concentration present in the material. This was done to prevent uncertainty of the initial mass within each CPB, based on density changes as a result of curing conditions.

2.9 Canadian and EPA Drinking Water Standards

Drinking water standards devised by Health Canada and the United States Environmental Protection Agency, as well as groundwater guidelines produced by Government of Canada are highlighted in Table 2.1.

Table 2.1. Drinking water standards and ground water quality guidelines for inorganic contaminants in Canada and the United States (Health Canada 2012; FCSAP 2010; US EPA 2013).

	Canada			EPA	
	Drinking Water		Groundwater Guideline	Drinking Water	
Inorganic Constituents	MAC (mg/L)	AO or OG (mg/L)	Lowest Guidance (mg/L)	MCLG (mg/L)	MCL or TT (mg/L)
Aluminum	NA	<1.0	NA	NA	NA
Ammonia	NA	NA	NA	NA	NA
Antimony	0.006	NA	1.6	0.006	0.006
Arsenic	**0.01**	**NA**	**0.005**	**0**	**0.01**
Asbestos	NA	NA	NA	7 MFL	7 MFL
Barium	1	NA	0.5	2	2
Beryllium	NA	NA	0.0053	0.04	0.04
Boron	5	NA	0.5	NA	NA
Cadmium	0.005	NA	0.000017	0.005	0.005
Calcium	NA	NA	NA	NA	NA
Chloride	NA	≤ 250	100	NA	NA
Chromium	0.05	NA	0.0089	0.01	0.01
Copper	NA	≤ 1	Variable	1.3	1.3
Cyanide	0.2	NA	0.001	0.2	0.2
Fluoride	1.5	NA	0.12	4	4
Iron	NA	≤ 0.3	0.3	NA	NA
Lead	**0.01**	**NA**	**Variable**	**0**	**0.015**
Magnesium	NA	NA	NA	NA	NA
Manganese	NA	≤ 0.05	0.2	NA	NA
Mercury	0.001	NA	0.000016	0.002	0.002
Nitrilotriacetic acid	0.4	NA	NA	NA	NA
Nitrate	3	NA	13	10	10
Nitrite	NA	NA	NA	1	1
Selenium	0.05	NA	0.001	0.05	0.05
Silver	NA	NA	0.0001	NA	NA
Sodium	NA	≤ 200	NA	NA	NA
Sulfate	NA	≤ 500	100	NA	NA
Sulfide	NA	≤ 0.05	0.002	NA	NA
Thallium	NA	NA	NA	0.0005	0.002
Uranium	0.02	NA	0.01	0	0.03
Vanadium	NA	NA	0.1	NA	NA
Zinc	NA	≤ 5	0.01	NA	NA

2.10 Association of Arsenic and Lead with Gold Mine Tailings

Arsenosulfides are commonly found in association with sulfide-bearing mineral deposits. These deposits include arsenopyrite (FeAsS), orpiment (As_2S_3), and realgar (AsS/As_4S_4). Formation of sulfide bearing ore arises principally in hydrothermal and magmatic veins where gold mineralization commonly. Additionally, other sulfide-bearing minerals such as galena (PbS), a lead bearing sulfide, are also commonly associated with hydrothermal and magmatic gold bearing deposits occurs (Flora 2015; Kretschmar and McBride 2016; Zhu et al. 2011). Non-sulfide minerals containing arsenic, such as loellingite ($FeAs_2$), are also regularly found in gold ore deposits (Hamberg et al. 2017). Extraction of gold from arsenic bearing ore can result in the production of arsenic trioxide. A documented example substantial As_2O_3 production through gold extraction comes from the Giant Mine in the North West Territories where 237 000 tonnes of arsenic trioxide waste was produced over the life of the mine (Government of Canada, 2018).

2.11 Cement and Hydrating Cement Systems

Cement or binder is an important part of CPB, since when mixed with water hydration occurs resulting in the cementation of the material. In CPB hydration results in strength gain as bonding occurs between tailings particles. Binders used in CPB are commonly composed of OPC and admixtures of other pozzolanic materials (Ghirian 2016).

2.11.1 Portland Cement Hydration

Anhydrous Portland cement clinkers commonly contain the following constituents; silicates: tricalcium silicate or alite (C_3S, 50 – 70 wt%) and dicalcium silicate or belite (20 – 30 wt%), and aluminates: tricalcium aluminate (C_3A 5 – 12 wt%) and tetracalcium alumina ferrite (5 – 12 wt%) (Cocke 1990; Ghirian 2016). These compounds hydrate to form three main types of hydration products; calcium silicate hydrate (C-S-H), calcium hydroxide ($Ca(OH)_2$ or CH), and ettringite ($3CaO{\cdot}Al_2O_3{\cdot}3CaSO_4{\cdot}31H_2O$) calcium sulphoaluminate (Ghirian 2016). A schematic of the hydration process of Portland cements is displayed in Figure 2.8.

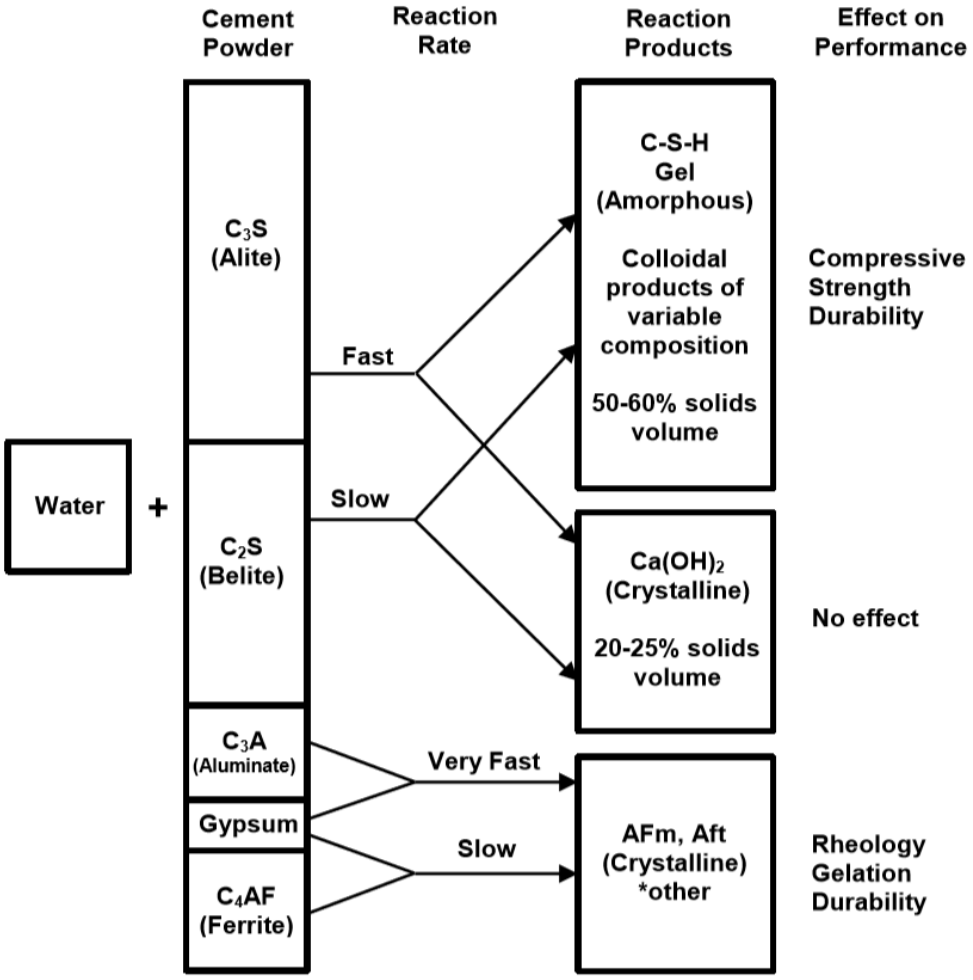

Figure 2.8. Hydration process of Portland cements where box size represents constituent/product volume (from Ghirian 2016, adapted from Double 1983)

2.11.2 Sequential Hydration Process

The reactions between the liquid phase and the clinkers (solid constituents that make up the cement powder) are exothermic chemical processes. The exothermic reactions occur in five distinct stages in the following order: initial, induction, acceleration (or settling), deceleration (or hardening) and densification, seen in Figure 2.9 (Bullard et al. 2011). This multi-step process is described in studies by (Neville, 1995; Swaddiwudhipong et al., 2002; Soroka, 2003; Bullard et al., 2011; Winter, 2012) are summarized below:

(1) Initial reaction: Upon addition of mixing water during the mixing period to about 30 minutes aluminates and gypsum undergo rapid dissolution releasing heat, Na, K, Ca, OH, and SO_4 into the pore solution.

(2) Induction: Calcium silicates react resulting in the initial formation of C-S-H gel. This occurs between 30 minutes and 3 hours. The porewater solution becomes supersaturated with Ca and OH. Ettringite forms as a product of reactions between gypsum and C_3A. The formation of these hydration products results in the retardation of hydration rate. Heat generation ceases, and the paste is plastic.

(3) Acceleration: Heat is generated in significant quantities as a result of C_3A and gypsum reactions initially and then C_3A and ettringite sequentially later. C-S-H and CH form resulting in refined pore space and increased strength. This takes place between 3 and 17 hours.

(4) Deceleration: undissolved clinkers are isolated by the continued formation of C-S-H and CH resulting in a slowed hydration rate. The porosity continues to decrease. This stage occurs between 17 and 48 hours.

(5) Densification: this occurs from the end of the deceleration stage to up to several years of curing. Remaining C_3S and C_2S dissolve at very slow rates by means of diffusion. This dissolution contributes to the formation of a solid C-S-H and CH mass, leading to low porosity, low hydraulic conductivity, and high strength.

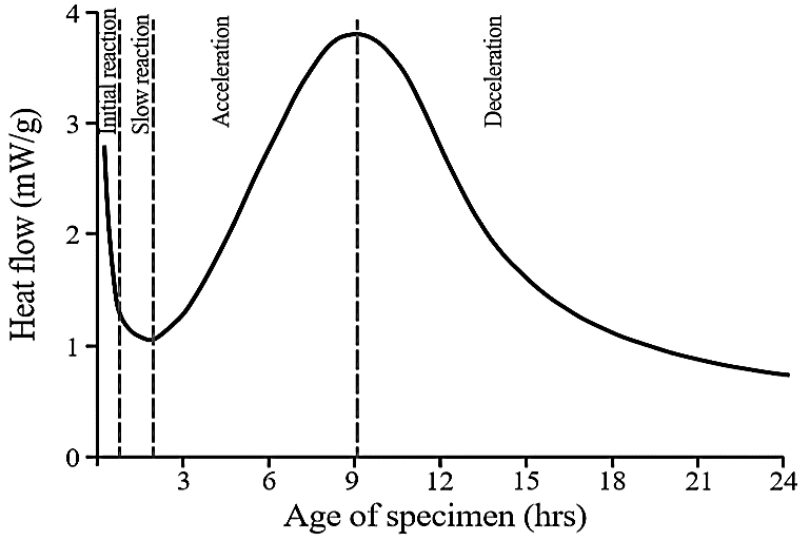

Figure 2.9. Rate of hydration with curing time (Bullard et al. 2011).

2.11.3 Factors That Affect Cement Hydration

The dominant factors that influence hydration include curing pressure, curing temperature, water to cement (w/c) ratio, and cement fineness (Lin and Meyer 2009).

Increased curing pressure can result in a high curing rate displayed in Figure 2.10 (a). The increase in hydration with pressure is explained by an increase in contact between hydration water and cement grains (Zhou and Beaudoin 2003). Increased curing pressure may also result in densification of the cement matrix, resulting in increased compressive strength (Roy et al. 1972).

As shown in Figure 2.10 (b), curing temperature has a substantial influence on hydration rate. Increased curing temperatures may result in more rapid hydration, producing increased early compressive strength and density. Consequently, high curing temperatures can result in decreased long term performance, because at advanced ages, porosity may be higher, and microstructure less uniform. These characteristics can be attributed to a decrease in mechanical strength (Kjellsen et al. 1990; Maltais and Marchand, 1997; Elkhadiri et al. 2009).

The rate of hydration may increase with a decrease in w/c ratio, as described in Figure 2.10 (c). Reduced w/c ratio can also lead to increased mechanical strength, decreased porosity and decreased hydraulic conductivity (Goto and Roy 1981, Bentz et al. 2009).

As a given mass of particles becomes finer the surface area increases. Increase surface area may allow for increased water contact with cement grains, creating a higher rate of hydration. Fineness of particles also influences the thickness of hydration products. Finer particles result in less thickness meaning setting time may be reduced, hardening process accelerated, and mechanical strength increased (Ginebra et al. 2004; Bentz et al. 2008; Lin and Meyer 2009).

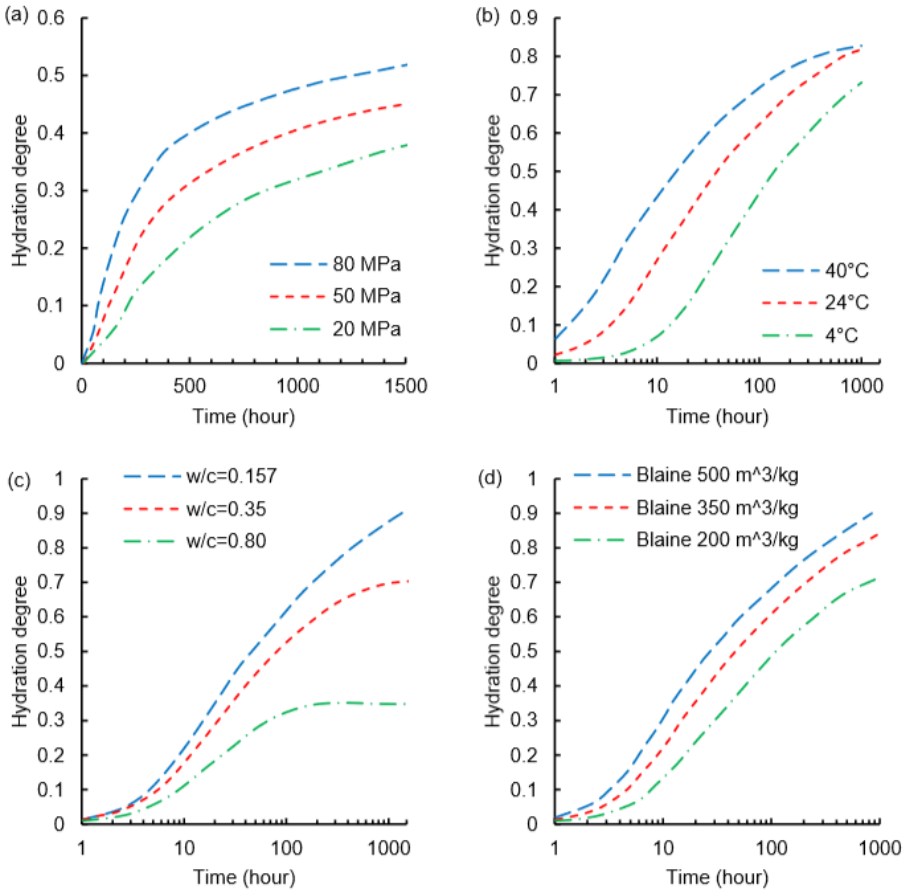

Figure 2.10. Cement hydration evolution under different conditions (a) curing stress, (b) curing temperature, (c) w/c ratio, and (d) cement fineness (from Lin and Meyer 2009).

2.11.4 Influence of Blast Furnace Slag

The four primary components of BFS are oxides: lime (CaO) 35-38 wt%, silica (SiO_2) 33-35 wt%, alumina (Al_2O_3) 17-20 wt%, and magnesia (MgO) 6-8 wt% (Liu et al. 2017; Prasad et al. 2018). Other components that may be present in minor amounts include (SO_3, FeO or Fe_2O_3, TiO_2, K_2O, Na_2O, etc.). Minor components may vary depending on the blast furnace however, the four major oxides remain relatively constant (Taylor 1997).

The latent hydraulic property of slag is an important consideration when supplementing the OPC binder. Slag will react with water, but the reaction rate is notably slow, unless an activator is involved. Common slag activators include Portland cement, sulfates, sodium silicate, and calcium hydroxide. These activators may be referred to as alkali activators due to their alkali metal content (Narang and Chopra

1983; Chen 2007). Activation of slag by Portland cement (activation utilized in this study) is a sequential process. First small amounts of BFS react with available calcium sulfides. Slag hydration then increases initially by activation due to alkalis and finally by CH produced in the Portland cement hydration reaction (Chen 2007). The reaction stoichiometry regarding the consumption of CH in slag hydration is outlined by Richardson et al. (2002):

$$C_{7.88}S_{7.39}M_3A + 2.6CH + bH \rightarrow 7.39C_{1.42}SH_mA_{0.046} + 0.66M_{4.6}AH_d$$

where:

$C_{7.88}S_{7.39}M_3A$ = empirical formula for BFS

$7.39C_{1.42}SH_mA_{0.046}$ = C-S-H

$0.66M_{4.6}AH_d$ = hydrocalcite

7.39m + 0.66d = b: dependent on slag to CH ratio and temperature

OPC-Slag cements result in different characteristics compared to an unblended OPC binder. Notable considerations when supplementing slag into the binder include: increased formation of hydration products (specifically at higher curing temperatures), increased 28-day and 90-day UCS, and increased susceptibility to sulfate attack in sulfide rich mixtures (Fall et al. 2014).

Chapter 3 – Theory and Objectives

3.1 Mine Flooding and Groundwater Flow Theory

During underground mining operations groundwater is pumped from the mine cavities via a sump station. Pumping is conducted to keep active mining areas dry by removing groundwater from the voids. Upon mine closure the sump is decommissioned, resulting in groundwater rebound (Alvarez et al. 2018). Groundwater rebound is the phenomena of groundwater rise and movement through interconnected pore spaces to achieve hydrodynamic equilibrium. Pumping depresses the groundwater surrounding the pumps area of influence. The equilibrium conditions of the system after backfilling and mine closure will be altered from the natural steady state conditions that existed prior to excavation of parent rock. Groundwater flow is governed by difference in hydraulic head. This is described by Darcy's Law, which defines groundwater flow through porous media (Fetter 2013). Darcy's Law in general terms:

$$Q = -KA(\frac{dh}{dl})$$

Q represents discharge, while K represents hydraulic conductivity, A represents the cross-sectional area of flow, and dh/dl represents the hydraulic gradient. Hydraulic gradient describes the change in hydraulic head (energy density) over a given distance. Thus, the hydraulic conductivity of porous media can be expressed as (Fetter 2013):

$$K = -\frac{Q}{A\left(\frac{dh}{dl}\right)}$$

Hydraulic conductivity is expressed in units of length per time and is the coefficient in Darcy's Law that relates to the nature of the porous medium (Fetter 2013). The rate of ground water rebound relates to the saturated hydraulic conductivity of the CPB. Assuming the (intrinsic) permeability of the CPB is greater than that of the parent rock, water will first move through the CPB to achieve hydrodynamic equilibrium. The hydraulic conductivity is directly related to permeability through the equation (Fetter 2013):

$$K = K_i\left(\frac{\gamma}{\mu}\right)$$

K_i represents permeability while μ and γ represent the dynamic viscosity and specific weight of the pore water solution, respectively. This means that hydraulic conductivity is a function of the porous medium, which in this case is CPB, and the pore solution (Fetter 2013). K_i is a material parameter of the porous medium, while γ and μ are properties of the pore water solution. The relationship between pore fluid and intrinsic permeability is important when considering the expected hydraulic conductivity of the CPB. The degree of saturation of the CPB must be considered because hydraulic conductivity is governed by the degree of saturation (1 fluid vs 2 fluid system). Air acts as a non-wetting fluid, retarding the hydraulic conductivity (unsaturated hydraulic conductivity). Based on cement chemistry and past research, CPB filled stopes can be assumed to remain highly saturated (near 100%) through hydration (Benzaazoua 2004). Therefore, saturated flow conditions may be assumed. Figure 3.1 displays how groundwater is expected to move through underground CPB structures.

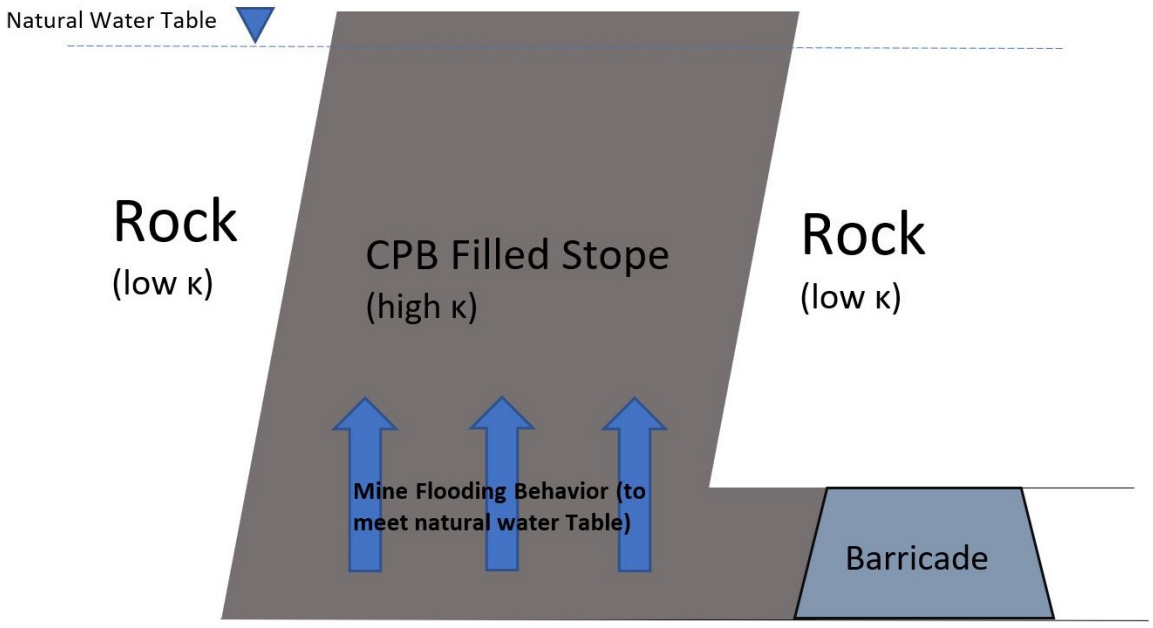

Figure 3.1. A simplified schematic of how groundwater is expected to move through a backfilled underground mine. Complex geology increases the complexity of flow. This schematic represents expected flow when parent rock is unfractured, and CPB is saturated (k: permeability).

3.2 Research Objectives

The primary objective of this research is to characterize the temperature dependence of the leachability of arsenic and lead from CPB, generated from gold mine tailings. This research assumes that the CPB remains saturated through hydration and acts as the primary conduit for ground water rebound upon mine closure. The objective of study can be met by assessing the individual and interrelated effects of curing temperature and binder composition on various CPB properties.

3.2.1 Influence of Hydraulic Binder on Leachability

As discussed previously, multiple hydraulic binders can be used as the binding agent for CPB, with OPC being the most common. In this experiment samples were cured under the same conditions with two binder compositions; OPC, and OPC/Slag mixed at a 50% blending ratio. The objective of this portion of study was to determine if the binder composition influences the leaching behavior of CPB specimens cured in the temperature range of 2°C to 35°C.

3.2.2 Influence of Hydraulic Binder on Microstructure

Microstructure analysis of each sample was conducted with the objective of understanding the relationship between microstructure and leachability. The microstructure of the CPB can be broken into subcategories of physical and mineralogical structure. The hydraulic binder may influence both the physical and mineralogical structure of the backfill.

3.2.3 Influence of Microstructure of Leachability

The microstructure of cemented specimens refers to both the mineralogical configuration and pore distribution of the structure. Both porosity and minerology can be expected to influence the pore water characteristics, including flow rate and chemistry. Microstructural characteristics such as the porosity and minerology can be related to the curing temperature and binder composition of each specimen. From this information the effect of microstructure on leachability was determined.

Chapter 4 – Experimental Program and Design

In this experiment, natural gold tailings were formed into CPB samples using two different binders, cured at three different temperatures. The samples were leached using the ASTM C1308-08 leaching protocol. The effluent water was collected and analyzed for arsenic, lead, and other major ions. Leached and unleached CBP samples were analyzed using SEM. PXRD and MIP were used for mineral phase characterization and pore structure analysis of unleached CPB samples.

4.1 Materials

The CPB specimens used for analysis were prepared using natural gold mine tailings from northern Quebec. The tailings were doped with arsenic and lead using As_2O_3 and PbS, respectively. Binders used for hydration were OPC and BFS. Tap water was used as mixing water.

4.2.1 Tailings

The mineral composition of tailings is highly variable and dependent on the parent material (bedrock) that the tailings are produced from, as well as the extraction method used to separate the valuable minerals from the valueless waste (Fall et al. 2010). Natural tailings sourced from a hard rock gold mine were used for this procedure. The natural tailings used were sourced from a CPB plant at a gold mine in northern Quebec. The tailings were homogenized using a double spiral mixer prior to sample preparation to achieve uniformity between samples.

Tailings were analyzed using both ICP-MS and PXRD to determine both their chemical and mineralogical composition. Understanding the makeup of the natural tailings was critical to ensure sufficient quantities of arsenic and lead existed in the tailings for detectability in the leachate. The concentrations of both arsenic and lead found were not expected to be enough for detection from leaching tests. This background information allowed for samples to be doped with arsenic and lead in the form of As_2O_3 and PbS, based on stochiometric conversion.

Analysis of metals was conducted using ICP-MS, and results are tabulated in Table 4.1. Tailings were digested by acidification by the Geochemistry Laboratory at the University of Ottawa. Dominate metals include aluminum, calcium and iron. Four replicate analysis were conducted, and the average value was considered. The primary importance of this test was to understand the availability of arsenic and lead. Physical properties of these tailings are outlined in Table 4.2.

Table 4.1. ICP analysis of natural gold tailings sourced from Northwestern Quebec

Element	Average Concentration (ppm)
Al	4265
Ca	6117
Cr	149
Cu	520
Fe	39374
K	936
Mg	866
Mn	203
Na	605
Ni	8.2
Zn	1399
As	**59.3**
Pb	**110.1**

Table 4.2. Physical properties of the tailings used.

Material	**Physical properties**				
	G_s	D_{10} (μm)	D_{30} (μm)	D_{50} (μm)	D_{60} (μm)
Natural tailings	3.1	3.2	15.8	35.5	49.5

G_s: specific gravity

The mineral composition of the tailings used is primarily composed of albite, quartz, and chlorite when broken down by weight percent. A complete breakdown of the major minerals is seen in Table 4.3.

Table 4.3. Mineralogical composition of the tailings used.

	Mineral												
	Quartz	Albite	Dolomite	Calcite	Chlorite	Magnetite	Pyrite	Talc	Pyrrhotite	Pyrrhotite	Spinel	Others	Total
wt%	15	32.8	15	4.2	16.1	2.4	1	7	1.8	0.3	1.8	2.6	100

The gradation of the tailings used was distributed primarily between sand and silt sized particles within the range of 10 – 100 µm as described in Figure 4.1.

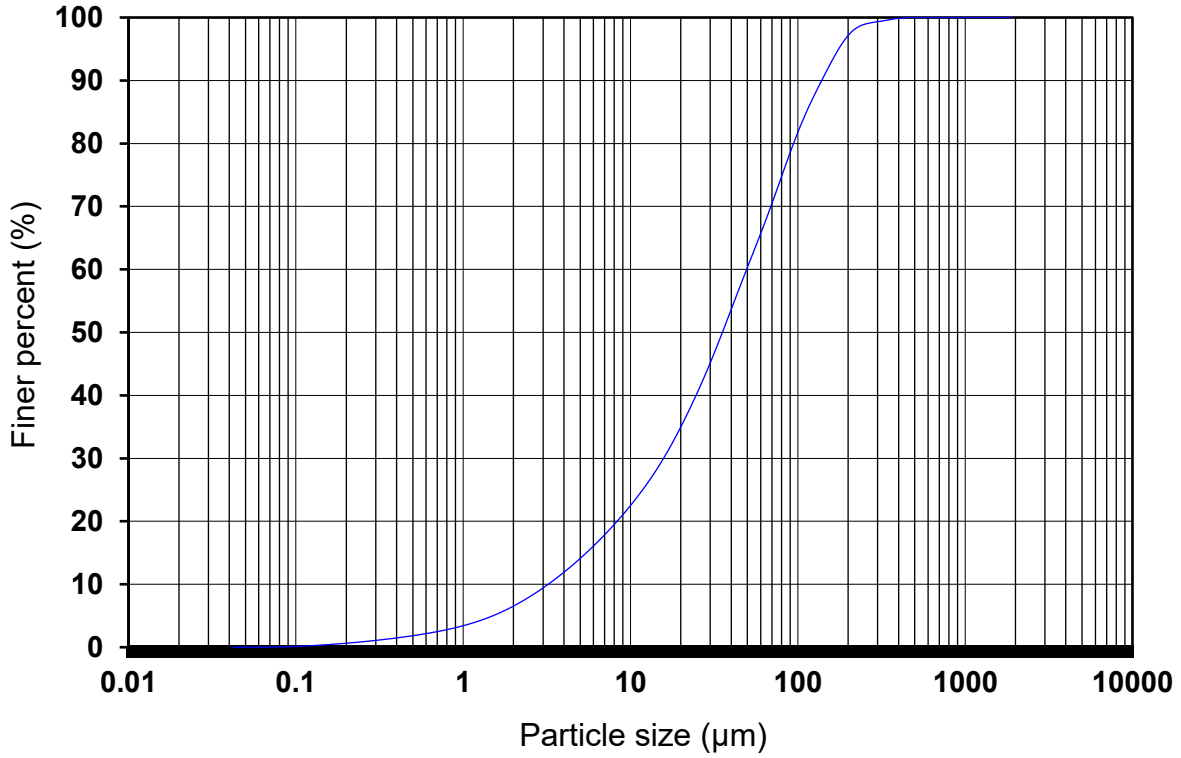

Figure 4.1. Grain size distribution of the tailings used (laser diffraction was used to determine the particle size).

4.2.2 Water

Tap water was used to mix binders with the tailings for hydration.

4.2.3 Binders

Two binder compositions were used for this experiment. One series of samples was prepared using OPC as a binder. The second set of samples was prepared using a mixture of OPC and BFS at a blending ratio of 50%. In cemented paste backfilling operations, OPC is the most common binder used. The use of OPC as a binder can account for up to 75% of the total cost of the CPB (Grice 1998). To reduce the cost of CPB operations, additives such as blast furnace slag and fly ash are implemented as a portion of the hydraulic binder (Tariq and Yanful 2013). With an increasing number of operations moving towards the use of additives to OPC as a hydraulic binder, it is important to understand the temperature effects on the leachability of different binder compositions. Experiments by Mácsik and Jacobsson (1996) found that release of constituents from monoliths bound using OPC, as well as OPC/LD slag mixes were not consistent. Therefore, a comparison was made between the leachability of samples cured with OPC, and an OPC/BFS mix at a blending ratio of 50% to determine the importance of the binder with respect to temperature dependent leaching.

4.2.4 Constituents of Potential Concern

Arsenic and lead were analyzed based on the nature of gold mine tailings, and the potentially hazardous effects of these two constituents. Arsenic (As) and lead (Pb) have been found to be associated with ore bodies containing gold. As and Pb are found in sulfides, such as arsenopyrite (FeAsS) and galena (PbS) that are common in gold bearing ore deposits (Kagambega et al. 2014). Arsenic trioxide is also by-product of gold extraction (Government of Canada 2018). This As(III) form is regarded to be the more toxic than other arsenic forms such as As(V) (Conner 1990). Arsenic and Lead pose environmental concerns based on their toxicologic properties at low concentrations. In Canada the guideline for arsenic in groundwater is 0.005 mg/L, and the guideline for lead is variable (FCSAP 2010). In drinking water the maximum allowable concentrations of both arsenic and lead are 0.01 mg/L (Health Canada 2012). Concentrations of As and Pb have been found at concentrations as high as 312000 ppm and 510 ppm respectively (Drage 2015; Fashola et al. 2016).

Laboratory analysis of the gold mine tailings acquired for this experiment resulted in low concentrations of both arsenic and lead. Average concentrations from four replicates were 59.3 ppm and 110.1 ppm of the solid portion, respectively. The maximum observed field value for arsenic in gold mine tailings is 312000 ppm (Drage 2015) and lead is 510 ppm (Fashola et al. 2016). Lead and arsenic are commonly found in gold mine tailings in the form of sulfide minerals galena and arsenopyrite (Kagambega et al. 2014). Supplementation of arsenic and lead to the tailings was done using arsenic trioxide and galena. Arsenopyrite was not available at a justifiable cost for use in the quantity required for this experiment. As_2O_3 was selected as a supplemental arsenic source for several reasons. The first reason being the low cost compared to other arsenic sources. This choice was also justified by the conclusion that As(III) is often found in tailings produced through gold, cobalt, and lead extraction. Furthermore As(III) more known to be toxic than As(V), and As_2O_3 is more soluble than other natural arsenic compounds (Conner 1990; National Academy of Sciences 1977). Arsenic was supplemented to achieve a solids concentration of 50000 ppm, while the lead was supplemented to achieve a concentration of 500 ppm.

4.3 Mixing Ratios and Sample Preparation

The paste backfill used was composed of tailings, supplemental constituents of potential concern, hydraulic binders, and water. Prior to mixing the residual water content of the tailings was determined by drying 20 g of the tailings in an oven at 40°C for four days. The high content of sulfidic materials in the tailings makes drying at a temperature greater than 40°C potentially dangerous due to the risk of fire and release of noxious gas. The tailings were weighed after drying and the change in mass corresponds to the wt% of water that is residual in the tailings. This residual water content was considered when determining the additional water needed to achieve the desired water to cement ratio. The tailings, constituents of potential concern, hydraulic binder, and water were homogenized in a double spiral mixer on level 6, for 7 minutes. This mixing protocol follows the protocol used by Fall and Samb (2009). The water-to-cement ratio (w/c) used was 6. The w/c ratio of 6 was chosen based on the consistency

of the mix in preliminary mix tests. The CBP samples were prepared using a constant binder proportion of 4.5 wt%.

As and Pb were added to the tailings slurry to ensure quantities high enough for detection in produced leachate, but still within the concentration range found in the field. The concentrations used are 50000 ppm As, and 500 ppm Pb. These concentrations correspond to 5% and 0.05% solids, respectively. Arsenic was supplemented as arsenic(iii) oxide (As_2O_3) and lead was supplemented as galena (PbS).

Samples were prepared using cylindrical molds with a 5 cm diameter and 10 cm height. Homogenized samples were poured into curing moulds, deaired by vibration, sealed, and placed into temperature-controlled chambers for 90 days.

4.4 Curing Temperature

Samples were cured in temperature-controlled chambers to simulate thermal conditions to which CPB structures can be subjected at mine sites. Three curing temperatures were adopted. Samples were cured at 2°C, 20°C, and 35°C. This temperature range was designed to simulate temperature variations in curing CPB structures based on self-heating through exothermic reactions during the hydration process, as well as temperature variation based on geographic location.

4.5 Curing Time

The goal of this experiment was to determine the leachability of mature CPB structures. For CBP samples to be considered mature they must cure for a period of (at least) 90 days prior to leaching. Past experiments conducted by (Benzaazoua et al. 2004; Aldhafeeri et al. 2016; Cui and Fall 2016) support that after 90 days the CPB structure shows negligible change. All CPB specimens studied in this experiment were cured for a 90-day period.

4.6 Leaching Test

ASTM C1308-08 was the leaching test chosen for this study because it is a standard test method designed to simulate accelerated leaching of monolithic materials.

A more detailed description of this leaching test is supplied in Appendix A. A standard test method was desired to ensure the leaching procedure consistency between samples. Samples were cut to 5.0 cm height by removing 2.5 cm from each end of the cylinder. The surface area and volume of the samples used in the ASTM C1308-08 test were 117.8 cm^2 and 98.2 cm^3, respectively. In this test the samples are suspended from the top of a container using monofilament for a duration of 11 days. The leachate was exchanged at 2, 5, 17, and 24 hours, then daily for the remainder of the protocol. This resulted in 14 leachate collections per sample. Each leachate collection was analyzed independently such that both incremental and total mass leached could be determined.

4.6.1 Leachant

The leachant used in the ASTM C1308-08 test was distilled water. Distilled water was chosen to reduce uncertainty in leachate analysis. The absence of ions in distilled water reduces the opportunity for error in analysis. 900 ml of leachant was used for each leaching interval, this resulted in a surface area to leachant volume ratio of 0.13 cm^{-1}.

4.6.2 Contaminate Analysis

The concentrations of the constituents of potential concern (As & Pb) were determined using ICP at the University of Ottawa Geochemistry Laboratory. Information from the ICP results provide the concentration of constituent for each leaching interval for the ASTM C1308-08 test. Results are displayed in the terms of mass of constituent leached at each extraction interval.

4.7 Microstructural Analysis

The microstructure of the monolithic samples was analyzed using SEM, PXRD, and MIP. The differences in the microstructure give insight to the processes that govern the leaching of CPB structures cured at different temperatures. MIP was used to determine the total porosity of the samples, as well as the pore size distribution. SEM allowed for the visual analysis of the pore structure before and after leaching, allowing for the change in the pores of each sample due to leaching to be observed.

Understanding the change in pore structure with respect to leaching will help to determine why contaminants leach differently at different curing temperatures. PXRD was used for phase characterization of each specimen. Understanding the presence of crystalline phases developed at different curing temperatures will help to understand why CPB structures may leach differently based on their curing temperature.

4.7.1 Mercury Intrusion Porosimetry

Mercury intrusion porosimetry (MIP) is an effective technique used to determine the total porosity and pore size distribution of geomaterials. The sample of interest is placed in a glass bulb connected to a finite tube containing mercury. Mercury is injected into the sample in a series of incrementally increased pressure steps. Results are then expressed as either total mercury volume intruded in the sample, or by incremental volume intruded at each pressure step (Ouellet et al. 2007). Winslow and Diamond (1970) describe the pore diameter that corresponds to the highest rate of mercury intrusion into the sample as the “threshold diameter”. This diameter is commonly understood to be the smallest diameter of pores with geometric continuity throughout the sample. In other words, the largest pore diameter at which appreciable amounts of intrusion occur. Above the threshold diameter only large capillary pores are intruded (Aligizaki 2006).

Samples from each curing temperature and binder condition were sent to Porous Materials Inc. laboratory for MIP analysis. Prior to submission samples were reduced in size to a diameter of approximately 3 cm and dried for 4 days at 45°C. MIP was used to characterize the pore size distribution and pore volume of each CPB sample. MIP tests were conducted on the samples by using a PMI Mercury/Nonmercury Porosimeter. Pressure was increased from 0 to approximately 30000 PSIA over 110 increments. Results were given in terms of total intrusion volume, total surface area, median and average pore diameter (based on surface area and volume), and logarithmic differential intrusion.

Critical pore diameter (d_c) is given as the maximum value of the logarithmic differential pore volume curve which is equivalent to the steepest slope on the cumulative intrusion curve. The critical pore diameter is generally assumed to be the

most frequently occurring pore diameter occurring in continuous pores (Aligizaki 2006). The threshold pore (d_{th}) diameter was interpreted by approximating the inflection point on the cumulative intrusion curve using judgment from Aligizaki (2006).

4.7.2 Scanning Electron Microscopy

Scanning Electron Microscopy (SEM) is an effective technique for characterizing microstructural properties of porous materials. SEM has been used by many researchers in the fields of CPB and cement stabilized materials (e.g., Aldhafeeri and Fall 2016; Benzaazoua et al. 2006; Cocke et al. 1991; Fall and Samb 2009; Ouellet 2005). SEM is commonly combined with energy dispersive spectrometry (EDS) to provide characterization of hydrated phases (Benzaazoua et al. 2006)

Scanning electron microscopy was conducted by the Materials Laboratory at the University of Ottawa to characterize the surface topography of each sample. Samples were reduced in size to approximately 1.5 cm in diameter, and to a thickness of approximately 3 mm. Sized samples were dried in an oven at 40°C for 4 days. After drying it was determined that sample faces could not be polished due to their delicate nature. Samples were analyzed raw which allowed for SEM to be conducted however, the ability to perform reproducible EDS results was compromised, due to scatter disturbance from the unaltered porous face of the specimen.

SEM images were used for visual comparative analysis between samples. Observations were justified by comparing to MIP, PXRD, and past literature. The images with the most suitable comparative properties were taken at 500X magnification using Zeiss instruments.

4.7.3 Powder X-Ray Diffraction

Powder X-Ray diffraction (PXRD) is mineral phase characterization technique commonly used by researchers in the field of CPB and other cement stabilized materials (e.g., Fall et al. 2010; Wu et al. 2015; Pokharel and Fall 2013). In this process powdered samples are placed on slides and subjected to beams of Cu Kα radiation through a range of contact angles. Crystals diffract the beams in unique diffraction patterns based on their planes. The intensity of diffraction at through a specified range

is given and can be plotted in the form of a diffractogram. The diffractogram is then used in software assisted phase characterization.

PXRD conducted by the University of Ottawa X-Ray Core Laboratory was used to characterize the mineralogical makeup of the CPB structures prior to leaching. The goal was to determine if different curing temperatures and binder compositions result in formation of phases that are resistant to leaching. Samples were cut to approximately 4 cm^3 and dried for 4-days at 40°C. After drying the samples were ground to a powder using a mortar and pestle.

Samples were analyzed using Rigaku software. Software assisted results were compared to previous CPB PXRD results from Pokharel (2008) for validation of software assisted uncertainties.

4.8 Rate of Mass Removal

The 11-day leaching protocol had 14 prescribed leachant renewals. At the time of renewal, the entire leachant volume was exchanged and the leachant from the previous time interval was collected as leachate. The arsenic concentration was determined at each exchange. The rate of mass removal for each submerged duration was then calculated using the formula:

$$Rd_i = \frac{m_i}{t_i}$$

where:

Rd_i = Mass removal rate per incremental leaching step (assumed diffusion based)

m_i = Mass removed per leaching step, (mg)

t_i = Submerged duration per leaching step, (hours)

The mass removal rate was then plotted using Method A (first order assumption) and Method B (modified from Kundu and Gupta 2007). Method A plots log(R_d) as ordinates and log(t) as abscissa, both using arithmetic scale. A linear fit is used to validate the assumption that leaching is governed by first order kinetics (diffusion based). A strong linear fit indicates that diffusion is the dominate leaching mechanism based on the first order assumption. Method B employs a similar method where

cumulative mass leached is plotted as ordinates and square root of leaching time is plotted as abscissa, both on the arithmetic scale. Again, a strong linear fit validates the assumption that leaching is diffusion based.

The Method A (Log, Log) graphs can be interpreted as follows. The intercept is representative of the initial leach rate (initial available quantity). In other words, a higher intercept suggests the presence of soluble salts on the pore surface. These pore linings leach readily resulting in a high initial leach rate. The slope is representative of rate change in diffusion as a function of time. Thus, a steeper negative slope represents a more rapid decrease in constituent available to leach. Since all specimens contain the same initial constituent concentration, slower diffusion (flatter negative slope) means higher quantity of constituent remaining to be leached at a given time. However, in this case diffusion occurs more slowly, and depending on the remaining phase(s) diffusion may become negligible.

Chapter 5 – Results and Discussions

5.1 Initial Observations

The measured arsenic concentrations in the leachates of the CPB samples with different binder types and cured at different temperatures are shown in Figure 5.1. The results clearly display that leaching of arsenic from CPB is temperature dependent. Moreover, the temperature dependent leaching behavior of the CPB differed based on the cement binder composition. The significant change in leachate concentration between each leaching interval for the initial 2-days of leaching is due to the leachate exchanges at variable submerged durations over this period of the protocol.

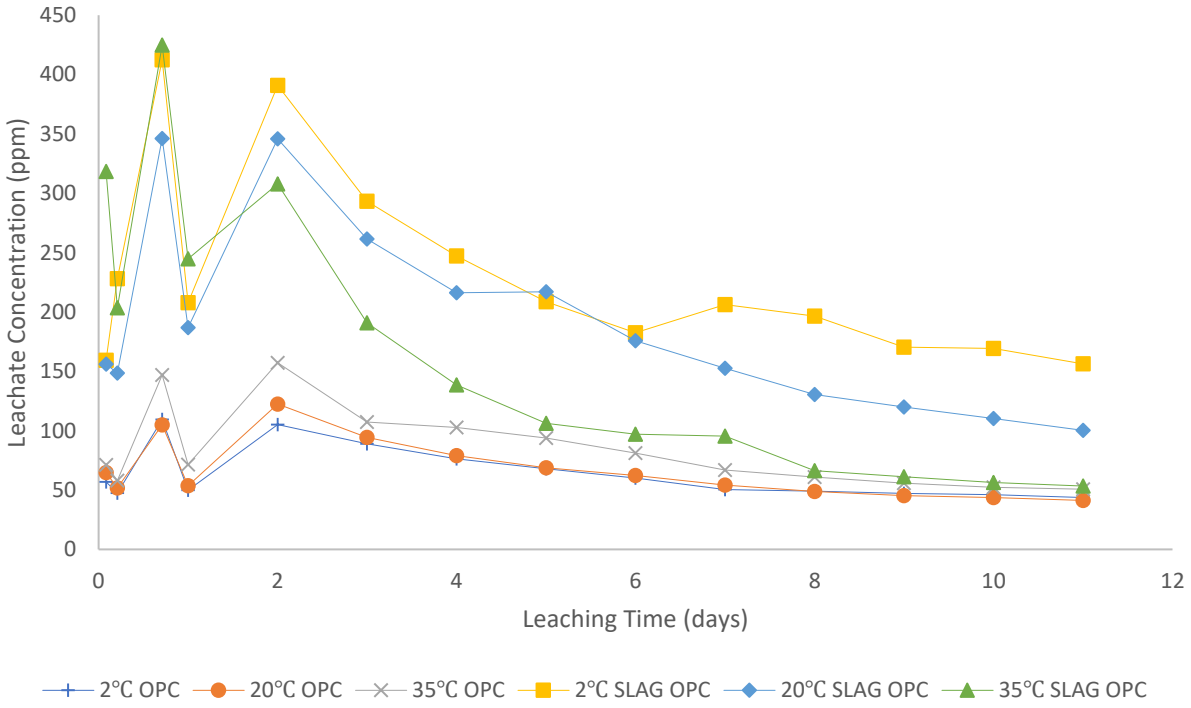

Figure 5.1. Arsenic concentrations from all test specimens observed through ICP analysis at leachate collection intervals.

These results clearly show that between the two binders tested (OPC and OPC/Slag), OPC performed better at all curing temperatures compared to the blended binder. This suggests that binder composition plays a strong role in the leachability of contaminates from mature CPB. This observation is further demonstrated when comparing the cumulative mass leached from each specimen in Figure 5.2. This figure

shows that a considerably greater amount of mass was leached from the CPBs cured with an OPC/Slag binder, while temperature also played a role in the mass leached between specimens cured using the same binder composition.

(a)

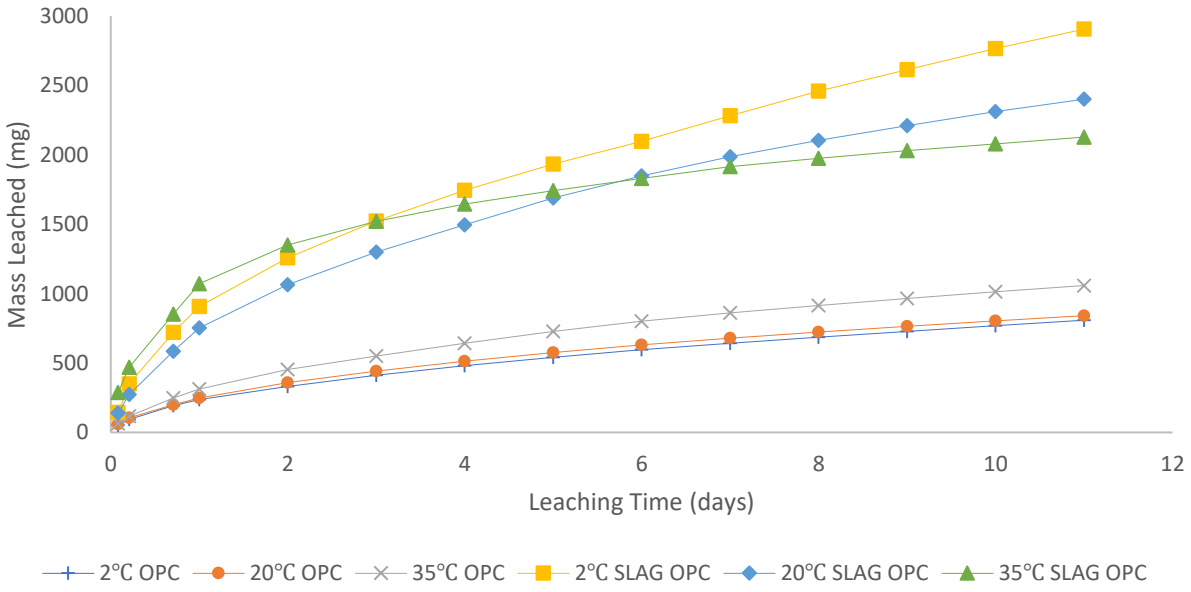

(b)

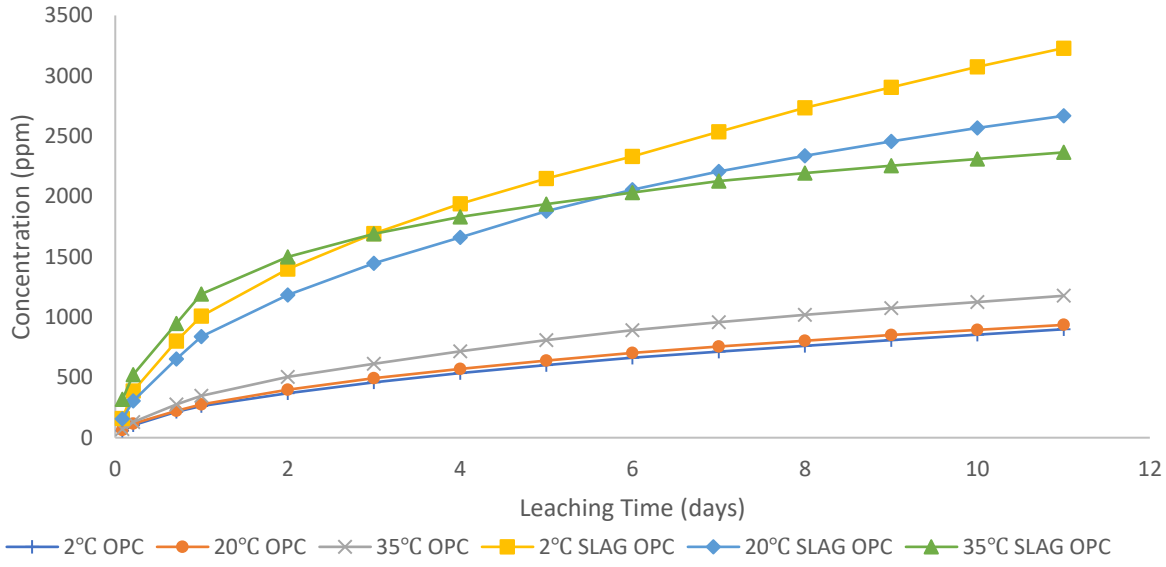

Figure 5.2. (a) Cumulative mass of arsenic leached from all test specimens (b) Cumulative leachate concentration.

Similar results were found with lead as the constituent of potential concern (Figure 5.3), however the concentrations of lead in the leachate were much lower due to a significantly lower initial lead concentration in each specimen. The lower solubility of galena compared to arsenic trioxide also played a role in the reduced lead concentration found in the leachate. Figure 5.3 displays that leaching of lead is temperature dependent, especially with specimens cured with the blended binder at low temperatures. Due to low concentrations of lead in the leachate, as a product of low concentrations in the CPB and low galena solubility, the leachability of arsenic is the dominant focus of the leaching test results to restrict the influence of uncertainties on the analysis and interpretation of the results.

(a)

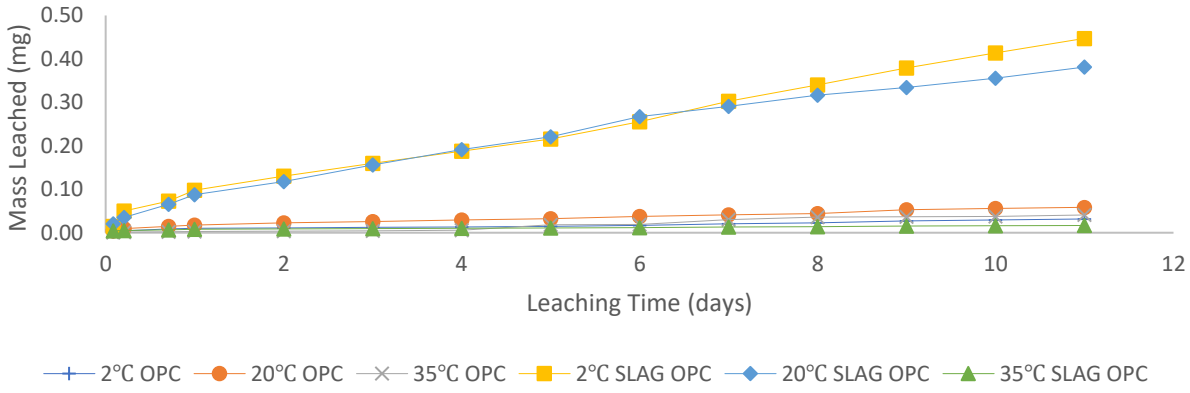

(b)

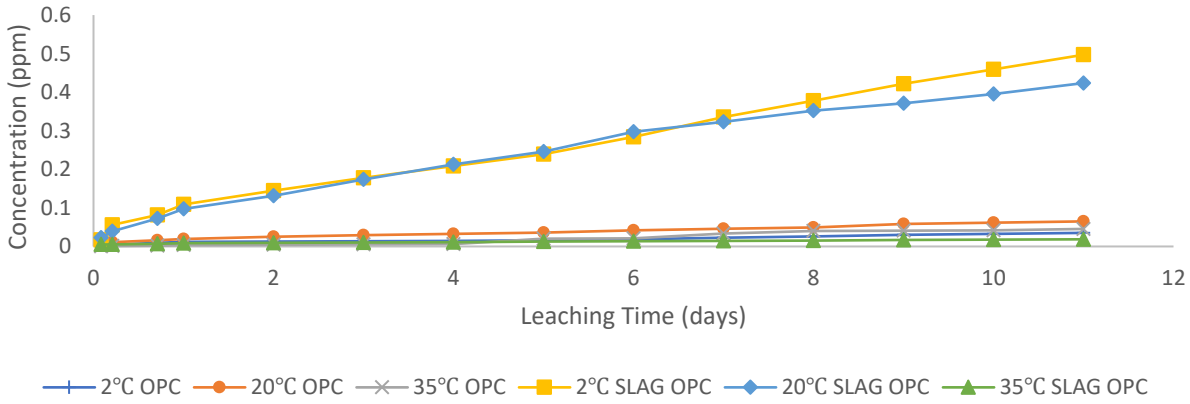

Figure 5.3. (a) Cumulative mass of lead leached from all test specimens (b) Cumulative leachate concentration.

5.2 Leachability of CPB that Contains OPC

CPB made with OPC (OPC-CPB) outperformed the CPB that contains OPC and Slag (OPC/Slag-CPB) at all tested curing temperatures with respect to arsenic leachability. It was observed that as curing temperature increased from 2°C to 35°C the performance of the OPC binder for arsenic immobilization decreased (Figure 5.4).

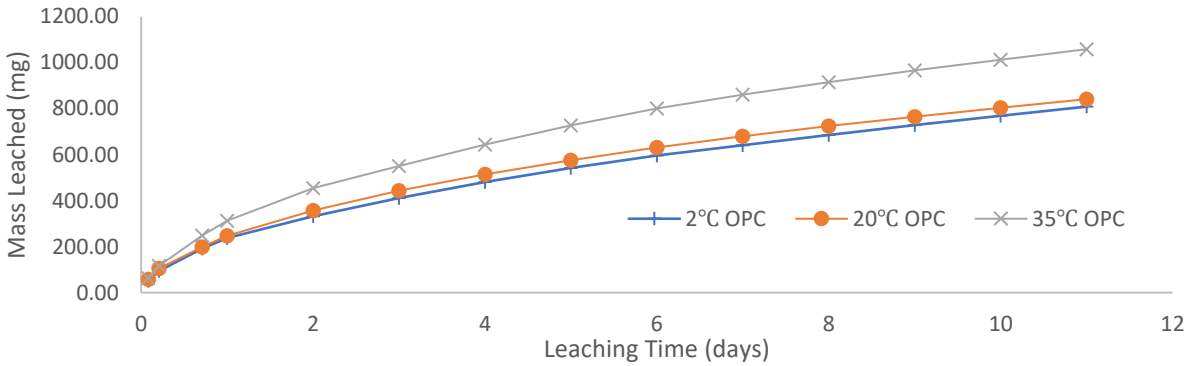

Figure 5.4. Cumulative mass of arsenic leached from OPC-CPB.

5.2.1 OPC-CPB at 2°C

The OPC-CPB cured at 2°C yielded the most favourable results for leaching of arsenic with a cumulative mass leached of 808.8 mg leached over the eleven-day leaching protocol. The cumulative mass of arsenic leached from this sample is approximately 4% lower than that of the sample cured at 20°C and approximately 25% less than the 35°C specimen. The cumulative mass leached from the 2°C OPC-CPB sample is highlighted in Figure 5.5. Over the initial two days of leaching, the rate of diffusion is highest with an initial value of 29.1 mg/h over the initial two hour submerged duration. After two days of leaching the rate of diffusion begins to decrease substantially and continues to decrease throughout the leaching test until the slope of the curve is near zero. This flattening slope means that the rate of diffusion is becoming close to constant. This is included in Figure 5.5. This plateau in the diffusion rate suggests a near constant diffusion rate from around two days of being submerged to the end of the test.

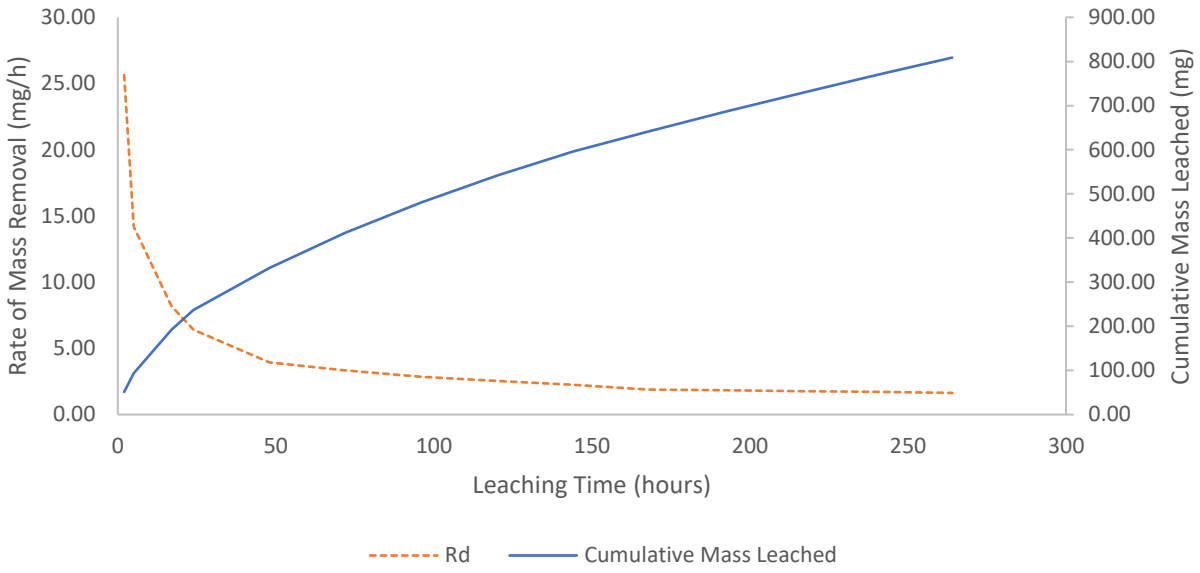

Figure 5.5. Mass removal and removal rate curves for the 2°C OPC-CPB (Rd: rate of mass removal).

5.2.2 OPC-CPB at 20°C

The results displayed that OPC-CBP cured at 20°C behaved very similarly to OPC-CPB cured at 2°C with respect to arsenic leachability. The sample cured at 20°C maintained a very similar leaching profile to the 2°C OPC-CPB with slightly higher leachate concentrations through the duration of the test. The cumulative mass leached from this specimen was 841.3 mg over the eleven-day test duration. Figure 5.6 displays that there is very little difference in the leaching profile between the 2°C and 20°C OPC CPBs. This suggests than the curing process at these two temperatures is very similar. This similar leaching profile also resulted in a similar dissipation in the rate of diffusion at around two days of being submerged. The initial rate of diffusion is higher for the 20°C OPC-CPB at 31.98 mg/h compared to 29.07 mg/h of the 2°C OPC-CPB over the initial two hours of soaking, however at the two-day interval, the diffusion profiles become very analogous. The slope of the rate of diffusion curve becomes close to zero around six days soaking as seen in Figure 5.6, meaning that at this point, the mass removal rate becomes near constant.

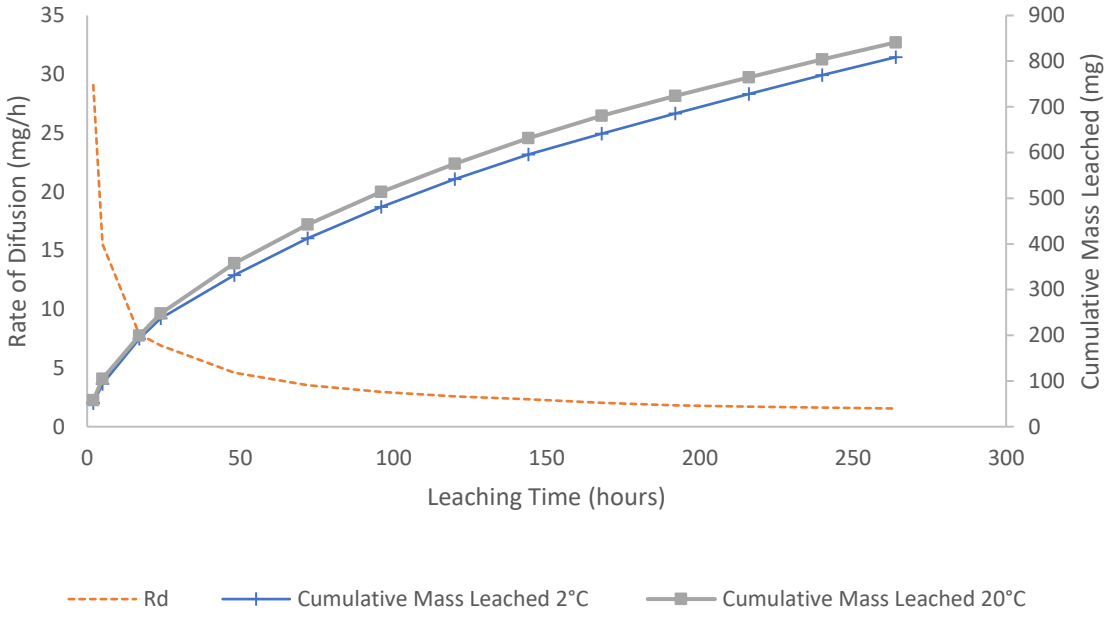

Figure 5.6. Comparison between the cumulative mass leaching profiles from OPC-CPBs cured at 2°C and 20°C with the rate of mass removal curve (Rd: rate of mass removal).

5.2.3 OPC-CPB at 35°C

Of the OPC-CPB samples the 35°C specimen showed the highest cumulative mass leached with 1058.5 mg over the 11-day test duration. This is substantially greater than both the 2°C and 20°C OPC-CPBs. The initial rate of diffusion is much higher than the other samples at 31.91 mg/h over the first two hours submerged. The rate of mass removal dissipation rate is least with the 35°C OPC-CPB, as the slope flattens at the three-day leaching interval. The flattening beyond this interval is more gradual and does not approach zero until the 9-day interval where the diffusion rate becomes near constant (Figure 5.7).

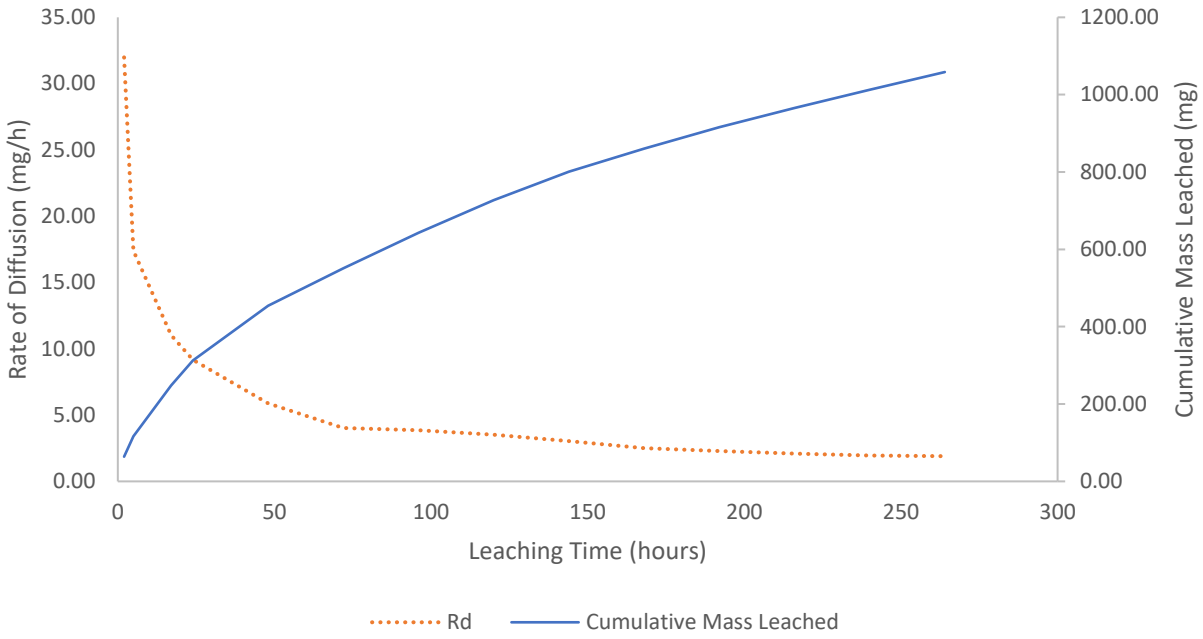

Figure 5.7. Mass removal and removal rate curves for OPC-CPB cured at 35°C (Rd: rate of mass removal).

5.2.4 Comparison and Discussion of OPC as a Binder

Differences in the leaching profiles of the OPC-CPBs cured at 2°C, 20°C, and 35°C can be described by differences in the microstructure and formation/development of hydration products during the curing process. These differences were observed through analysis of samples from this experiment using SEM, MIP, and PXRD with the support of literature from past research in the field of cement stabilized materials.

5.2.4.1 Comparison of OPC Samples Using Microstructural Analysis

SEM images allow for qualitative comparison which is further supported through quantitative data from MIP, and PXRD. SEM was utilized to visually compare the porosity and formation of hydration products with respect to specimens cured at three temperatures. Figures 5.8 through 5.13 were used to compare the microstructural properties of unleached OPC samples cured at various temperatures (2°C, 20°C and 35°C).

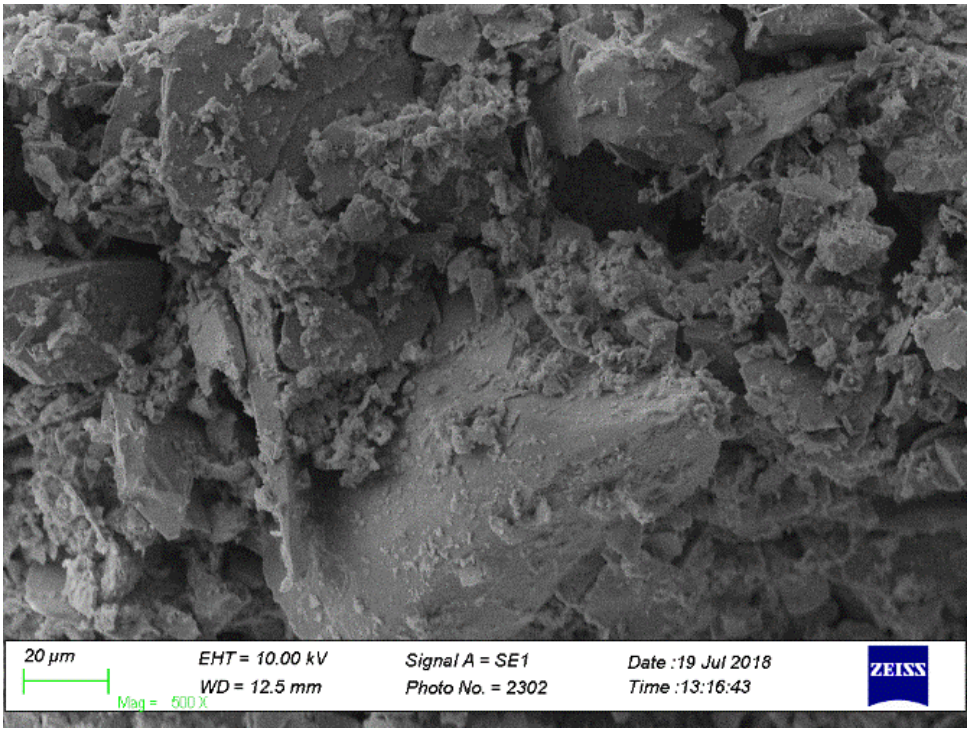

Figure 5.8. SEM image of OPC-CPB cured at 2°C (500X magnification)

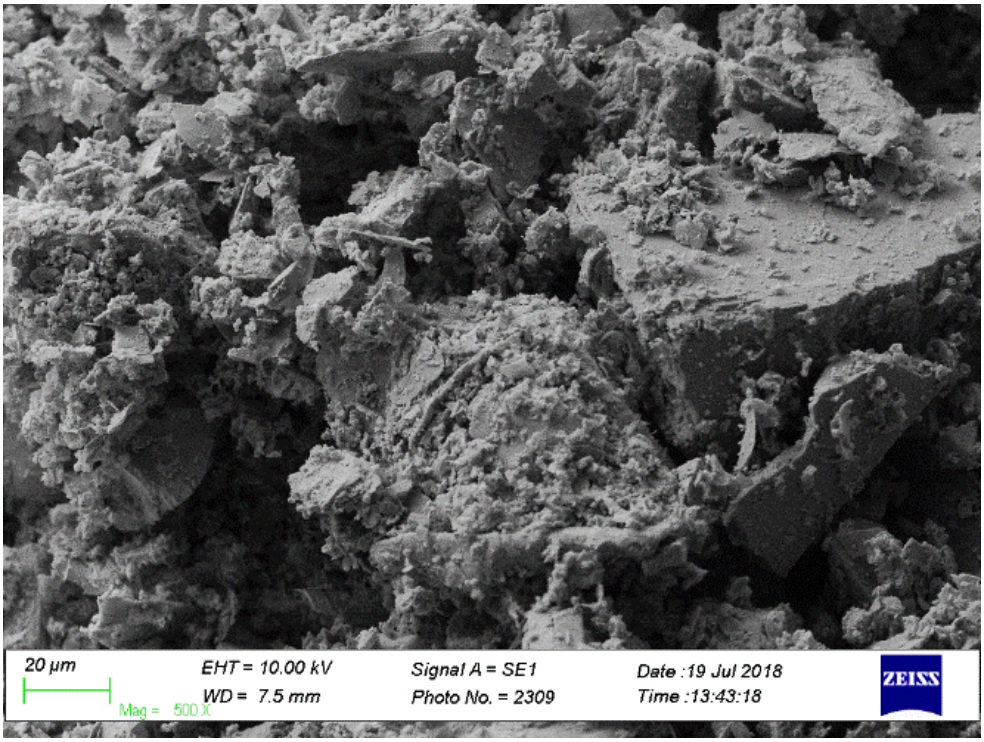

Figure 5.9. SEM image of OPC-CPB cured at 20°C (500X magnification)

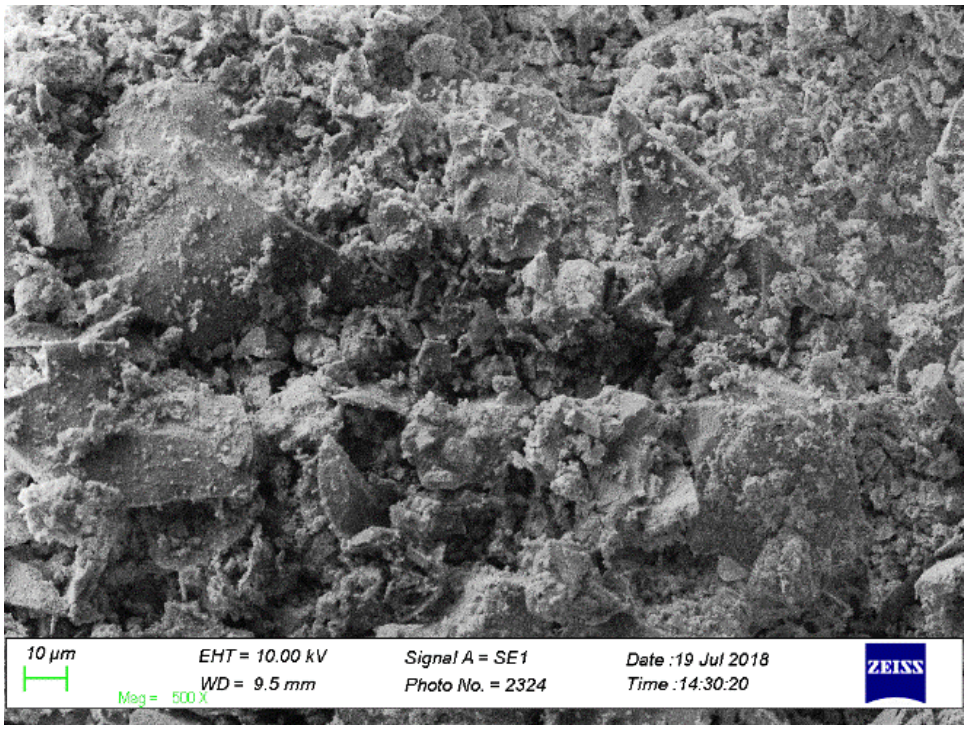

Figure 5.10. SEM image of OPC-CPB cured at 35°C (500X magnification).

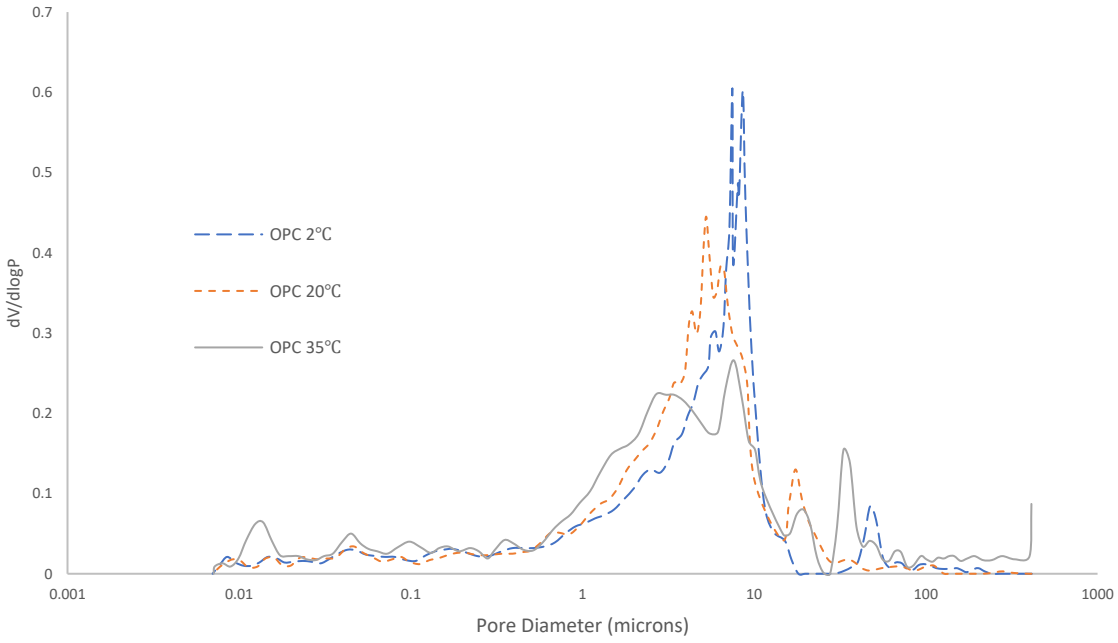

Figure 5.11. MIP data highlighting pore size distribution of OPC-CPBs.

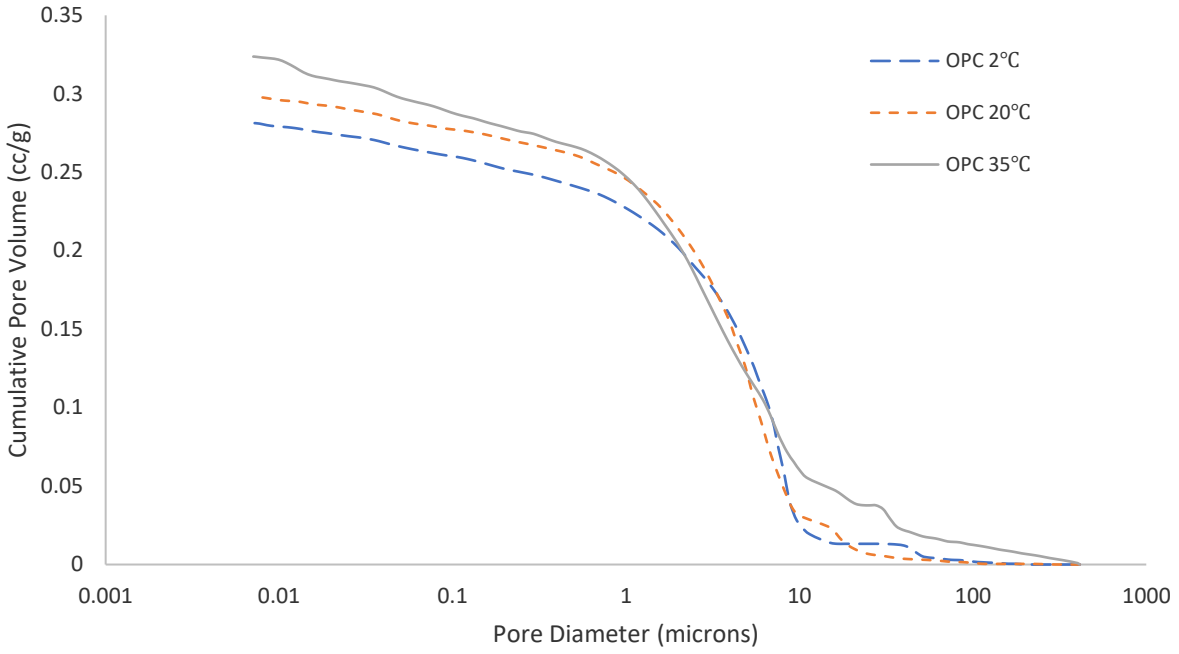

Figure 5.12. Cumulative pore volume of OPC-CPBs.

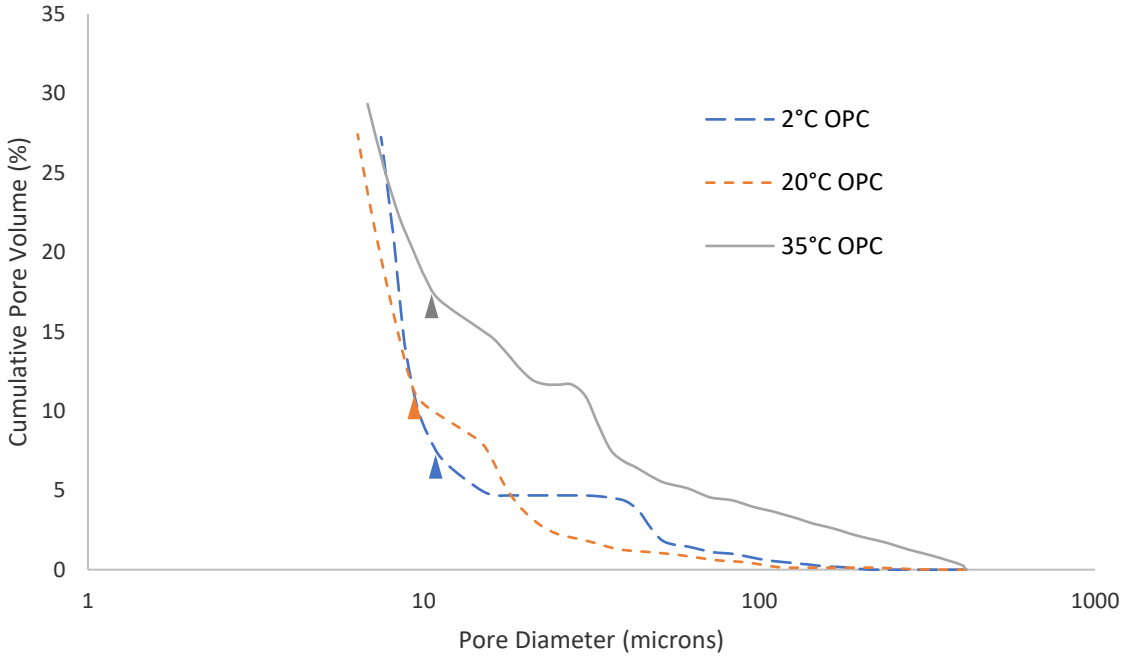

Figure 5.13. Cumulative porosity curve for OPC-CPBs with triangle markers indicating the inflection point representative of threshold pore diameter.

The SEM images (Figures 5.8 through 5.10) provide a basis for visual differentiation of microstructural characteristics between OPC-CPBs. Following are the trends noticed in these samples as curing temperature increases: hydration product formation increases; increased hydration product formation suggests increased pore surface area. These observations are in agreement with those made by Fall et al. (2010) who state that increased curing temperature results in accelerated hydration and increased formation of hydration products.

The increase in pore surface observation is analogous to the MIP data. The pore surface is approximately the same for the 2°C and 20°C OPC-CPBs. With the 20°C being 0.18 m^2/g less that the 2°C OPC-CPB. However, the total surface area of the 35°C OPC-CPB is 3.14 m^2/g greater than that of the 2°C OPC-CPB. Table 5.1 describes the porosity characteristics from each OPC-CPB.

Table 5.1. Porosity characteristics of OPC-CPBs

	OPC 2°C	OPC 20°C	OPC 35°C
TOTAL INTRUSION VOLUME (cc/g)	0.2814	0.2982	0.3237
TOTAL SURFACE AREA (m^2/g)	4.4201	4.2403	7.5568
VOLUME BASED MEDIAN PORE DIAMETER (µm)	4.7937	4.1292	3.1592
SURFACE AREA BASED MEDIAN PORE DIAMETER (µm)	0.0175	0.0202	0.0141
AVERAGE PORE DIAMETER (µm)	0.2547	0.2813	0.1714
CRITICAL PORE DIAMETER (µm)	7.46	5.25	7.60
THRESHOLD PORE DIAMETER (µm)	11	9	11

OPC-CPBs cured at 2°C and 20°C have similar pore characteristics in terms of total intrusion porosity and total surface area. This coincides with their similar leaching profiles. The 35°C OPC-CPB has a substantially increased pore volume, and pore surface area while the median and average pore diameter is decreased. The cumulative curves for the 2°C and 35°C OPC-CPBs are quite different, however the pore parameters, threshold and critical pore diameter, are very similar. These parameters significantly influence fluid transport in porous media (Garboczi 1989; Ma 2013). The threshold pore diameter diameters for the 2°C and 35°C both occur at the inflection point on the curve at the 11-micron diameter. Although this inflection point occurs at approximately the same pore diameter, the percent of intruded volume is much

different. The 2°C OPC-CPB sees a threshold diameter at near 7% of the total intrusion porosity, while the 35°C OPC-CPB has a threshold diameter reflecting to about 17% of the total intrusion volume. These CPBs exhibit the greatest difference in cumulative arsenic leached.

PXRD was conducted on all OPC-CPBs. The major component of the natural tailings used (SiO_2), unhydrated cement components and hydration products ettringite (Et), Gypsum (Gpm), portlandite (CH), calcite or lime ($CaCO_3$), anhydrite ($CaSO_4$), and C-S-H were detected. Figures 5.14 through 5.16 display the mineral phase characterization of each OPC-CPB. The SiO_2 can be considered constant in each CPB since the same mix proportioning was used and SiO_2 is relatively inert. Using the SiO_2 as a reference peak, the relative quantities of hydration products can be determined, specifically in the low angle range (5 – 30 degrees 2-theta – Cu Kα Radiation). It is notable that the relative quantities of hydration products increase as the curing temperature increases through the 2°C to 35°C range. The differences in relative hydration product quantities between the 2°C and 20°C (Figures 5.14 and 5.15) are less obvious than the 35°C OPC-CPB (Figure 5.16) where there is certainly increased ettringite, gypsum and CH detected in the low angle range. The increased quantities of hydration products support visual SEM image observations.

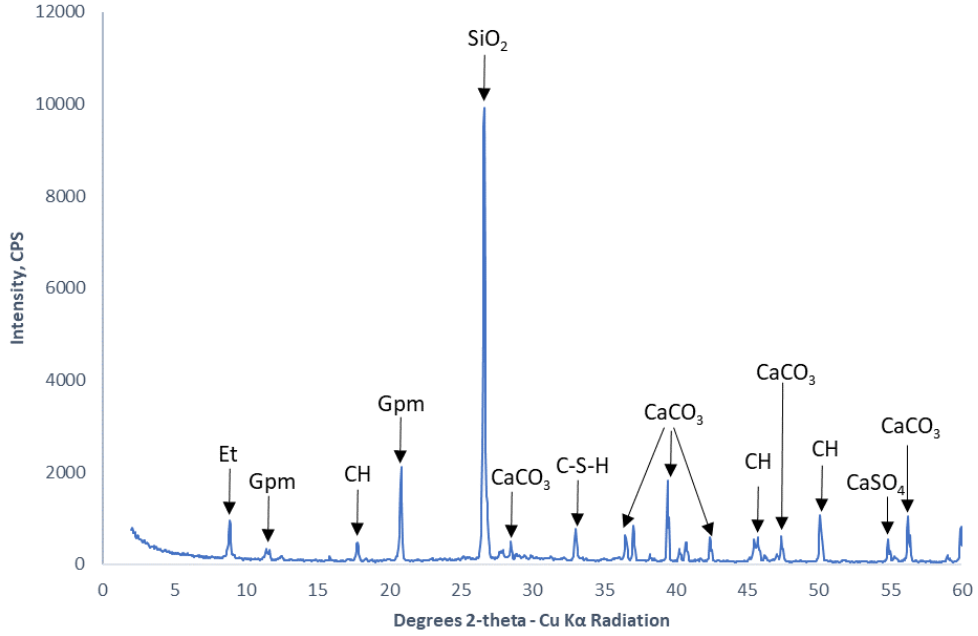

Figure 5.14. PXRD diffractogram of 2°C OPC-CPB.

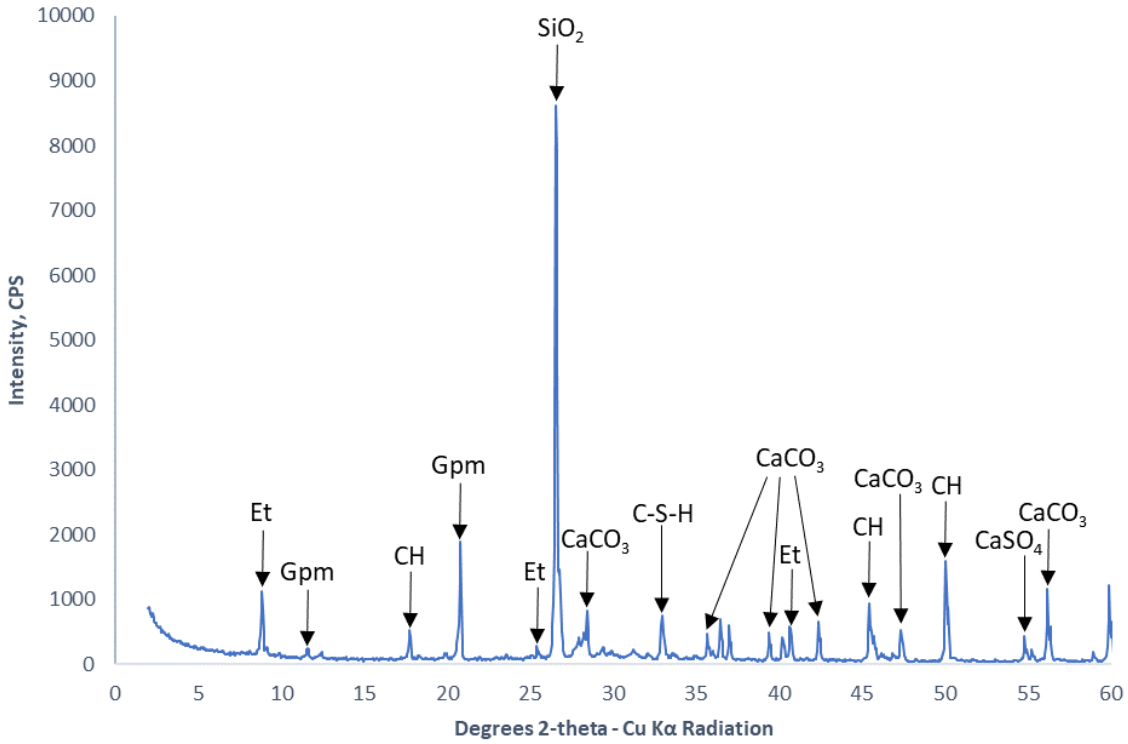

Figure 5.15. PXRD diffractogram of 20°C OPC-CPB.

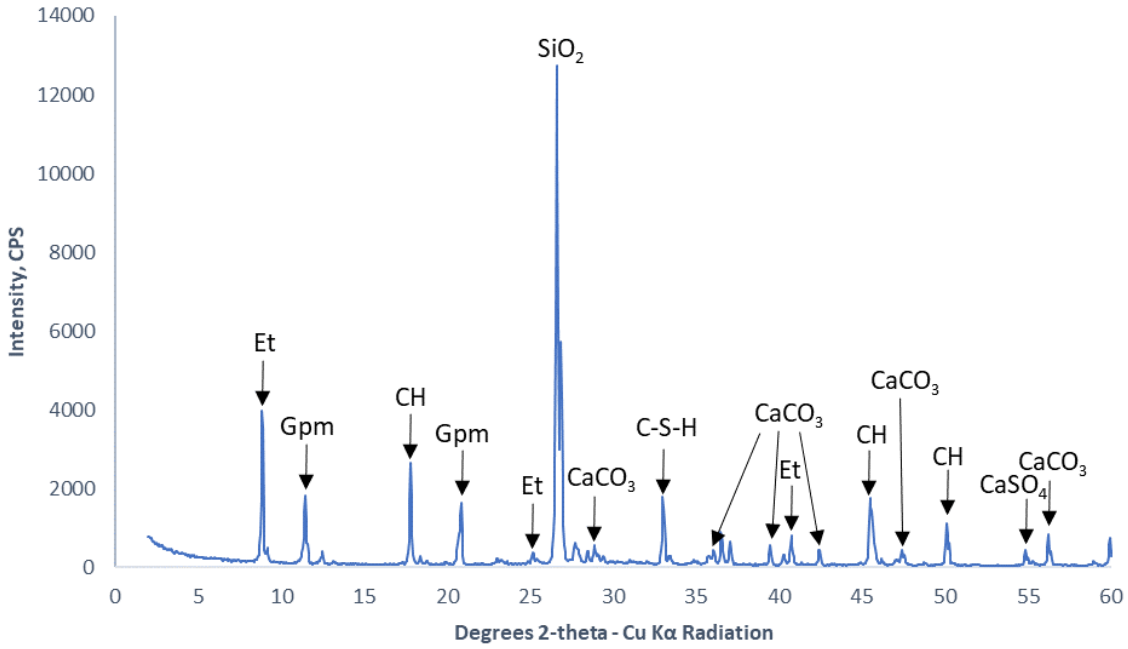

Figure 5.16. PXRD diffractogram of 35°C OPC-CPB.

5.2.4.2 OPC-CPB Leachate pH Observations

The pH of the bulk leachate was measured at each leachate exchange. This pH is likely not equal to the pH of the porewater due to concentration gradients, however it should approximately represent the pH of the pore solution. Figure 5.17 displays the pH of the leachate for the 2°C, 20°C, and 35°C OPC-CPBs.

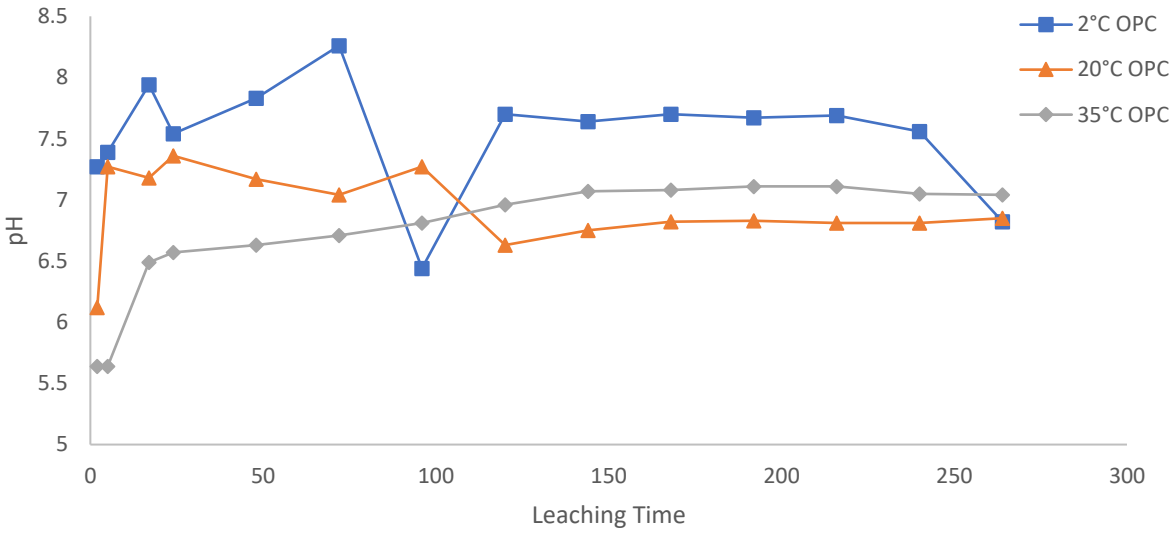

Figure 5.17. Leachate pH of OPC-CPBs.

The pH of the 2°C OPC-CPB leachate is in the range of 6.4 to 8.3. Most of the measurements for the 2°C OPC-CPB leachate were between pH 7 and 8. The 20°C OPC-CPB leachate had a pH range of 6.1 to 7.3. Most of the measurements for the 20°C OPC-CPB leachate were between 6.5 and 7.5. Finally, the 35°C OPC-CPB leachate had pH in the range of 5.6 to 7.1. During the period where the slope of the cumulative mass curves is greatest (0 – 72 hours) the pH range for the 2°C, 20°C, and 35°C leachates were 7.3 to 8.3, 6.1 to 7.4, and 5.6 to 6.7 respectively.

5.2.4.3 Discussion and support from past research

Notable trends and observed differences in microstructure can be explained by past research from the field of CPB and other cement stabilized materials. The formation of hydration products, specifically the calcium-silicate-hydrate (C-S-H) and portlandite (CH) phases responsible for strength gain in CPB cured using Portland cement, are temperature dependent. Elevated curing temperatures result in increased

early age unconfined compressive strength (UCS) of CPB due to increased production of C-S-H and CH (Fall et al. 2010). The rapid hydration of CPB samples cured at elevated temperatures has a profound influence on the pore structure of CPB at all curing ages. Unlike many concretes and cement stabilized materials, CPB cured with OPC as the sole binder shows a reduction in porosity as curing temperature increases at advanced curing times. CPB cured with OPC at high temperature can show a decrease in strength at advanced curing time. This temperature induced strength decrease can be explained by the crossover effect. In a CPB system the crossover effect may not be evident until the age of the monolith reaches 150 days (Fall et al. 2010). However, the curing time at which the crossover effect may take place in CPB depends on many other parameters, such as the chemical composition of the cement, the w/c ratio and chemistry of the pore water of CPB (Fall et al. 2010). This may explain the notably wide distribution of pores between 0.8 and 20 microns for the 35°C OPC-CPB. The pore distribution and cumulative curves for the 35°C OPC-CPB are obviously different than the 2°C and 20°C OPC-CPBs at this stage of curing. This may give reason for the similarities in both threshold and critical pore diameter between the 2°C and 35°C samples despite very different pore characteristics and leaching profiles. This suggests that the 35°C OPC-CPB may not be mature enough to determine a representative mature age porosity if the crossover effect has yet to occur. Garboczi (1989) states that the pores can only significantly contribute to flow if they are relatively large in diameter, and continuous across the media. Based on this theory, the most appreciable amount of flow through the media occurs where $d > d_{th}$. Since permeability of cement-stabilized materials is influenced by d_{th} the effective diffusion coefficient (D_e) may also be related to d_{th} (Garboczi 1989). This relationship suggests that the increased percent of cumulative pore volume greater than d_{th} may result in greater D_e. This may explain the difference in cumulative mass leached between each OPC-CPB. The pore volume greater than d_{th} for the 2°C, 20°C, and 35°C samples are 0.021 cc/g, 0.036 cc/g, and 0.055 cc/g respectively. This may provide explanation for the increased cumulative mass leached from the 35°C OPC-CPB compared to the 2°C, and 20°C OPC-CPBs. The higher percent of cumulative pore volume greater than d_{th} is, the easier it is for the leachant to reach the reaction site; therefore, more of the arsenic can be

leached out. Moreover, the size of the available surface area (reaction site) is an additional mechanism or factor that contributes to the increase in cumulative mass leached from the 35°C OPC-CPB compared to the 2°C, and 20°C OPC-CPBs. It is well established that the rate of leaching of contaminant (metal) from a porous waste material stabilized with cement or binder is significantly affected by the amount of available surface area (e.g., Bishop et al 1992). Leaching is a mechanism in which the contaminants in the solid phase are transported to the liquid phase in contact with it. Consequently, the area of the interface between the solid phase and the liquid in the pores of the cemented waste material is vital. The bigger the available surface area is, more of the contaminant can be leached out. This argument is consistent with the results of MIP tests presented in Table 5.1 and discussed above. From Table 5.2, it can be observed that the total surface area of the 35°C OPC-CPB (7.6 m^2/g) is considerably bigger than that of the 20°C OPC-CPB (4.2 m^2/g) and 2°C OPC-CPB (4.4 m^2/g).

Not only can the formation of C-S-H contribute to the strength and pore structure of a cement monolith, but it can provide hydroxyl anions to bind with trace metals resulting in chemical stabilization within the monolith (Hamberg 2018). The phase formation does influence the leachability of arsenic from cement stabilized materials. Kundu and Gupta (2008) found that curing of cement and other pozzolanic materials results in multiple arsenic bearing phases. The solubility of these phases varies. Common phases found include: Calcium arsenite (Ca-As-O), Calcium arsenates ($CaAs_2O_6$, $Ca_2As_2O_7$, $CaO–As_2O_5$), Calcium hydrogen arsenate hydrates ($Ca_5H_2(AsO_4)_4 \cdot 9H_2O$, $CaHAsO_4 \cdot 2H_2O$, $Ca_5H_2(AsO_4)_4 \cdot 5H_2O$), Calcium hydroxide arsenate hydrate ($CaAsO_3(OH) \cdot 2H_2O$), and Calcium hydrogen arsenates ($CaHAsO_4$, $CaH_4(AsO_4)_2$, $Ca(H_2AsO_4)_2$). These arsenic bearing phases are likely doped to the both identified and unidentified peaks observed on the PXRD diffractograms. The Rigaku software was unable to detect any arsenic doped phases, possibly due to low relative arsenic quantities within each CPB and high amounts of noise, especially at higher diffraction angles.

Based on solubility of these arsenic bearing phases, $CaHAsO_4$ and $CaHAsO_4 \cdot 2H_2O$ are expected contributors of arsenic leached from a cement stabilized matrix (Kundu and Gupta 2008). The phase of arsenic used to dope the samples, As_2O_3, is

also highly soluble and if not dissociated by hydration waters, may remain in the matrix as an arsenic bearing phase available to contribute leachable arsenic. As(III) has been found to sorb to C-S-H. This sorption capacity of C-S-H is reduced by the increases in the Ca/Si ratio (Stronarch et al. 1997; Walker 1993). Stronarch et al. (1997) performed experiments based specifically around the reactions of As_2O_3 in cement. The resulting dominant arsenic phases from reactions between As_2O_3 and cement detected by PXRD were As_2O_3 + $Ca(AsO_2)_2$, $CaAsO_2OH$ + $Ca(OH)_2$ and $Ca(AsO_2)_2$ + $CaAsO_2OH$. Findings suggested that Portland cement stabilized materials can provide effective immobilization capacity for As(III). This is explained by the availability of both $Ca(OH)_2$ and C-S-H to react with As(III) resulting in immobilization. This agrees with Kundu and Gupta (2008), where arsenic was found to produce insoluble compounds within cements and other pozzolanic materials through reactions with $Ca(OH)_2$. Coussy et al. 2011 found that arsenic may substitute in ettringite to form stable calcium arsenate. Although researchers (Fall et al. 2010) have found lower quantities of ettringite in CPBs cured at low (2°C) temperatures, ettringite is known to destabilize at high curing temperatures (Escadeillas et al, 2007). These past findings suggest the lower curing temperatures may result in formation of a more stable arsenic bearing phase within the paste.

Arsenic mobility has been described as pH dependent (Halim 2004). In leaching test performed by Halim (2004), arsenic was found to be least mobile in the pH 7-8 range. This result shows strong correspondence with the pH of the OPC-CPB leachate. The 2°C and 20°C OPC-CPB leachate had pH values within the range where arsenic is most stable, while the 35°C OPC-CPB leachate pH reading was outside the range towards more acidic conditions. The notable increase in hydration products as temperature increases suggests that the pore structure, pH, and possible variations in arsenic bearing phases that were undetected by PXRD analysis, play the greatest role in the temperature dependent leachability of arsenic from OPC-CPBs.

5.2.4.4 Discussion of the Leaching Mechanism

Diffusion stands out as the dominant leaching mechanism of arsenic at all tested curing temperatures. When plotting both Log (Rd) as a function of Log (t), and cumulative mass leached as a function of the square root of leach time, the trend

produced is linear with an R^2 values ranging from 0.98-0.99. The linear nature of these graphs (Figures 5.18 – 5.20) provides evidence that the leaching mechanism is certainly diffusion. This is supported by Kundu and Gupta (2008) who also found a linear relationship between cumulative fraction leached and the square root of leaching time regarding arsenic leach rates from cement stabilized materials.

(a)

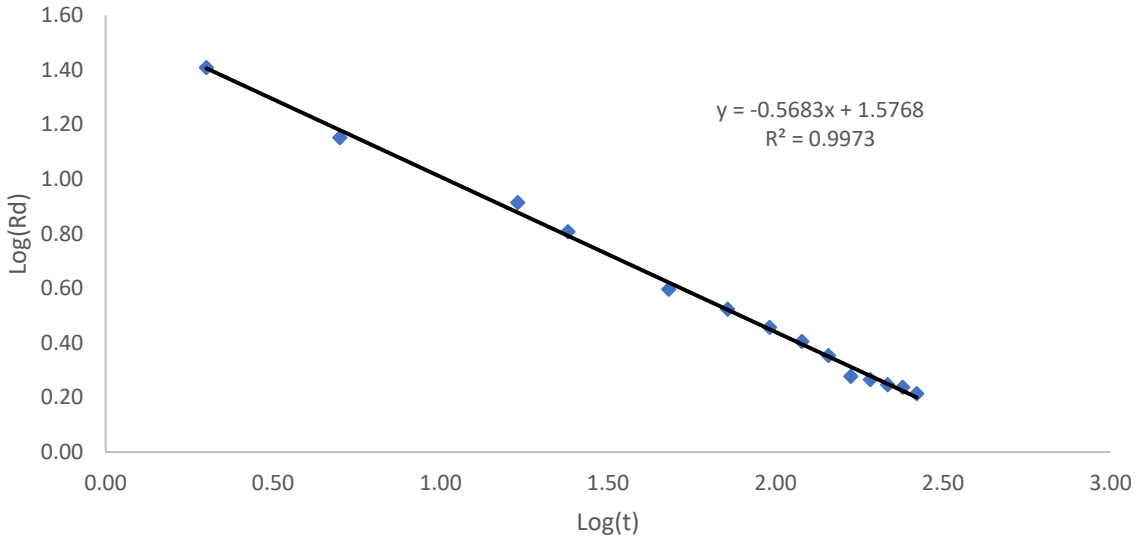

(b)

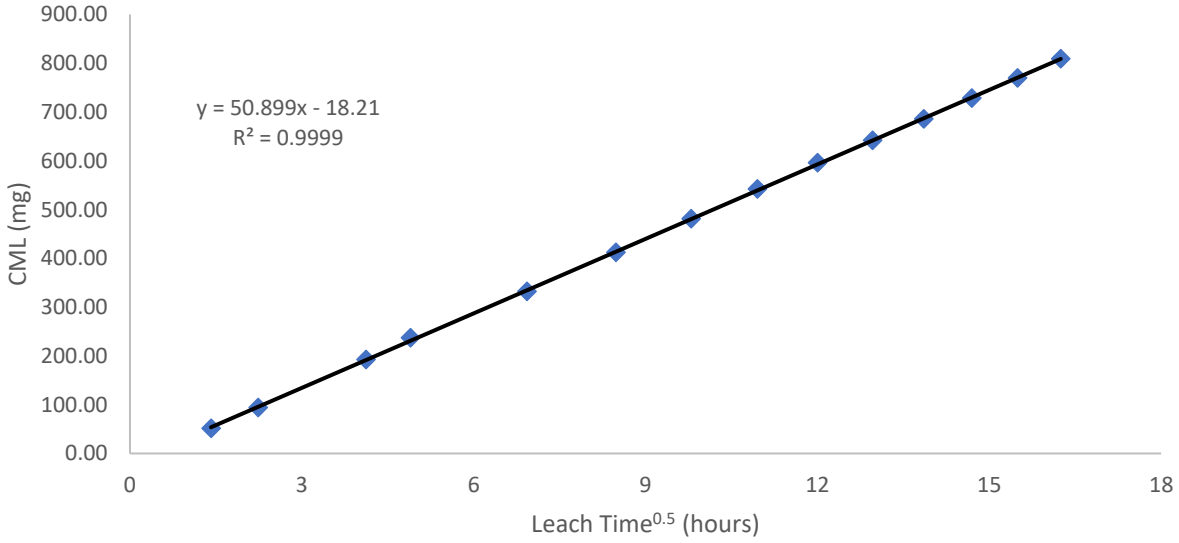

Figure 5.18. (a) Plot of Log rate of mass removal as a function Log time for the OPC-CPB cured at 2°C (Rd: rate of mass removal). (b) Plot of cumulative mass leached as a

function the square root of leaching time for the OPC-CPB cured at 2°C (CML: cumulative mass leached).

(a)

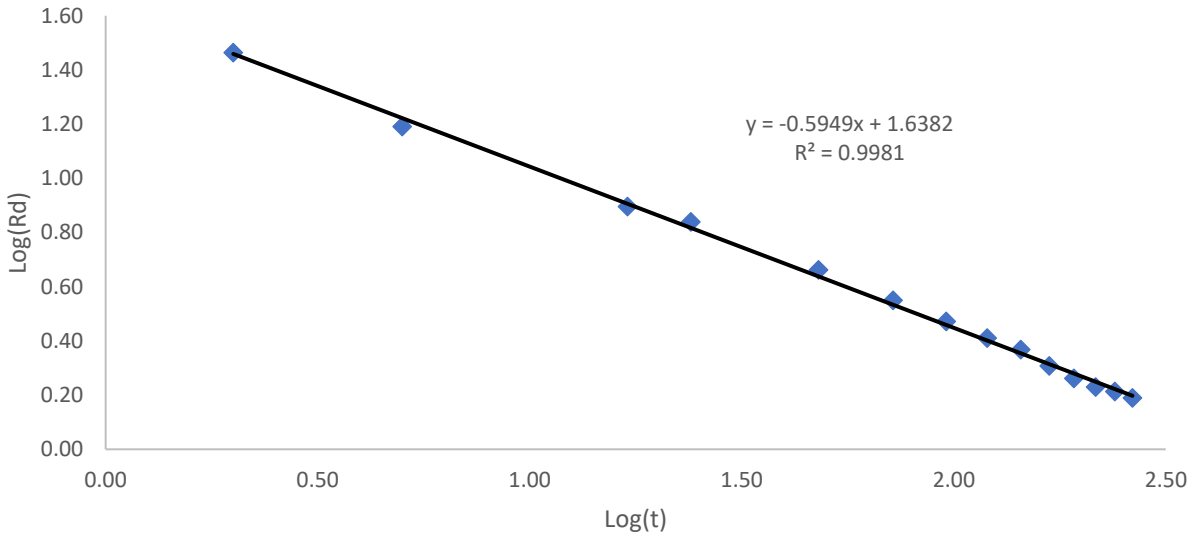

(b)

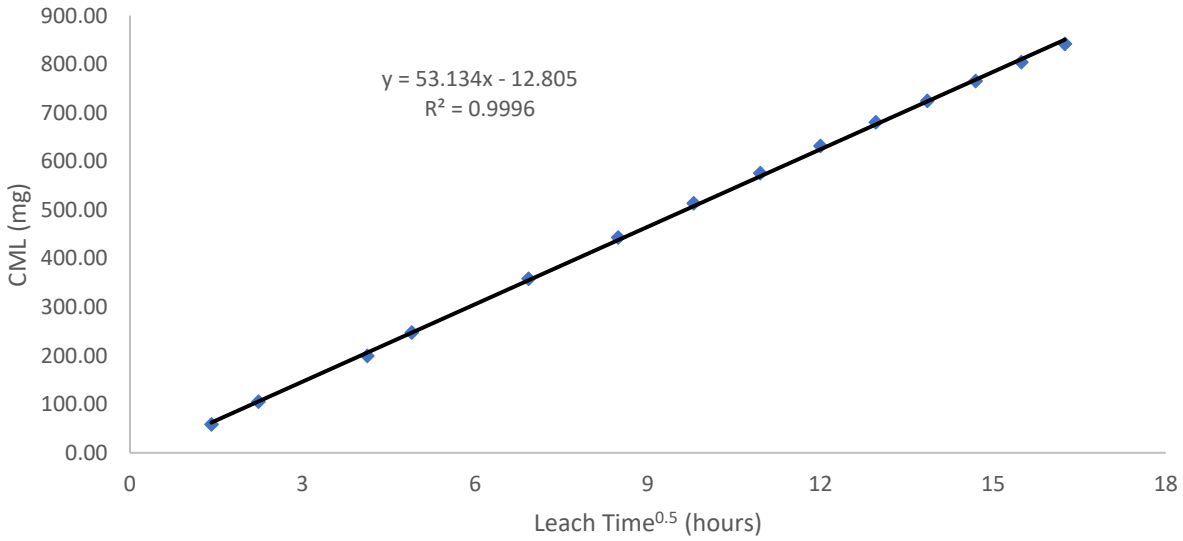

Figure 5.19. (a) Plot of Log diffusion rate as a function Log time for the OPC-CPB cured at 20°C (Rd: rate of mass removal). (b) Plot of cumulative fraction leached as a function the square root of leaching time for the OPC-CPB cured at 2°C (CML: cumulative mass leached).

(a)

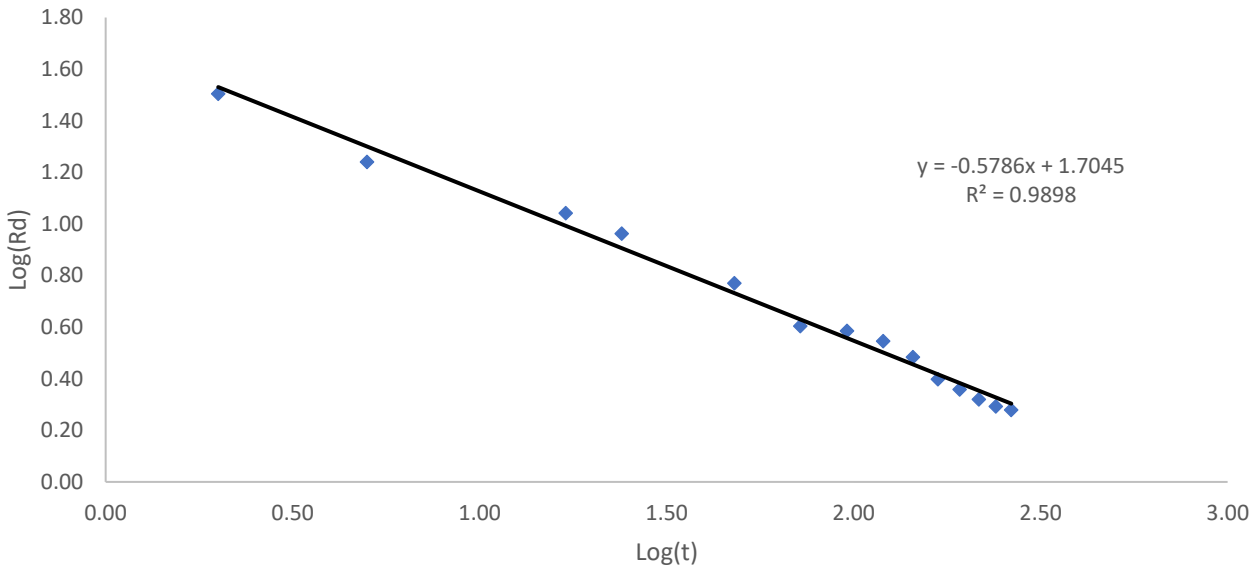

(b)

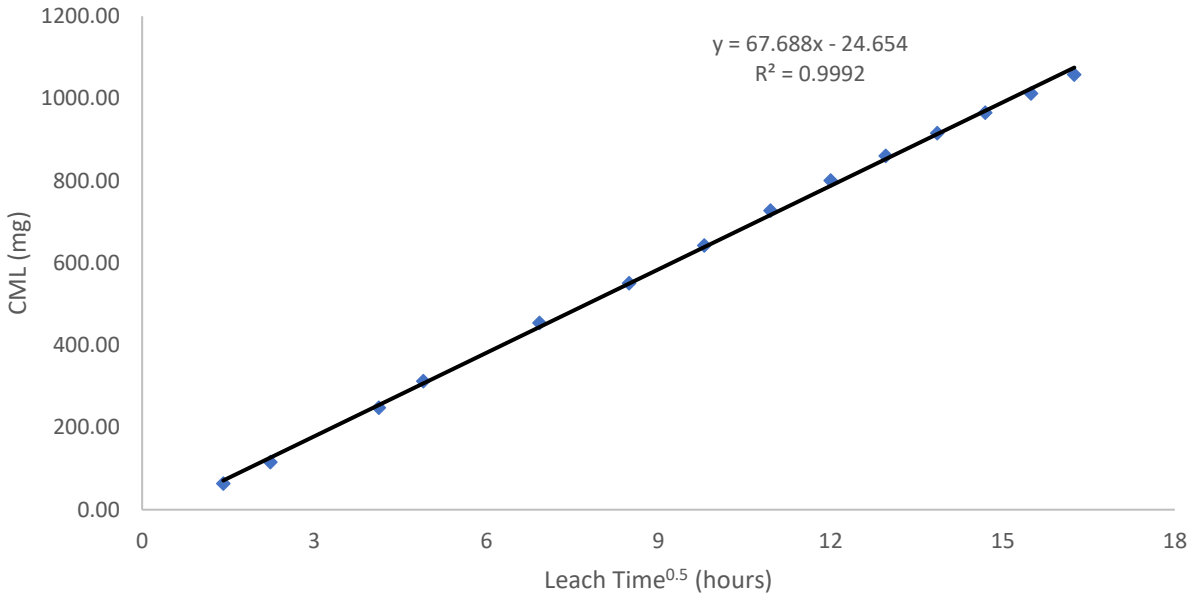

Figure 5.20. (a) Plot of Log mass removal rate as a function Log time for the OPC-CPB cured at 35°C (Rd = rate of mass removal). (b) Plot of cumulative fraction leached as a function the square root of leaching time for the OPC-CPB cured at 35°C (CML: cumulative mass leached).

These plots suggest that the leaching mechanism is independent of curing temperature. This means that diffusion dominates as the leaching mechanism through

the studied temperature range. However, temperature does control the availability for arsenic to leach. There is a significant difference between the leaching of arsenic within the experimental temperature range, suggesting that although the mechanism is the same, temperature does control availability through speciation and porosity characterization. Through the range of curing temperatures studied diffusion can be considered the dominant mechanism for mass removal. Due to this observation, the change in cumulative mass leached must be attributed to the way in which arsenic is held by the matrix. The 35°C OPC-CPB does have the highest pore surface area suggesting more opportunity for diffusion. Contrarily the 2°C OPC-CPB has a slightly greater pore surface area compared to the 20°C OPC-CPB, yet it leached marginally less arsenic.

5.3 Leachability of CPB Cured Using OPC/Slag at a 50% Blending Ratio

Samples cured with 4.5 wt% binder composed of a 50% blending ratio of OPC and BFS did not match the performance of the OPC binder. Cumulative mass leached from all three curing temperatures exceeded the cumulative mass leached from the OPC-CPBs by substantial margins. It was found that curing temperature had the opposite effect on the OPC/Slag-CPBs compared to OPC-CPBs. Increased curing temperature yielded lower arsenic mass removal over the duration of the leaching test. Figure 5.21 displays the leaching profiles of the blended binder samples. The 2°C and 20°C OPC/Slag-CPBs follow a similar leaching profile throughout the test, however the 35°C OPC/Slag-CPB follows a different mass removal curve.

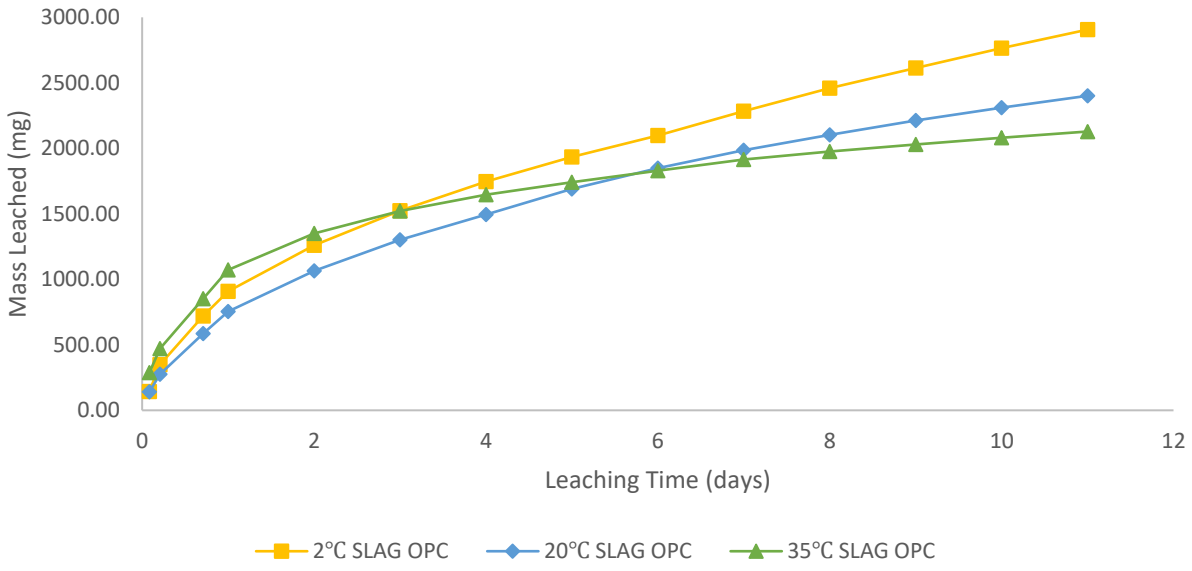

Figure 5.21. Cumulative mass leaching profiles of OPC/Slag-CPBs cured at 2°C, 20°C, and 35°C.

5.3.1 OPC/Slag-CPB cured at 2°C

The obtained results displayed that the OPC/Slag-CPB cured at 2°C allowed the greatest cumulative mass of arsenic to be leached with a value of 2906.2 mg (Figure 5.21). This was 2097.4 mg more than the cumulative arsenic mass leached from the OPC-CPB cured at the same temperature. The mass removal rate of 71.74 mg/h over the first two hours of being submerged was intermediate to the 20°C and 35°C OPC/Slag-CPBs. The rate of mass removal plateaued and became nearly constant at approximately 120-hours of submerged leaching time. The profile of the rate of diffusion throughout the leaching protocol is displayed in Figure 5.22.

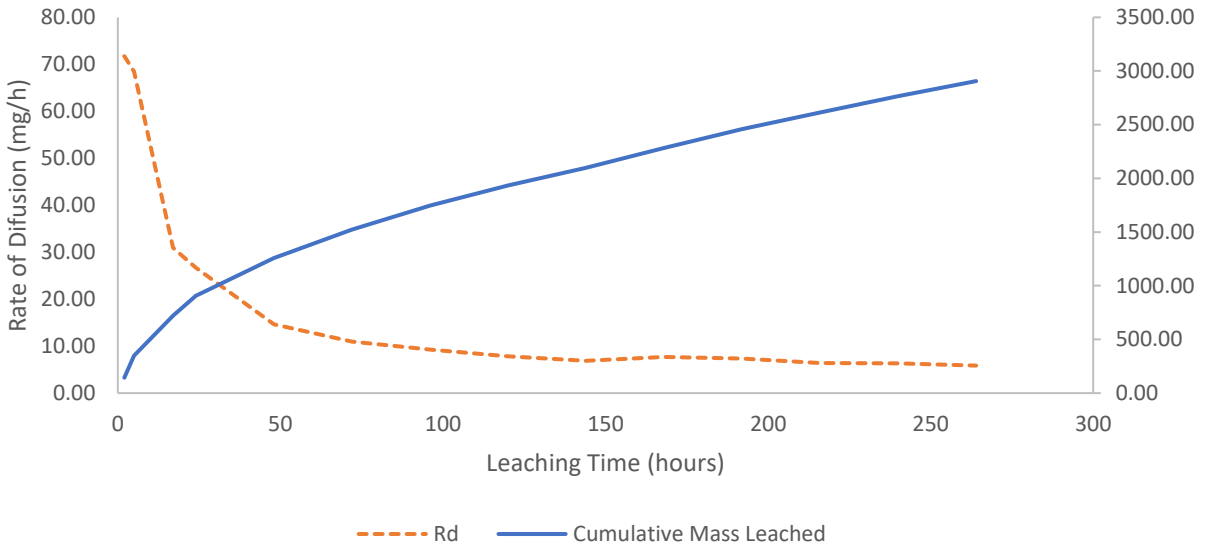

Figure 5.22. Mass removal and removal rate curves for the 2°C OPC/Slag-CPB (Rd: rate of mass removal).

5.3.2 OPC/Slag-CPB at 20°C

The 20°C OPC/Slag-CPB sample followed a similar mass removal profile to the 20°C OPC-Slag CPB. However, both the initial rate of mass removal over the first two hours of leaching and cumulative mass leached were lower with values of 70.26 mg/h and 2401.09 mg respectively (Figure 5.23).

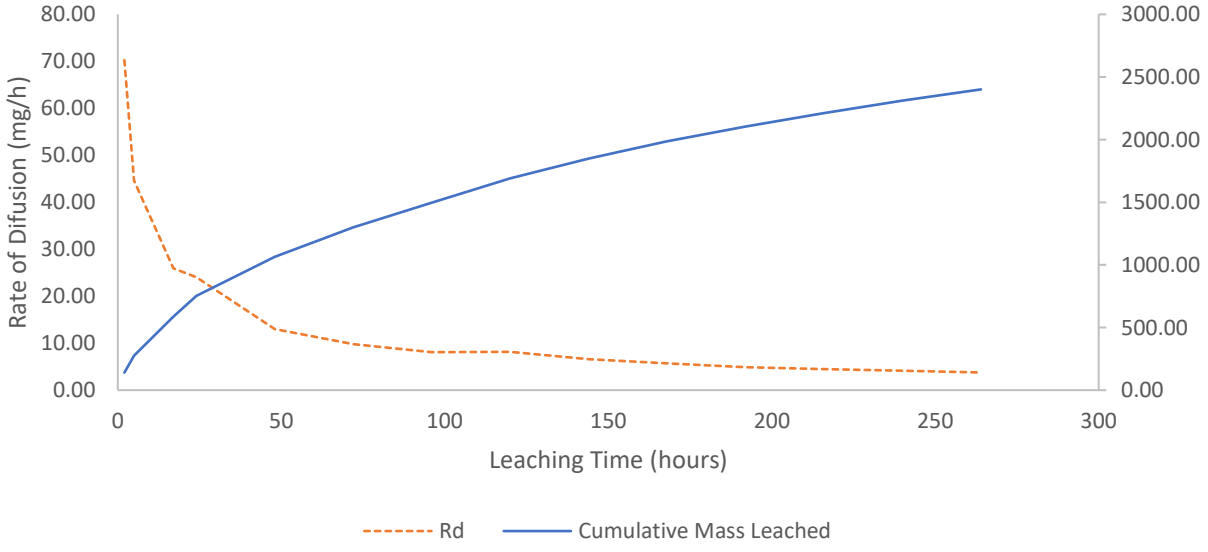

Figure 5. 23. Mass removal and removal rate curves for the 20°C OPC/Slag-CPB (Rd: rate of mass removal).

The rate of diffusion becomes near stable at approximately 192 hours of submerged duration and follows a curve of similar shape to the 2°C OPC/Slag-CPB.

5.3.3 OPC/Slag-CPB cured at 35°C

Of the three curing temperatures tested, 35°C provided the best results for samples OPC/Slag-CPB. Although the 35°C specimen had the highest mass removal rate over the initial two hours of leaching (143.23 mg/h) it resulted in the lowest cumulative mass of arsenic leached of the samples cured using the blended binder; 2128.23 mg (Figure 5.24).

The shape of the mass removal profile is different for the 35°C sample compared to that of the other two samples cured using the OPC/Slag binder. Mass transfer is rapid in the initial 24 hours of leaching but drops quite low and becomes near constant at approximately 96 hours of leaching (Figure 5.24). Between two and four days the cumulative mass leached from the 35°C OPC/Slag-CPB drops below that of the 2°C OPC/Slag-CPB. The cumulative mass of arsenic leached from the 35°C OPC/Slag-CPB then drops below the cumulative mass of arsenic leached form the 20°C OPC/Slag-CPB between five and 6 days of leaching (Figure 5.21).

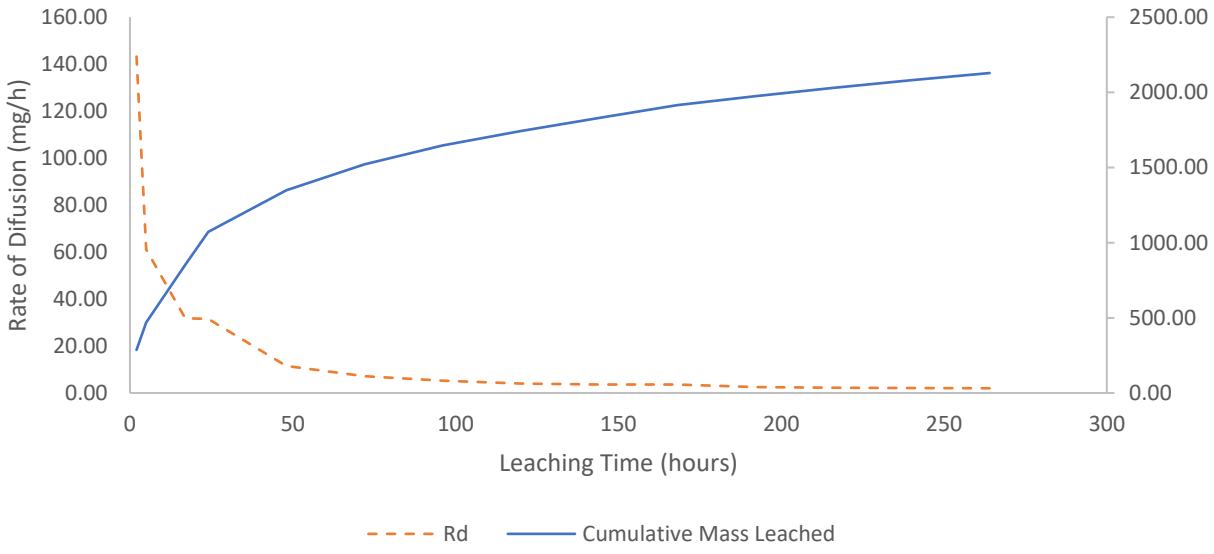

Figure 5.24. Mass removal and removal rate curves for the 35°C OPC/Slag-CPB (Rd: rate of mass removal).

5.3.4 Comparison and Discussion of OPC/Slag at a 50% Blending Ratio as a Binder

Using the same comparison techniques as the OPC-CPBs, SEM, PXRD, and MIP were used to compare the microstructure of the OPC/Slag-CPBs, providing explanation for the observed results from ASTM C1308-08.

5.3.4.1 Comparison of OPC/Slag-CPBs Using Microstructural Analysis

SEM images (Figure 5.25 through 5.27) of the OPC/Slag blended samples suggest little change in the microstructure with curing temperature. Differentiation between microstructural properties cannot be visually assessed with confidence. Tabulated values (Table 5.2) from MIP, suggest that curing temperature influences the pore structure of CPBs cured with an OPC/Slag blend. When looking at the pore size distribution in Figure 5.28, the results indicate that as curing temperature increases so does the critical pore diameter for the 2°C and 20°C OPC/Slag-CPBs. The critical pore diameter for the 35°C OPC/Slag-CPB is the lowest of the CPBs analyzed in for both OPC and OPC/Slag binders. These results suggest that the characteristics of the stability of the hydration products formed using the blended binder pose a considerable influence on leachability, along with the porosity characteristics. The threshold pore diameters increase as temperature increases (Figure 5.30).

Table 5.2. Porosity characteristics of OPC/Slag-CPBs cured between 2°C and 35°C.

	OPC/SLAG 2°C	OPC/SLAG 20°C	OPC/SLAG 35°C
TOTAL INTRUSION VOLUME (cc/g)	0.2899	0.2799	0.2711
TOTAL SURFACE AREA (m^2/g)	3.5966	3.4273	4.0629
VOLUME BASED MEDIAN PORE DIAMETER (µm)	2.451	3.0022	2.0607
SURFACE AREA BASED MEDIAN PORE DIAMETER (µm)	0.0274	0.0205	0.0312
AVERAGE PORE DIAMETER (µm)	0.3224	0.3266	0.2669
CRITICAL PORE DIAMETER (µm)	3.55	4.53	2.0
THRESHOLD PORE DIAMETER (µm)	4.8	6.1	11

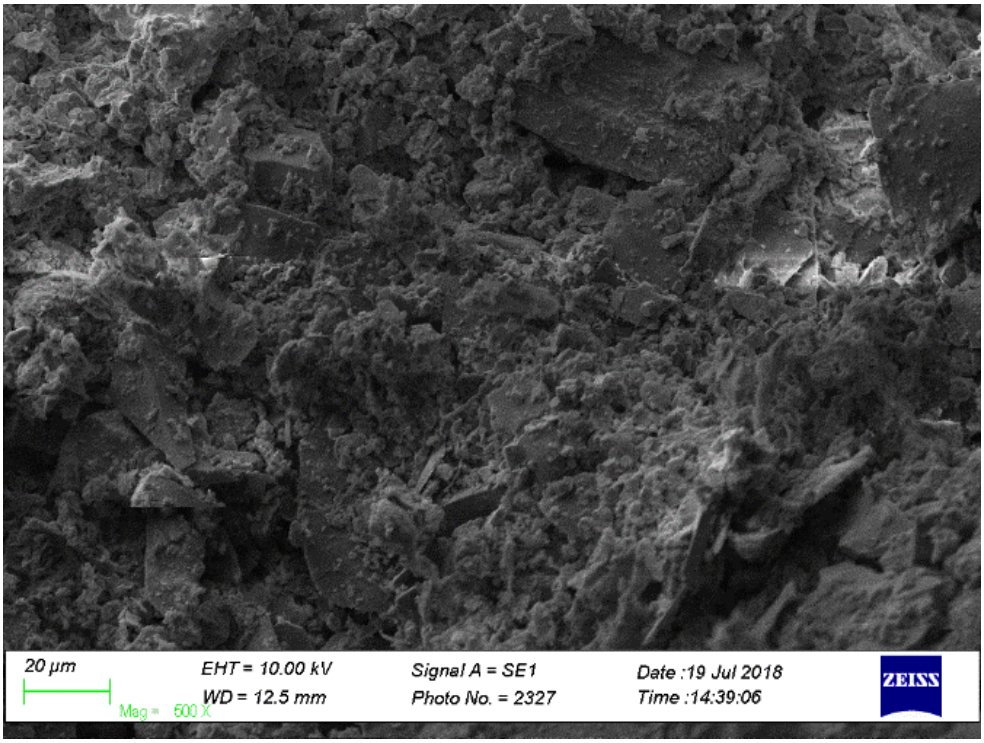

Figure 5.25. SEM image of OPC/Slag-CPB cured at 2°C (500X magnification).

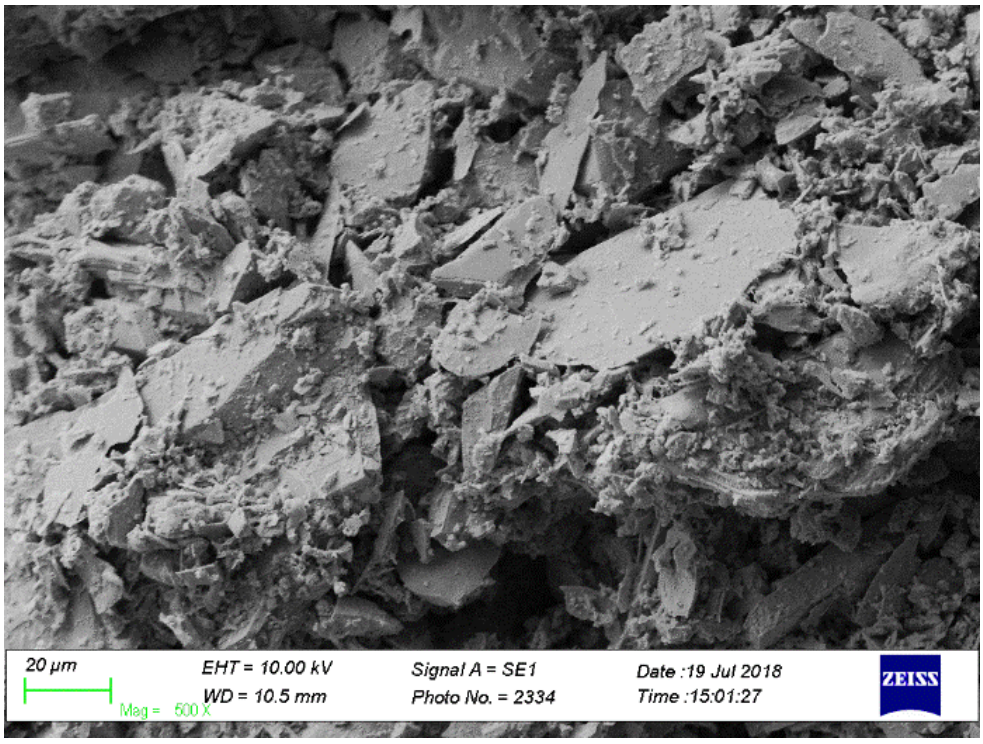

Figure 5.26. SEM image of OPC/Slag-CPB cured at 20°C (500X magnification)

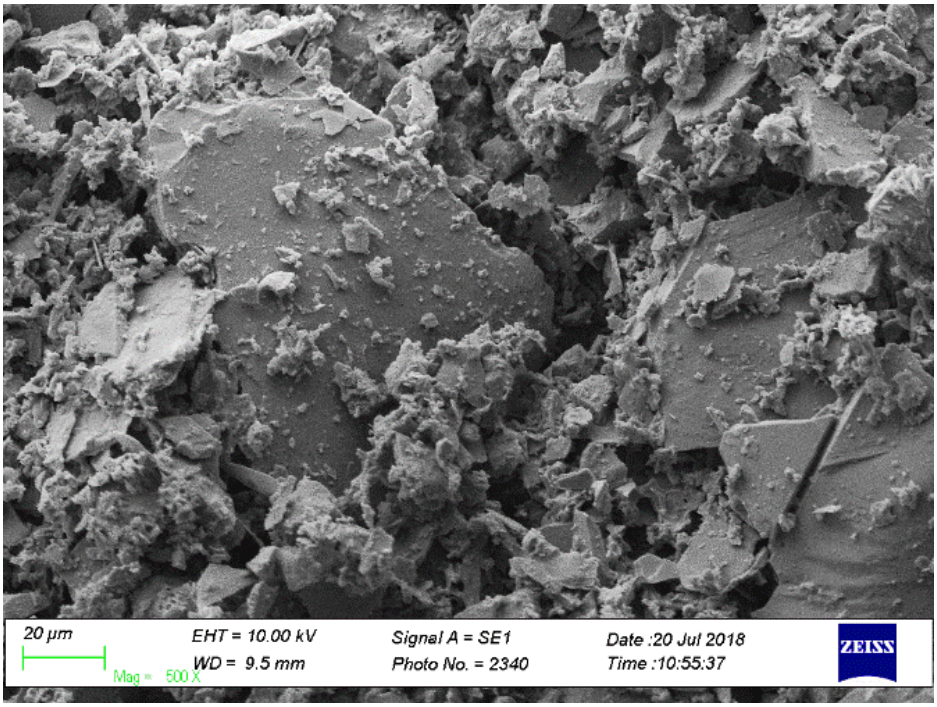

Figure 5.27. SEM image of OPC/Slag-CPB cured at 35°C (500X magnification)

The threshold pore diameter is the parameter with the greatest influence on fluid transport, and diffusion in a CPB system, as discussed in previous sections. The threshold pore diameters for the 2°C, 20°C, and 35°C OPC/Slag CPBs were 4.8 µm, 6.1 µm, and 11 µm respectively (Figure 5.30). 6.1 percent of the pore volume within the 2°C OPC/Slag-CPB was greater than d_{th}, which corresponds to 0.018 cc/g. The 20°C OPC/Slag-CPB had a 4.6 percent of the pore volume greater then d_{th}, which resulted in 0.013 cc/g of pores conductive to fluid transport. 5.7 percent of the pore space in the 35°C OPC/Slag-CBP was greater than d_{th}, which is equal to 0.015 cc/g. This means that there is a decrease in connective pores as curing temperature increases. The combined influence of d_{th} and the volume of pores greater then d_{th} likely influence the diffusion of arsenic due to an increased D_e as described by Garboczi (1989). These results are congruent with the observed cumulative mass leached (Figure 5.21). As threshold diameter decreases, the cumulative mass of arsenic leached increases. This agrees with Garboczi (1989) that threshold diameter is of more interest with respect to diffusion-based leaching compared to other porosity measurements, such as total pore volume or critical pore diameter.

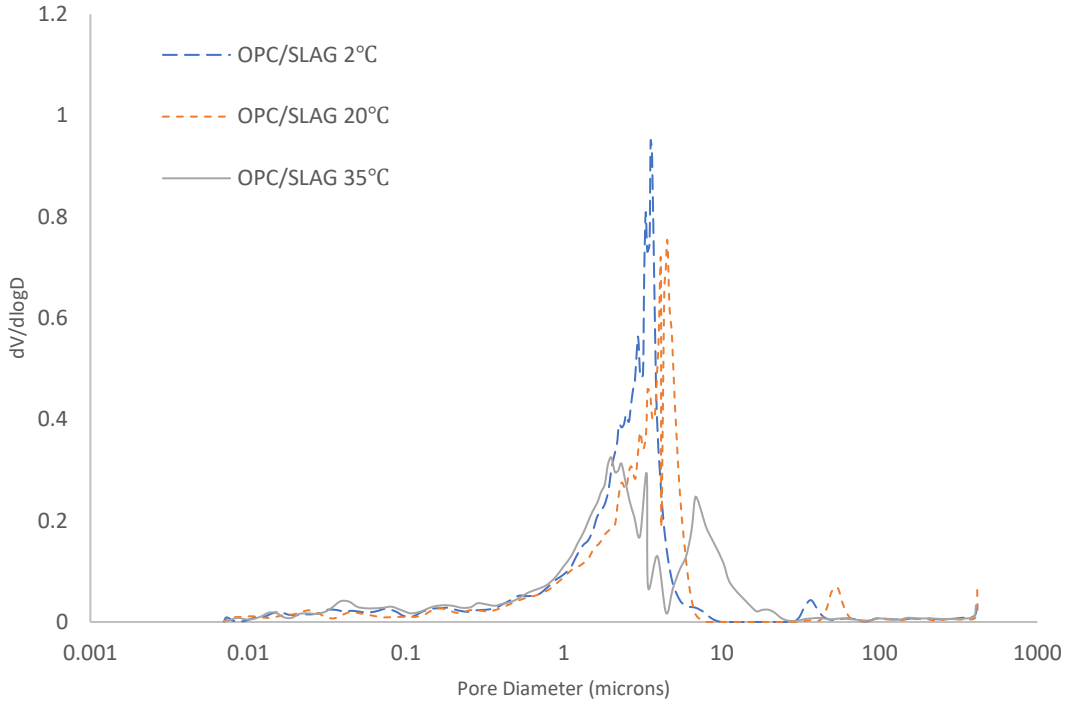

Figure 5.28. MIP data highlighting pore size distribution of OPC/Slag-samples.

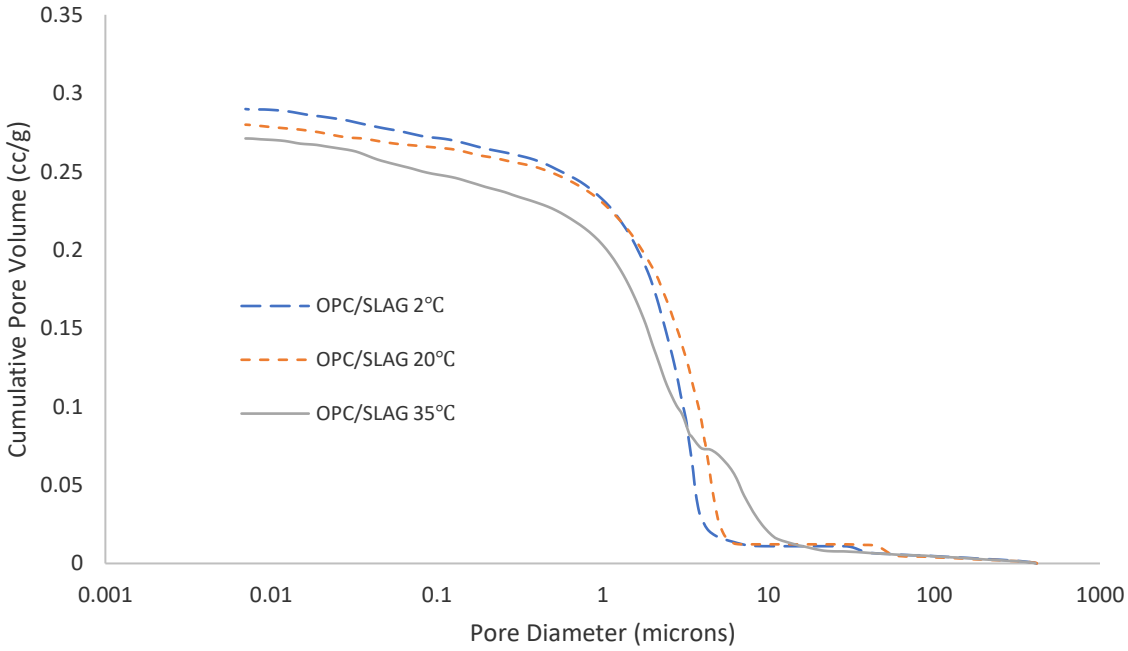

Figure 5.29. Cumulative intrusion curves for OPC/Slag-samples.

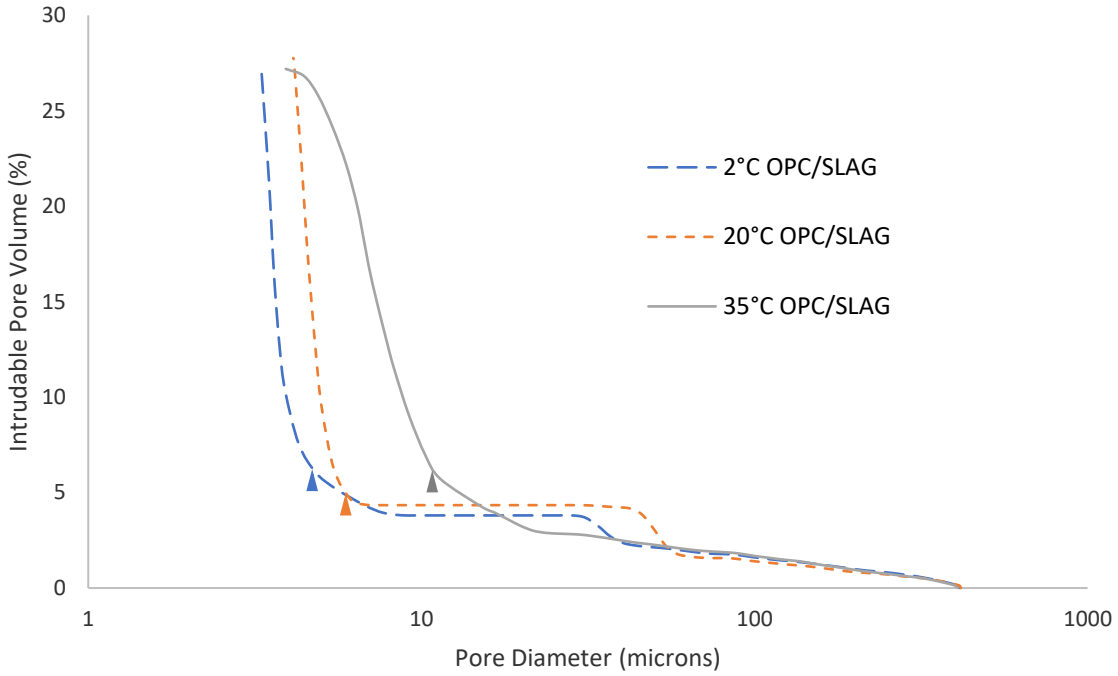

Figure 5.30. Cumulative porosity curve for OPC/Slag-CPBs with triangle markers indicating the inflection point representative of threshold pore diameter.

PXRD was conducted on OPC/Slag-CPBs as displayed in Figures 5.31 through 5.33. The results show that there were differences in phase formation at all three curing temperatures. This can be seen at low angles (less than 30 degrees 2-theta – Cu Kα radiation). Relative quantities of ettringite, CH, and gypsum are lowest for the 2°C OPC/Slag-CPB (Figure 5.31). However, the 2°C OPC/Slag-CPB has the greatest relative quantity of Ca_2SiO_4. Figure 5.32 shows that Ca_2SiO_4 was detected in the 20°C OPC/Slag-CPB, but not the 35°C OPC/Slag-CPB (Figure 5.33). Development of monosulfate is evident in in the 20°C OPC/Slag-CPB, with a more significant amount in the 35°C OPC/Slag-CPB. There was no detection of monosulfate in the OPC/Slag-CPB cured at 2°C. At angles greater than 30 degrees 2-theta Cu Kα radiation the differences in the diffraction pattern are less notable, with consistent relative quantities of CH, C-S-H, $CaCO_3$, $CaSO_4$, and ettringite.

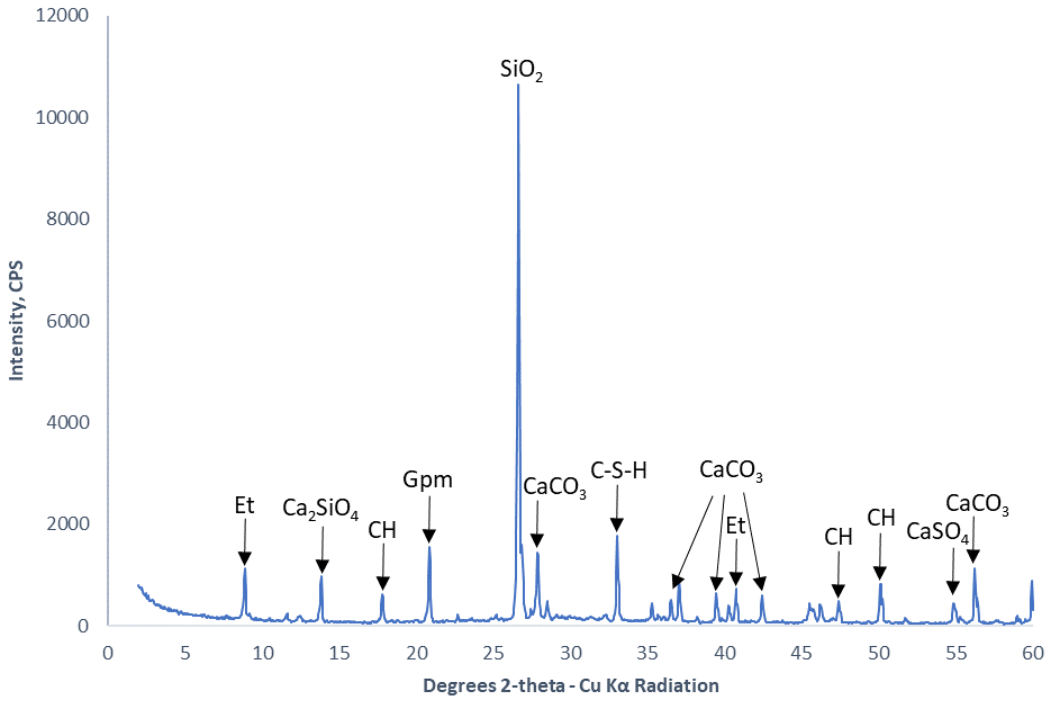

Figure 5.31. PXRD diffractogram for 2°C OPC/Slag-CPB.

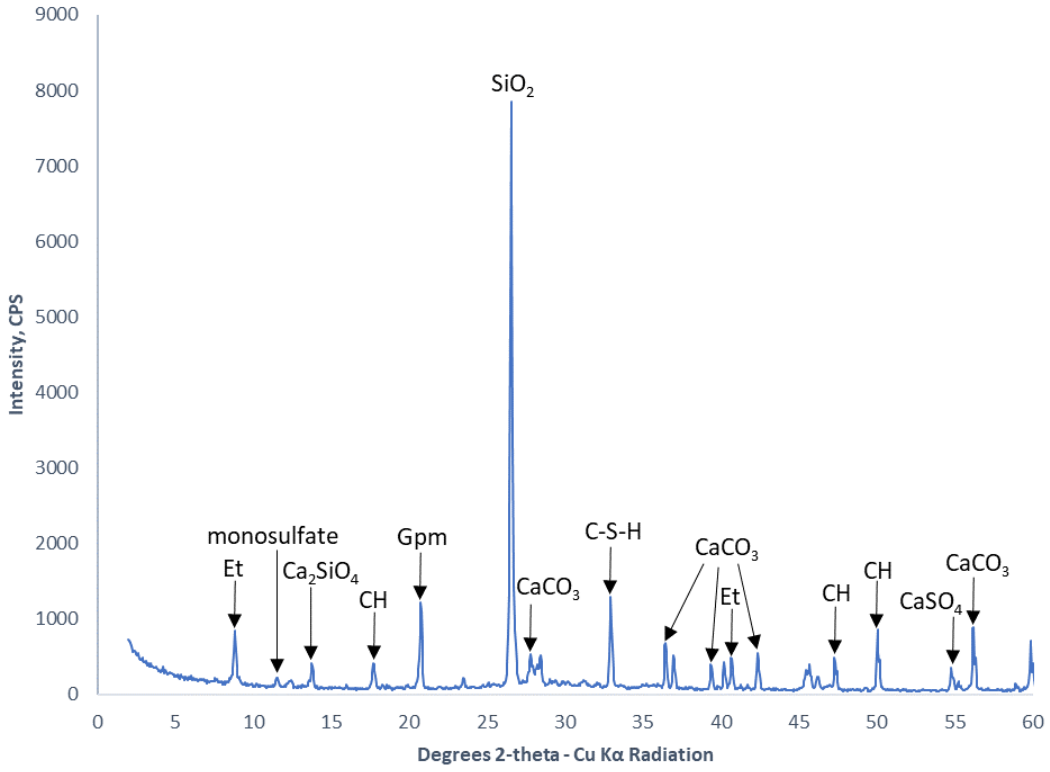

Figure 5.32. PXRD diffractogram for 20°C OPC/Slag-CPB.

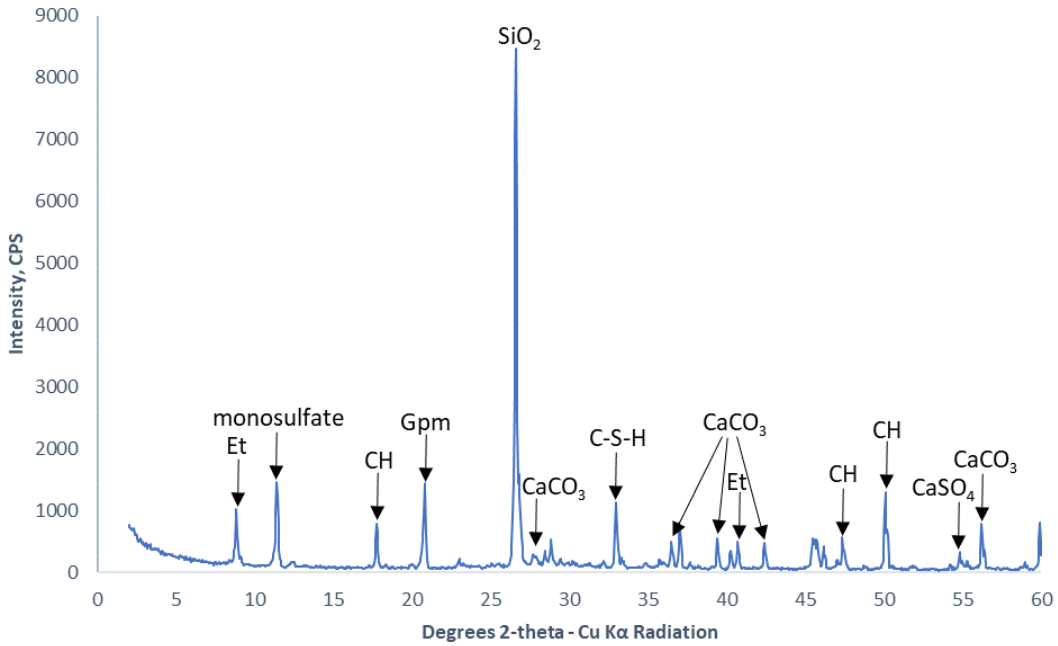

Figure 5.33. PXRD diffractogram for 35°C OPC/Slag-CPB.

5.3.4.2 Discussion and support from past research

As discussed previously, past research that has found that both C-S-H and $Ca(OH)_2$ are responsible for the immobilization of As(III) in a cement stabilized material (Stronarch et al. 1997). In CPB cured at low binder proportions using OPC/BFS mixed at a 50% blending ratio one can expect less available $Ca(OH)_2$ due to consumption during hydration, through the empirical reaction explained in section 2.11.4. $Ca(OH)_2$ is consumed leaving C-S-H to limit the mobility of As(III) through its sorption (Lui et al. 2017; Stronach et al. 1997). PXRD diffractograms agree with this research, showing relatively less CH in the OPC/Slag-CPBs compared to the OPC-CPBs. Certainly, there are still detectable quantities of CH in the OPC/Slag-CPBs. This may contribute to the overall increase in cumulative mass leached from samples cured at all three curing temperatures. It is assumed that arsenic bearing phases that are responsible for arsenic leachability are dominant in OPC/Slag-CPBs due to the quantity of arsenic leached. Kundu and Gupta (2008) describe CH as the primary hydration product responsible for immobilizing arsenic through pozzolanic reactions. Although no arsenic bearing phases

were detected by PXRD with certainty, it is expected that arsenic is doped to CH peaks, and other uncharacterized peaks. The combined effect of the arsenic bearing phases present in the hydration products, and the porosity characteristics are expected to be accountable for the difference in arsenic leached in the CPBs cured at different temperatures.

The porosity characteristics, specifically the threshold pore diameter, and pore volume greater than d_{th}, also likely play a significant role in the leachability of OPC/Slag-CPBs. The expected result of an increase in cumulative mass leached with decreasing threshold pore diameter based on the relationship between D_e and d_{th} as described by Garboczi (1989) was observed. Of the CPBs cured with the OPC/Slag binder, the greatest threshold pore diameter observed was in the CPB cured at 35°C. This CPB also showed the lowest cumulative mass leached of this group. This suggests that the reduction in continuous pores left much of the arsenic bound within the monolith, due to the reduced contact with percolating pore water. At lower temperatures the threshold pore diameter decreased, meaning there was an increased pore volume available for ion transfer. Thus, D_e presumably increased and resulted in the increased cumulative mass leached as highlighted in Figure 5.21.

5.3.4.3 Discussion of the Leaching Mechanism

Like the CPBs cured with OPC as the sole binder the OPC/Slag-CPBs experienced diffusion as the dominant leaching mechanism. Again, this is supported by the linear relationship of the graphs cumulative mass leached as a function of the square root of leaching time and, Log (Rd) as a function of Log (t). These charts are displayed as Figures 5.34 through 5.36. Like the samples cured using OPC as a binder, this result is supported by Kundu and Gupta (2008). R^2 values ranging from 0.97-0.99 show a strong linear relationship with respect to both plots.

(a)

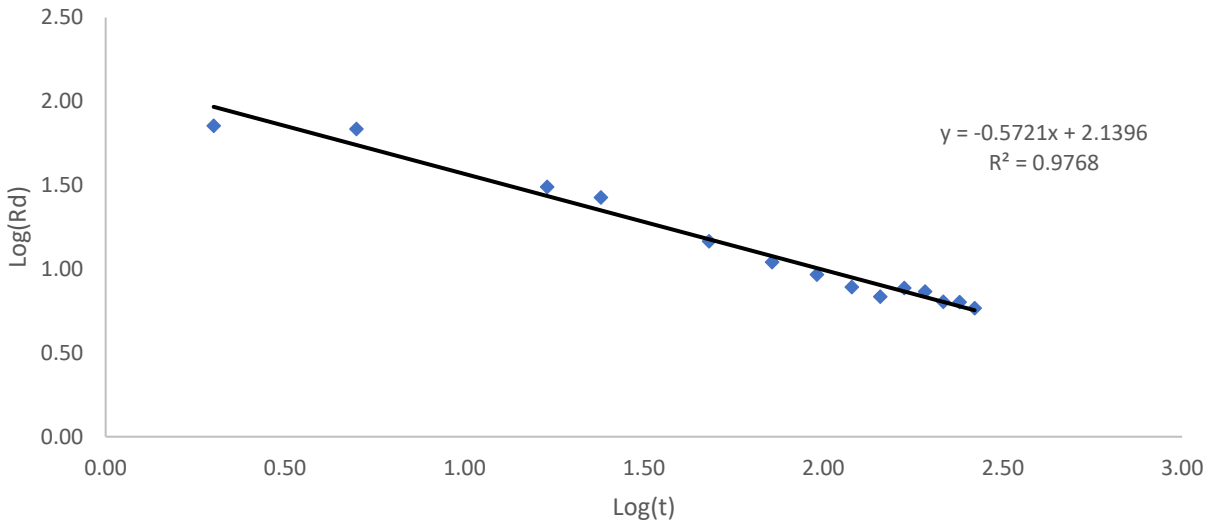

(b)

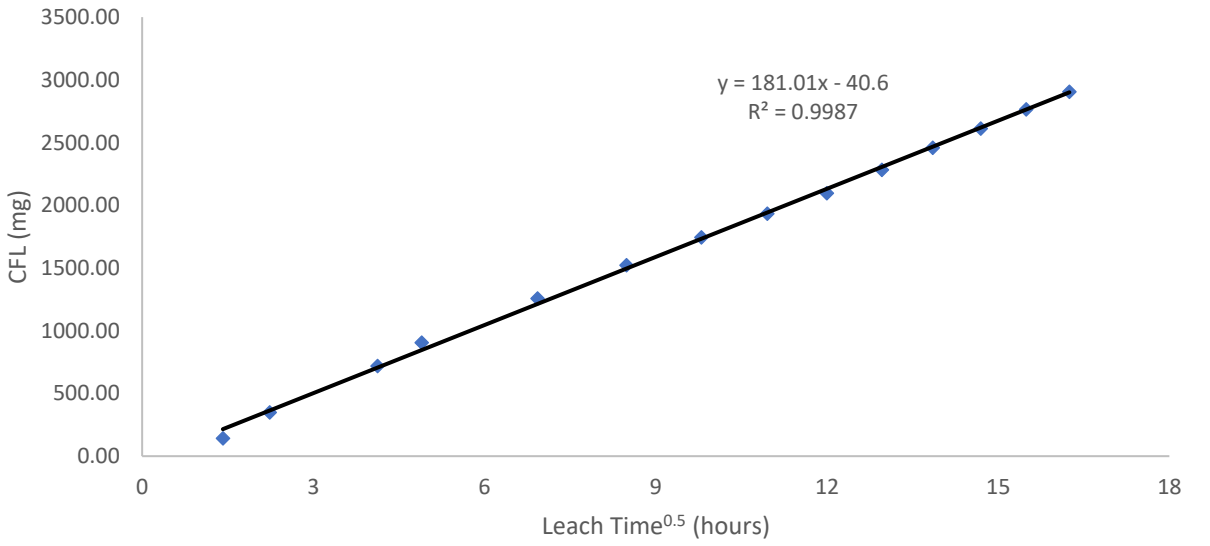

Figure 5.34. (a) Plot of Log rate of mass removal as a function Log time for the OPC/Slag-CPB cured at 2°C (Rd: rate of mass removal). (b) Plot of cumulative mass leached as a function the square root of leaching time for the OPC/Slag-CPB cured at 2°C. (CML: cumulative mass leached).

(a)

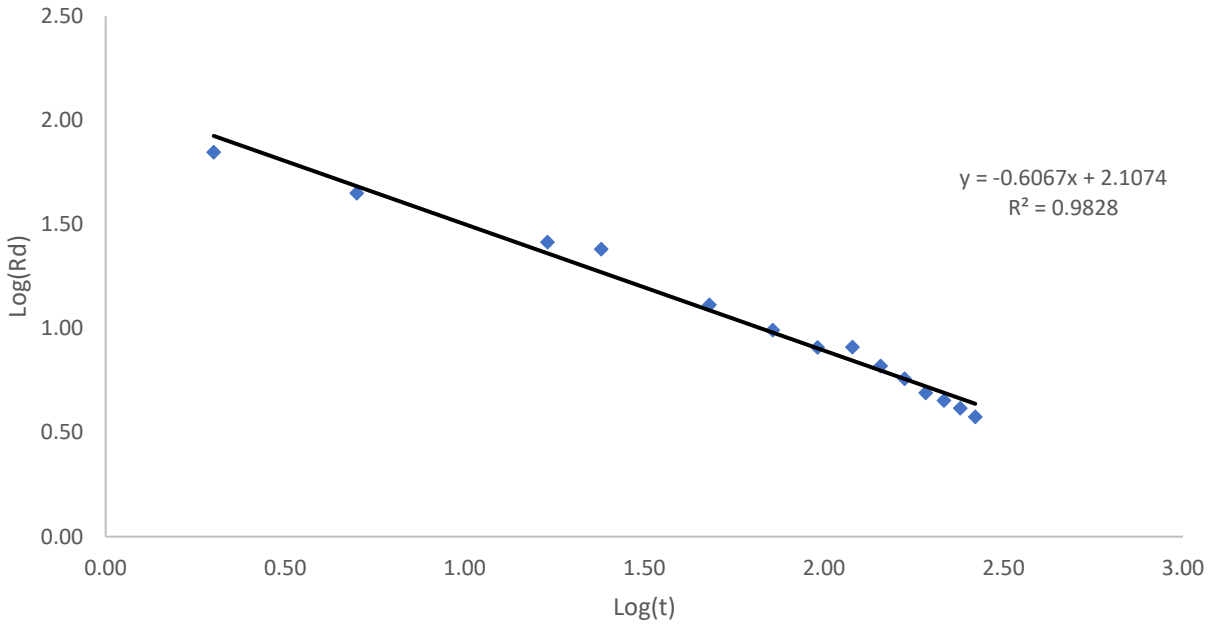

(b)

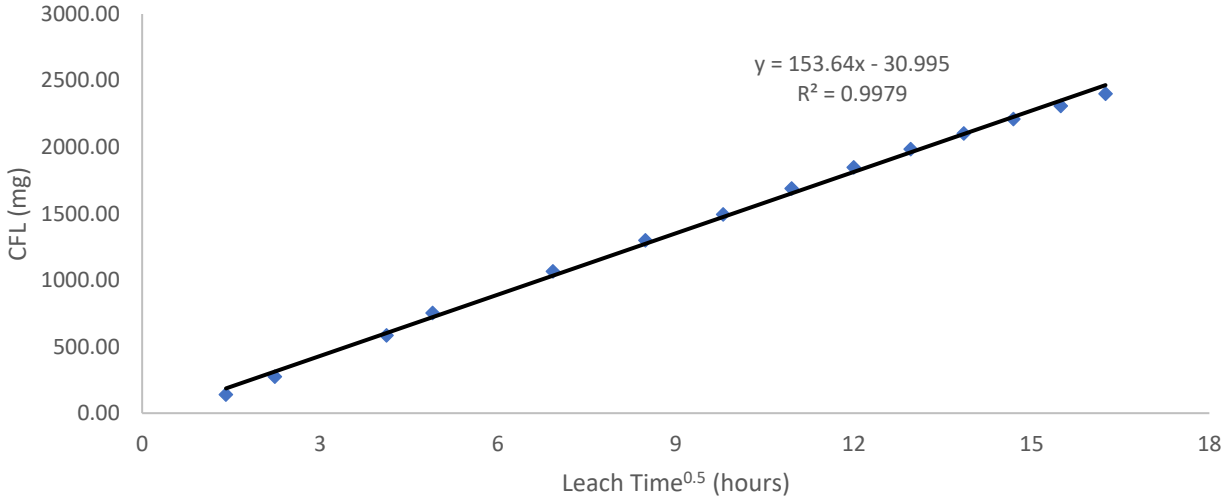

Figure 5.35. a) Plot of Log rate of mass removal as a function Log time for the OPC/Slag-CPB cured at 20°C (Rd: rate of mass removal). (b) Plot of cumulative mass leached as a function the square root of leaching time for the OPC/Slag-CPB cured at 20°C (CML: cumulative mass leached).

(a)

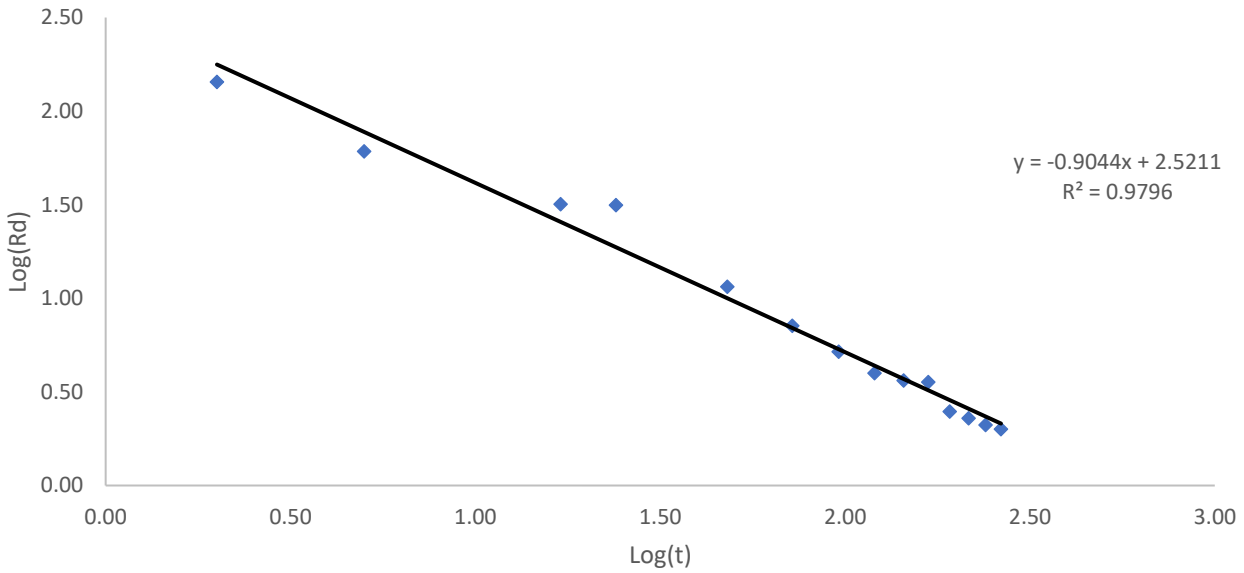

(b)

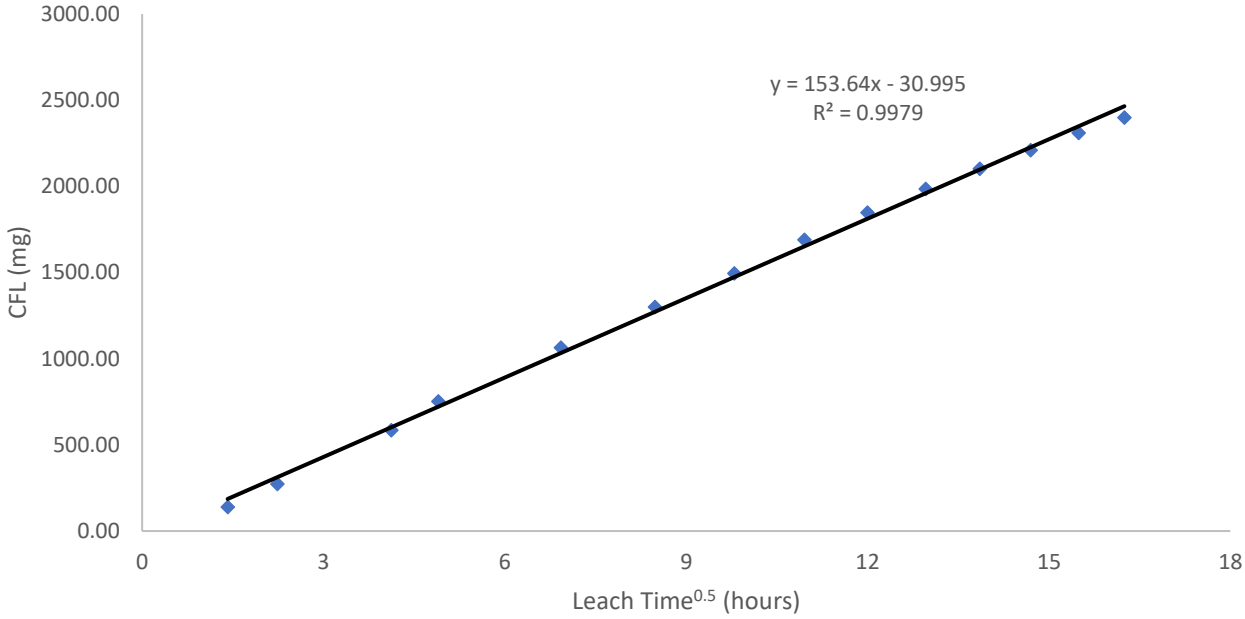

Figure 5.36. (a) Plot of Log rate of mass removal as a function Log time for the OPC/Slag-CPB cured at 35°C (Rd: rate of mass removal). (b) Plot of cumulative mass leached as a function the square root of leaching time for the OPC/Slag-CPB cured at 35°C (CML: cumulative mass leached).

5.4 Comparison and Discussion of Binder Choice

Past literature (e.g., Coussy et al. 2011; Stronarch et al. 1997; Hamberg et al. 2017) suggests that the mobilization of As(III) from cement stabilized materials is governed by the availability of C-S-H and $Ca(OH)_2$ within the matrix. The sorptive properties of C-S-H and binding properties of $Ca(OH)_2$ together provide optimal conditions for arsenic immobilization in the cement matrix. Blended binders can result in the increased consumption of $Ca(OH)_2$ during curing, thus reducing its availability to aid in the binding of arsenic to insoluble forms (Stronarch et al. 1997). Past researchers (Coussy et al. 2011; Hamberg et al. 2017) suggest that increasing $Ca(OH)_2$ content can stabilize As in CPB. Furthermore Coussy et al. 2011 conducted leaching test on CPB cured using OPC, OPC/Fly Ash, and OPC/Slag. The OPC/Slag mix was blended at 20% OPC, 80% Slag. Arsenic stabilization was best seen in the OPC samples. Results were intermediate for the OPC/Slag CPB and OPC-Fly Ash CPB yielded the least immobilization capacity for arsenic. The cause of this difference is explained by the difference in the formation of arsenic bearing compounds. In the OPC samples calcium arsenates formed, while OPC-Slag samples were dominated by the physical entrapment of arsenopyrite in the C-S-H matrix.

The incorporation of As(III) to a cement stabilized material can be achieved by physical encapsulation or chemical inclusion (Dermatas and Meng 1996; Cocke 1990). Physical encapsulation refers to the inclusion in the cement matrix without chemical interaction. Chemical inclusion refers to the incorporation of As(III) to pozzolanic products formed during hydration. Sorption also plays a role in how As(III) is incorporated in the cement stabilized matrix (Dermatas and Meng 1996). Cocke (1990), further suggests heavy metals can be incorporated in cement stabilized matrices by chemisorption, precipitation, inclusion, chemical incorporation, surface compounds, and other unknown forms as displayed in Figure 5.37. This figure may be interpreted as a representation of the hydration products formed amongst the natural tailings within a CPB system. Cement chemistry is complex, leading to the various outlined possibilities for incorporation of hazardous materials in the cement matrix, which is dependent on the curing conditions (Cocke 1990). The effect of curing temperature and choice of

binder are considerable factors regarding the dominant physical or chemical mechanisms responsible for binding As(III).

The chemistry of the binder governs the chemistry of the resulting hydration products. Portland cements are composed primarily of four compounds; C_3SiO_5 50-70 wt%, Ca_2SiO_4 20-30 wt%, $Ca_3Al_2O_6$ 5-12 wt%, and $Ca_4Al_2Fe_2O_{10}$ 5-12 wt%. Hydration of these compounds results in the solution being saturated with respect to KOH, NaOH, and $Ca(OH)_2$ during early curing stages. Further curing results in C-S-H formation. The ion chemistry of C-S-H is important because it provides sites for ion exchange with metals ions, meaning chemisorption is controlled by the surface structure and presence of C-S-H (Cocke 1990).

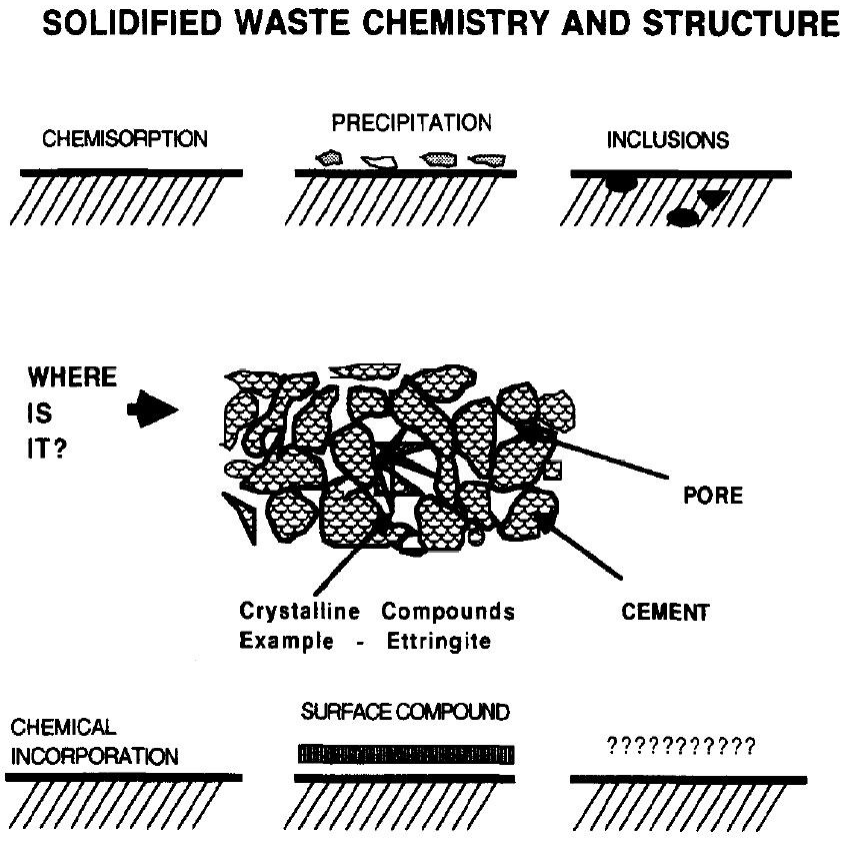

Figure 5.37. Potential sites for heavy metal additions to cement stabilized materials (Cocke 1990).

Blast furnace slag, a co-product of iron production, has a chemical makeup that shows latent hydraulic activity, making it a suitable for incorporation with Portland cements. The four dominant compounds that make up slag are CaO 35-38 wt%, SiO_2

33-35 wt%, Al_2O_3 17-20 wt%, and MgO 6-8 wt% (Liu et al. 2017; Prasad et al. 2018). XRD results from Lui et al. (2017) suggest that BFS produces both CH and C-S-H during early hydration stages as C_3S and C_2S are consumed. At later curing times (28 days) CH is consumed, suggesting as curing progresses C-S-H is available for sorption of As(III), however the availability of CH for chemical interactions is limited. As CH is consumed in a binder containing slag there is less opportunity for As(III) to be stabilized by the matrix because the system is relying on primarily on the sorptive capacity of the C-S-H.

Based on the chemistry of the OPC and slag hydration, slag substitutions limit the immobilization capacity of a cement stabilized material with respect to arsenic. The hydration of OPC alone yields a higher quantity of unconsumed CH while still providing an ample amount of C-S-H to take advantage of the properties of each product. Diffusion is the dominant leaching mechanism with respect to As(III) in a CPB system as suggested by the findings of this experiment. Higher OPC content yields a greater immobilization of arsenic by chemically binding the arsenic to hydration products. This limits the availability of As(III) for diffusion resulting in an increased immobilization performance when comparing CPBs produced with OPC and OPC/Slag of equal mixing ratios.

The pore distributions differed greatly between the OPC-CPBs and the OPC/Slag-CPBs. The threshold pore diameter of the OPC-CPBs were greater than or equal to the threshold diameters of the OPC/Slag-CPBs cured at equivalent temperatures. This suggests that the threshold pore diameter plays a considerable role in diffusion based arsenic leachability since the samples with greater threshold pore diameters (or pore volumes at $d > d_{th}$) exhibited significantly less leaching. However, it should be noted that the 35°C OPC-CPB and 35°C OPC/Slag-CPB had the same observed threshold pore diameter (11 μm) and the OPC-CPB leached substantially less arsenic, therefore supporting previous statements that the arsenic bearing phases formed in hydration reactions play a critical role in arsenic mobility during mature age leaching.

Chapter 6 – Conclusion and Recommendation for Future Research

The principal finding from this study is that in an CPB system cured with 4.5 wt% binder an OPC binder outperforms an OPC/Slag binder blended at 50 percent within the curing temperature range of 2°C to 35°C, by substantial margins. Although statistical conclusions cannot be made due to the lack of replaces utilized in this research, OPC is recommended as a binder in situations where the principal design parameter is immobilizing As(III). This statement is supported by subsequent important findings.

There was in an increase in the performance of the studied OPC-CPB in immobilizing As(III) at lower curing temperatures between the range of 2°C and 35°C. Cumulative mass of arsenic leached from the OPC-CPB cured at 2°C was 808.8 mg compared to 1058.5 mg at 35°C. The difference between the cumulative mass leached between the 2°C and 20°C OPC-CPB was insignificant at the experimental scale.

OPC/Slag-CPB showed the opposite effect when exposed to curing temperatures between 2°C and 35°C. As(III) immobilization was greater at 35°C (2128.2 mg leached) compared to 2°C (2906.2 mg leached). Ultimately the performance of arsenic immobilization was greatly reduced when the OPC binder was supplemented with 50% Slag.

Leaching of As(III) from both OPC and OPC/Slag CPB is dominated by diffusion. This mechanism of metals leaching through the diffusion process has been well documented by previous researchers (e.g., Kundu and Gupta 2008; Ekström 2003; Garboczi 1989). Observations from this research support these previous works.

Past research (e.g., Coussy et al. 2011; Stronarch et al. 1997; Hamberg et al. 2017; Cocke 1990) suggests that As(III) is immobilized by the sorptive capacity of C-S-H, and the binding properties of CH. PXRD results from this research seemingly support this statement. However, this cannot be stated with great confidence since arsenic bearing phases are assumed to be doped to existing CH and C-S-H peaks. The capability of the Rigaku software was limited in determining the specific phases produced during hydration.

Threshold pore dimeter is an important material characteristic when considering leachability of arsenic in CPBs. Connectivity of pores is related to the threshold and critical diameters. These properties of the CPB were influenced by both curing temperature and binder composition. These properties do not stand alone as the parameters that govern leachability. The pore surface was also noted to influence the mobility of arsenic, by increasing the area of reaction sties. This finding was supported by Bishop et al. (1992).

As_2O_3 was the only source of arsenic used to supplement the arsenic content in the CPBs studied. Different arsenic sources may result in immobilization to be observed differently in a cement stabilized material. The solubility of the arsenic bearing phase used may change the expected results based on how the arsenic becomes bound by the CPB matrix during hydration. All arsenic bearing minerals cannot be expected to exhibit leaching behave similar to As_2O_3. In practice the properties of the arsenic bearing mineral phase present in the tailings should be considered. This research may be used to aid in understanding how arsenic bearing phases are expected to behave when subject to leaching in CPBs.

This research serves as preliminary findings on how curing temperature and binder composition influence leachability of CPB. Next research steps in this field should aim to use replicates and additional leaching tests for statistical conclusions to be made. It is recommended that future researchers consider different blending ratios and binder proportions to combine the optimization of both leaching characteristics and long-term strength of CPB structures. Both environmental and geotechnical performance must be considered when designing CPBs. Higher curing temperatures should also be analyzed because, as shallow reserves are depleted mining at greater depth will become more common practice. Mines will begin to exceed depths of 5000 meters. At such depths the geothermal gradient may produce rock temperatures exceeding 70°C (Fall et al. 2014). The effect of pressure during curing stages is also something that should be considered in future leaching experiments, to simulate stress conditions noticed in full scale backfill operations. Various mixing waters should be tested since initial temperature variations hydration waters many influence the curing of CPBs. Other non-standard leaching tests such as a variation of the triaxial leaching test

developed by Butcher et al. 1993 should be considered since the conditions of the test simulate ground water flow through a permeable vein between impermeable parent rock.

7. References

Al, T. 2017. Geochemistry of Natural Waters; GEO 5147 University of Ottawa [Lecture Notes]

Aldhafeeri, Z., and Fall, M. 2016. Time and damage induced changes in the chemical reactivity od cemented paste backfill. Journal of Environmental Chemical Engineering. 4, 4038-4049

Aldhafeeri, Z., Fall, M., Pokharel, M., Pouramini, Z. 2016. Temperature Dependence of the Reactivity of Cemented Paste Backfill. Applied Geochemistry 72. Elsevier Ltd: 10–19.

Aligizaki, K.K. 2006. Pore structure of Cement-Based Materials: Testing, Interpretation and Requirements. Taylor & Francis, London

Álvarez, R., Ordóñez, A., García R., Loredo, J. 2018. An estimation of water resources in flooded, connected underground mines. Engineering Geology 114-122.

Amaratunga, L.M., and Yaschyshyn, D.N. 1997. Development of a high modulus paste fill using fine gold mill tailings. Geotech. Geol. Eng. 15, 205–219.

ASTM. 2017. Standard Test Method for Accelerated Leach Test for Diffusive Releases from Solidified Waste and a Computer Program to Model Diffusive , Fractional Leaching from Cylindrical Waste (Vol. 08).

Azam, S., and Li, Q. 2010. Tailings dam failures: A review of the last one hundred years. Geotechnical News, 28(4), 50–53.

Balsubramanian, A. 2015. Overview of Mineral Processing Methods. Centre for Advanced Studies in Earth Science. University of Mysore.

Belem, T., and M. Benzaazoua. 2004. An Overview on the Use of Paste Backfill Technology as a Ground Support Method in Cut-and-Fill Mines. Proceedings of the 5th Int. Symp. on Ground Support in Mining and Underground Construction. Villaescusa & Potvin (Eds.), 637 – 650.

Bentz, D., Peltz, M. and Winpigler, J., 2009. Early-age properties of cement-based materials: II. Influence of water-to-cement ratio. ASCE Journal of Materials in Civil Engineering, 21(9): 512–517.

Bentz, D., Sant, G. and Weiss, W., 2008. Early-age properties of cement based materials: I. Influence of cement fineness. ASCE Journal of Materials in Civil Engineering, 20(7): 502–508.

Benzaazoua, M., Fall, M., and Belem, T. 2004. A Contribution to Understanding the Hardening Process of Cemented Pastefill. Minerals Engineering 17 (2): 141–52.

Benzaazoua, M., Fiset, J.F., Bussiere, B., Villeneuve, M., Plante, B. 2005. Sludge recycling within cemented paste backfill: Study of the mechanical and leachability properties. Minerals Engineering 19: 420-432

Benzaazoua, M., Belem T., and Bussière B., 2002. Chemical Factors That Influence the Performance of Mine Sulphidic Paste Backfill. Cement and Concrete Research 32 (7): 1133–44.

Benzaazoua, M., Bussière, B., Demers, I., Aubertin, M., Fried, É., Blier, A. 2008. Integrated Mine Tailings Management by Combining Environmental Desulphurization and Cemented Paste Backfill: Application to Mine Doyon, Quebec, Canada. Minerals Engineering 21 (4): 330–40.

Bernier, L.R. and Li, M. 2003. High temperature oxidation (heating) of sulfidic paste backfill: A mineralogical and chemical perspective, Proceedings of Sudbury 2003: Mining and Environment III Conference, held May 25-28 in Sudbury, Ontario, Canada.

Bishop P. L., Gong R., Tim C. Keener (1992). Effects of leaching on pore size distribution of solidified/ stabilized wastes. Journal of Hazardous Materials, 31 (1992) 59-74

Blight, G.E., and Bentel, G.M. 1983. The behaviour of mine tailings during hydraulic deposition. Journal of The South African Institute of Mining and Metallurgy, (APRIL), 73–86.

Bullard, J.W., Jennings, H.M., Livingston, R.A., Nonat, A., Scherer, G.W., Schweitzer, J.S., Scrivener, K.L., Thomas, J.J., 2011. Mechanisms of cement hydration. Cement and Concrete Research 41, 1208-1223.

Butcher, E.J., Cheeseman, C.R., Sollars, C.J., Perry, R. 1993. Flow-through Leach Testing of Solidified Waste Using a Modified Triaxial Cell. Environmental Technology 14 (2013): 113–24.

Chen, W. 2006. Hydration of Slag Cement: Theory, Modeling and Application. Ph.D. Thesis University of Twente, The Netherlands

Cocke, D.L. 1990. The Binding Chemistry and Leaching Mechanisms of Hazardous Substances in Cementitious Solidification / Stabilization Systems. Journal of Hazardous Materials, 24, 231–253.

Cooke, D.L., Mollah, M.Y.A., Parga, J.R., Hess, T.R., Ortego, J.D. 1991. An XPS and SEM/EDS characterization of leaching effects on lead-and zinc-doped portland

cement. Journal of Hazardous Materials, 30: 83-95

Conner, J.R. 1990 Chemical Fixation and Solidification of Hazardous Wastes. Van Nostrand Reinhold, New York, p. 104.

Coussy, S., Benzaazoua, M., Blanc, D., Moszkowicz, P., Bussière, B., 2011. Arsenic stability in arsenopyrite-rich cemented paste backfills: a leaching test-based assessment. Journal of Hazardous Materials 185;1467–1476

Cui, L., and Fall, M. 2016. An Evolutive Elasto-Plastic Model for Cemented Paste Backfill. Computers and Geotechnics 71. Elsevier Ltd: 19–29.

Dell'Orso, M., Mangialardi, T., Paolini, A.E., Piga, L. 2012. Evaluation of the Leachability of Heavy Metals from Cement-Based Materials. Journal of Hazardous Materials 227–228. Elsevier B.V.: 1–8.

Dermatas, D., and Meng, X. 1996. Stabilization/Solidification (S/S) of Heavy Metal Contaminated Soils by Means of a Quicklime-Based Treatment Approach Stabilization and Solidification of Hazardous, Radioactive, and Mixed Wastes. ASTM STP 1240, American Society for Testing and Materials, Philadelphia, pp. 449–513.

Double, D., Hewlett, P., Sing, K., Raffle, J., 1983. New developments in understanding the chemistry of cement hydration and discussion. Philosophical Transactions of the Royal Society of London A: Mathematical, Physical and Engineering Sciences 310, 53-66.

Drage, J. 2015. Review of the Environmental Impacts of Historic Gold Mine Tailings in Nova Scotia.

Ekström, T. 2003. Leaching of Concrete: The Leaching Process and Its Effects. Ph.D Thesis. Lund University. Lund Sweden.

Elkhadiri, I., Palacios, M., and Puertas, F., 2009. Effect of curing temperature on cement hydration, Ceramics-Silikáty, 53(2): 65-75.

Escadeillas, G., Aubert, J.E., Segerer, M., Prince, W. 2007. Some factors affecting delayed ettringite formation in heat-cured mortars. Journal of Cement and Concrete Research 37 1445-1452

Fall, M. 2017. Geotechnical Hazards; CVG 5314 University of Ottawa [Lecture Notes]

Fall, M., Adrien, D., Célestin, J.C., Pokharel, M., Touré, M. 2009. Saturated Hydraulic Conductivity of Cemented Paste Backfill. Minerals Engineering 22 (15). Elsevier Ltd: 1307–17.

Fall, M., and Benzaazoua, M. 2005. Modeling the Effect of Sulphate on Strength Development of Paste Backfill and Binder Mixture Optimization. Cement and Concrete Research 35 (2): 301–14.

Fall, M., Benzaazoua, M. and Saa, E.G. 2008. Mix Proportioning of Underground Cemented Tailings Backfill. Tunnelling and Underground Space Technology 23 (1): 80–90.

Fall, M., Célestin, J.C., Pokharel, M., Touré, M. 2010. A Contribution to Understanding the Effects of Curing Temperature on the Mechanical Properties of Mine Cemented Tailings Backfill. Engineering Geology 114 (3–4). Elsevier B.V.: 397–413.

Fall, M., and Samb, S.S. 2009. Effect of High Temperature on Strength and Microstructural Properties of Cemented Paste Backfill. Fire Safety Journal 44 (4): 642–51.

Fall, M., Wu, D., and Pokharel, M. 2014. Effect of deep mine temperature conditions on the heat development in cemented paste backfill and its properties. In Deep Mining 2014 (pp. 0–5).

Fashola, M.O., Ngole-jeme, V.M., and Babalola, O.O. 2016. Heavy Metal Pollution from Gold Mines : Environmental Effects and Bacterial Strategies for Resistance. International Journal of Environmental Research and Public Health.

FCSAP. 2010. Guidance Document on Federal Interim Groundwater Quality Guidelines for Federal Contaminated Sites. http://ec.gc.ca/Publications/default.asp?lang=En&xml=423951F2-3B17-4348-A71C-62A7DB96D1D6.

Fetter, C.W., 2013. Applied Hydrogeology, 4th Edition. Pearson Prentice Hall, USA..

Flora, S.J.S. 2015. Arsenic: Chemistry, Occurrence, and Exposure. Handbook of Arsenic Toxicology.

Gandhi, S.M., and Sarkar, B.C., 2016. Essential of Mineral Exploration and Evaluation. Elsevier

Garboczi, E.J. 1989. Permiability, Diffusivity, and Microstructural Parameters: A Critical Review. Cement and Concrete Research . 20. 591 – 601.

Ghirian, A. 2016. Coupled Thermo-Hydro-Mechanical-Chemical (THMC) Processes in Cemented Tailings Backfill Structures and Implications for Their Engineering Design. Ph.D Thesis. University of Ottawa. Ottawa Canada.

Ghirian, A., and Fall, M. 2015. Strength Evolution and Deformation Behaviour of Cemented Paste Backfill at Early Ages: Effect of Curing Stress, Filling Strategy and Drainage. International Journal of Mining Science and Technology. China

University of Mining & Technology.

Ginebra, M.P., Driessens, F.C.M., and Planell, J.A., 2004. Effect of the particle size on the micro and nanostructural features of a calcium phosphate cement: a kinectic analysis. Biomaterials, 25(17): 3453-62.

Goto, S. and Roy, D.M., 1981. The Effect of W/C Ratio and Curing Temperature on the Permeability of Hardened Cement Paste. Cement and Concrete Research, 11(4): 575-580.

Government of Canada. 2018. Arsenic trioxide and underground issues at Giant Mine. 04 13. https://www.aadnc-aandc.gc.ca/eng/1100100027413/1100100027417#how.

Grice, T., 2001. Recent mine developments in Australia. Proceeding of the 7th International Symposium on Mining with Backfill (MINEFILL), pp. 351–357.

Hamberg, R. 2018. Cementation of cyanidation tailings – Effects on the release of As, Cu, Ni and Zn. Ph.D Thesis. Luleå University of Technology. Luleå, Sweden.

Hamberg, R., Maurice, C., and Alakangas, L. 2017. Lowering the water saturation level in cemented paste backfill mixtures – Effect on the release of arsenic. Minerals Engineering 112 (February). Elsevier: 84–91.

Halim, C.E., Amal, R., Beydoun, D., Scott, J.A., Low, G. Implications of the structure of cementitious wastes containing Pb(II), Cd(II), As(V), and Cr(VI) on the leaching of metals, Cem. Concr. Res. 34 (2004) 1093–1102.

Health Canada. 2012. Guidelines for Canadian Drinking Water Quality Summary Table Prepared by the Federal-Provincial-Territorial Committee on Drinking Water of the Federal-Provincial-Territorial Committee on Health and the Environment March 2006. Environments.

Kagambega, N,, Sawadogo, S., Bamba, O., Zombre, P., Galvez, R. 2014. Acid Mine Drainage and Heavy Metals Contamination of Surface Water and Soil in Southwest Burkina Faso – West Africa. International Journal of Multidisciplinary Academic Research 2 (3): 9–19.

Kjellsen, K.O., Detwiler, R.J. and Gjørv, O.E., 1990. Pore structure of plain cement pastes hydrated at different temperatures, Cement and Concrete Research, 20(6): 927–933.

Kogbara, R.B., Al-Tabbaa, A., and Stegemann, J.A. 2013. Relating Monolithic and Granular Leaching from Contaminated Soil Treated with Different Cementitious Binders. Journal of Environmental Science and Health - Part A Toxic/Hazardous Substances and Environmental Engineering 48 (12): 1502–15.

Kretschmar, U.H., and McBride, D. 2016. Felsic Volcanism Associated with Mineralization in the Chester Complex-Type Gold Deposits. In The Metallogeny of Lode Gold Deposits, 137–50. Elsevier Inc.

Kundu, S., and Gupta, A.K. 2008. Immobilization and leaching characteristics of arsenic from cement and / or lime solidified / stabilized spent adsorbent containing arsenic. Journal of Hazardous Materials, 153, 434–443.

Lin, F., and Meyer, C. 2009. Hydration kinetics modeling of Portland cement considering the effects of curing temperature and applied pressure. Cement and Concrete Research 39, 255-265.

Liu, J., Yu, Q., Zuo, Z., Yang, F., Duan, W., Qin, Q. 2017. Blast furnace slag obtained from dry granulation method as a component in slag cement. Construction and Building Materials, 131, 381–387.

Lothenbach, B., Matschei, T., Möschner, G., Glasser, F.P. 2008. Thermodynamic modelling of the effect of temperature on the hydration and porosity of Portland cement. Cement and Concrete Research, 38, 1–18.

Lottermoser, B. 2007. Mine Wastes. Mine Wastes (Second Edition): Characterization, Treatment and Environmental Impacts (Second). Berlin: Springer.

Ma, H. 2013. Mercury intrusion porosimetry in concrete technology: tips in measurement, pore structure parameter acquisition and application. Journal of Porous Materials 21: 207-215.

Mácsik, J., and A. Jacobsson. 1996. Leachability of V and Cr from LD-Slag/Portland Cement Stabilised Sulphide Soil. Waste Management 16 (8): 699–709.

Maltais, Y. and Marchand, J. (1997). Influence of Curing Temperature on Cement hydration and Mechanical Strength Development of Fly Ash Mortars, Cement and Concrete Research, 27(7): 1009-1020.

Martinson, M.J., 1977. Heat stress in Witwatersrand gold mines. Journal of Occupational Accidents, 1: 171-193.

McLeod, H. and Bjelkevik, A. 2017. Tailings Dam Design: Technology Update (ICOLD Bulletin), in Proceedings of the 85th Annual Meeting of International Commission on Large Dams, July 3-7, 2017. Prague, Czech Republic: Czech National Committee on Large Dams.

Nagaraj, D.R. 2005. Minerals Recovery and Processing. In Kirk-Othmer Encyclopedia of Chemical Technology (pp. 595–668). Hoboken, NJ, USA: John Wiley & Sons, Inc.

Narang, K.C. and Chopra, S.K. (1983). Studies on alkaline activation of BF, steel and

alloy slags, silicates industrials, Silicates Industriels 9: 175–182.

National Academy of Sciences, 1977. National Research Council (US) Committee on Medical and Biological Effects of Environmental Pollutants. Arsenic: Medical and Biologic Effects of Environmental Pollutants. Washington (DC): National Academies Press (US); 1977. 2, Chemistry of Arsenic.

Neville, A.M., 1995. Properties of Concrete. Pearson Education Limited. Harlow, England.

New Gold. 2017. New Afton - Geology, Exploration & Technical Reports. New Gold. http://www.newgold.com/operations/new-afton/geology-and-mineralization/default.aspx

Orejarena, L., and Fall, M. 2008. Mechanical Response of a Mine Composite Material to Extreme Heat. Bulletin of Engineering Geology and the Environment 67 (3): 387–96.

Ouellet, S., Bussière, B., Aubertin, M., Benzaazoua, M., 2007. Microstructural evolution of cemented paste backfill: mercury intrusion porosimetry test results. Cement and Concrete Research 37, 1654-1665.

Ouellet, S., Bussière, B., Mbonimpa, M., Benzaazoua, M., Aubertin, M., 2005. Reactivity and mineralogical evolution of an underground mine sulphidic cemented paste backfill. Mineral Engineering, 19(5): 407-419.

Pareja, L.D., 2000. Deep Underground Hard-Rock Mining – Issues, Strategies, and Alternatives. Ph.D Thesis. Queens University. Kingston, Ontario, Canada.

Pokharel, M. 2008. Geotechnical and Environmental Response of Paste Tailings Systems to Coupled Thermo-Chemical Loadings. Ph.D Thesis. University of Ottawa. Ottawa, Canada.

Poon, C.S., Chen, Z.Q. and Wai, O.W.H. 2001. The Effect of Flow-through Leaching on the Diffusivity of Heavy Metals in Stabilized/Solidified Wastes. Journal of Hazardous Materials 81 (1–2): 179–92.

Prasad, K., Srishilan, C., Kumar, A., Kaza, M. 2018. Thermodynamic assessment and experimental validation of clinker formation from blast furnace slag through lime addition. Ceramics International, 44(16), 19434–19441.

Rankine, R. and Sivakugan, N. 2007. Geotechnical properties of cemented paste backfill from Cannington Mine, Australia. Geotechnical and Geological Engineering, 25: 383–393.

Rawlins, CA and Phillips, HR. 2001, Reduction of mine heat loads, in S Wasilewski

(ed.), Proceedings of the 7th International Mine Ventilation Congress, Research & Development Center for Electrical Engineering and Automation in Mining, pp. 381-389.

Rennie, D.W., Bergen, R.D., and Krutzelmann, H. 2015. Technical Report on the New Afton Mine , British Columbia , Canada NI 43-101 Report. Vol. 1.

Richardson, J.M., Biernacki, J.J., Struzman, P.E., Bentz, D.P. 2002. Stoichiometry of Slag Hydration with Calcium Hydroxide. Journal of the American Ceramic Society 85 (4) 947-953

Roy, D.M., Gouda, G., Bobrowsky, A., 1972. Very high strength cement pastes prepared by hot pressing and other high pressure techniques. Cem Concr Res 2, 349-366.

Shahavari, M., and Grabinsky, M. 2016. Pore Water Pressure Variations in Cemented Paste Backfilled Stopes. Geo-Chicago Conference 2016

Singer, P., and Stumm, W. 1970. Acidic Mine Drainage : The Rate-Determining Step. American Association for the Advancement of Science, 167(3921), 1121–1123.

Soroka, I., 2003. Concrete in hot environments. CRC Press.

Stronach, S.A., Walker, N.L., Macphee, D.E., Glasser F.P. 1997. Reactions between cement and As(III) oxide: the system $CaO–SiO_2–As_2O_3–H_2O$ at 25°C, Waste Manage. 17 (1997) 9–13.

Swaddiwudhipong, S., Chen, D., Zhang, M., 2002. Simulation of the exothermic hydration process of Portland cement. Advanced Cement Research 14, 61-69.

Tabelin, C.B., Hashimoto, A., Igarashi, T., Yoneda, T. 2014. Leaching of boron, arsenic and selenium from sedimentary rocks: II. pH dependence, speciation and mechanisms of release. Science of the Total Environment, 473–474, 244–253.

Tariq, A., and Yanful, E.K. 2013. A Review of Binders Used in Cemented Paste Tailings for Underground and Surface Disposal Practices. Journal of Environmental Management 131. Elsevier Ltd: 138–49. doi:10.1016/j.jenvman.2013.09.039.

Taylor, H.F.W. (1997). Cement chemistry, 2nd edn, Thomas Telford Publishing, London, U.K.

Udd, J.E., 2006. A bibliography on deep mining. Proceedings of the Core Project on Deep Mining. 10p.

US EPA. 2013. National Primary Drinking Water Regulations. Drinking Water

Contaminants.

Usiyama, T, and Fukushi, K. 2016. Predictive Model for Pb(II) Adsorption on Soil Minerals (Oxides and Low-Crystalline Aluminum Silicate) Consistent with Spectroscopic Evidence. Geochimica et Cosmochimica Acta 190. Elsevier Ltd: 134–55.

Villaescusa, E., 2003. Global extraction sequences in sublevel stoping. MPES 2003 Conference, Kalgoorlie, April 2003

Vick, S. G. 1983. Planning, design, and analysis of tailings dams. Vancouver, Canada: BiTech.

Vollpracht, A., and Brameshuber, W. 2016. Binding and Leaching of Trace Elements in Portland Cement Pastes. Cement and Concrete Research 79. Elsevier Ltd: 76–92.

Waihi Gold, 2015. The Mining Process. http://www.waihigold.co.nz/mining/

Walker, N.L. 1993. Arsenic sorption by C-S-H. Technical report, Department of Chemistry, University of Aberdeen.

Washington State Department of Ecology. 2003. An Assessment of Laboratory Leaching Tests for Predicting the Impacts of Fill Material on Ground Water and Surface Water Quality. A Report to the Legislature.

Williams, T.J., Denton D.K., and Larson, M.K. 2001. Geomechanics of Reinforced Cemented Backfill in an Underhand Stope at the Lucky Friday Mine, Mullan, Idaho.

Wills, B.A., and Finch, J.A. 2015. Wills' Mineral Processing Technology : An Introduction to the Practical Aspects of Ore Treatment and Mineral Recovery (8th ed.). Butterworth-Heinemann.

Winslow, D.N., and Diamond, S. 1970. A mercury porosimetry study of the evolution of porosity in portland cement, Journal of Materials. 5(3) 564 – 584.

Winter, N.B., 2012. Understanding cement: An introduction to cement production, cement hydration and deleterious processes in concrete. Microanalysis Consultants.

Wu, A., Wang, Y., Wang, H., Yin, S., Miao, X. 2015. Coupled Effects of Cement Type and Water Quality on the Properties of Cemented Paste Backfill. International Journal of Mineral Processing 143. Elsevier B.V.: 65–71.

Yin, C.Y., Shaaban, M.G., and Mahmud, H.B. 2007. Chemical Stabilization of Scrap Metal Yard Contaminated Soil Using Ordinary Portland Cement: Strength and Leachability Aspects. Building and Environment 42 (2): 794–802.

Zhou, Q., Beaudoin, J.J., 2003. Effect of applied hydrostatic stress on the hydration of Portland cement and C3S. Advanced Cement Research 15, 9-16.

Zhu, Y., An, F. and Tan, J. 2011. Geochemistry of Hydrothermal Gold Deposits: A Review. Geoscience Frontiers 2 (3). Elsevier B.V.: 367–74.

Appendix A. Abreviated ASTM C 1308 Procedure

A.1 Materials

A.1.1 Leaching Containers

Leaching vessles used were 1000 ml HDPE bottles. HDPE has been found to be a suitable container such that it does not react with the leachate or the specimine. The bottles used had a screw cap that fit tightly to minimize evaporative losses. Each container was labled with its specimine number. Two containers were used for each specimine such that the specimine could be transferred directly to fresh lechant at each exchange. This minimized the time the CPBs were exposed to the atmosphere to just a few seconds per exchange.

A.1.2 Specimine Supports

Specimine supports were used to suspend the specimine within the leaching vessel. Monofiliment was used becaue it is inert and the could be used to suspend the CPB in the middle of the leaching vessel withouot contacting greater than 1 % of the specimine's cylindrical surface area. Below the specimine the monofiliment was connected to mesh to better support the specimine in a vertical position. Specimines were suspended from the lid of the container using the monofiliment and mesh to allow for efficient leachate exchanges. This allowed for the lid containing the specimine to be transferred to the subsiquent leaching container.

A.1.3 Sample Containers

50 ml HDPE centrafuge tubes were used as containers to hold aquilots of leachate from each exchange.

A.1.4 Extraction Equiptment

50 ml pipettes were used to extract leachate from the leaching container and transfer it to the 50 ml centrafuge tubes.

A.1.5 Specimines

Cylindrical CPB specimines were used with a 1:1 diameter to height ratio of 5cm:5cm. Samples were cured in standard 5X10 molds. 2.5 cm was cut from each end of the specimine to ensure the same boundray on each end of the specimine. Calipers were used to ensure the sample dimensions were within a 0.01 cm tolerance.

A.2 Procedure

Specimines were cut to specified dimensions and placed on the mesh base connected to the monofiliment. The monofiliment was threded through holes punched in the leaching vessel cap, then tied off. The holes were then taped over to minimize evaporative loss. The leachant volume used for each leaching step was 900 ml. This was measured using a graduated cylinder to ensure constant surface area to leachate ratio for the test durration between all samples. All leaching tests were conducted at room temperature. At the end of each leaching interval the container lid was removed and the specimine was placed in the subsiquent leaching vessle prepard with 900 ml of leachant. The pipette was then used to homoginize the leachate, then extract two aquilots of 50 ml for leachate analysis. Aquilots were then refrigerated at 4°C until analysis was conducted by the geochemistry laboratory. The remainder of the leachate was contained in a hazardous waste container. The leaching vessel was then cleaned thouroughly with distilled water and prepared with 900 ml of water, to be used as the leaching vessel for the following leaching interval. Leachate exchange was conducted at 2, 5, 17, and 24 hours, then at each 24 hour interval for the remainder of the 11 day protocol. This resulted in 14 data points per specimine leached.